

## ABSTRACT

Sampling of the partially-saturated zone at the site of regular, long-term dumping and burning of jet fuels revealed vapor-phase concentrations of volatile organic compounds up-gradient from the point of dumping. This suggests that significant amounts of volatile compounds may be transported through the partially-saturated zone by vapor-phase diffusion. The laboratory component of this research examined both the steady-state and transient diffusion behavior of toluene, a volatile organic compound, in 6-cm long columns packed with glass beads and soil. One end of a column was exposed to toluene vapor and the other was sampled periodically using an activated carbon trap. The results of these diffusion experiments, when compared to column diffusion simulated with a one-dimensional finite difference model, revealed a retardation effect during the approach to steady state. The retardation effect was attributed to vapor-aqueous and aqueous-solid phase partitioning. Linear sorption constants were determined for the experimental data using the finite difference model. Although there was some variability in the data from one set of column runs to another, one set of experiments run with soil at 50-70% of saturation, was closely approximated using a linear sorption coefficient consistent with the linear coefficient found for a saturated system in an independent batch experiment. Sorption parameters for the saturated system were determined with a bottle-point equilibrium study and a non-linear Freundlich sorption model was found to describe the saturated system more accurately than a linear model. For several of the diffusion columns however, the model, run with linear sorption parameters, predicted transient diffusion behavior that fit the experimental data well.

## ACKNOWLEDGEMENTS

This research was made possible by a grant from the Water Resources Research Institute.

I would like to thank Dr. Cass T. Miller for his patience, guidance, and assistance, and especially for providing me with the opportunity to do this work. Also, thanks to my committee for their involvement, and to my fellow students, whose encouragement and endless ideas were essential.

## TABLE OF CONTENTS

	<u>Page</u>
Abstract . . . . .	i
Acknowledgements . . . . .	ii
Table of Contents . . . . .	iii
List of Figures . . . . .	v
List of Tables . . . . .	vii
1. Introduction . . . . .	1-1
2. Theoretical Background . . . . .	2-1
2.1 Darcy's Law . . . . .	2-1
2.2 Partially-Saturated Flow . . . . .	2-3
2.3 Fluid-Phase ADR Equation . . . . .	2-7
2.3.1 Velocity Vector . . . . .	2-8
2.3.2 Hydrodynamic Dispersion . . . . .	2-8
2.4 Vapor-Phase ADR Equation . . . . .	2-10
2.5 Diffusion . . . . .	2-11
2.5.1 Steady State . . . . .	2-11
2.5.2 Transient . . . . .	2-12
2.6 Reactions . . . . .	2-14
2.6.1 Aqueous-Solid Equilibrium . . . . .	2-14
2.6.2 Aqueous-Solid Rate . . . . .	2-16
2.6.3 Vapor-Liquid Equilibrium . . . . .	2-18
2.7 Governing Equations . . . . .	2-20
3. Experimental Methods . . . . .	3-1
3.1 Introduction . . . . .	3-1
3.2 Materials . . . . .	3-3
3.3 Analytical Methods . . . . .	3-6
3.3.1 Extraction Methods . . . . .	3-6
3.3.2 Measurement Methods . . . . .	3-7
3.4 Experimental Methods . . . . .	3-9
3.4.1 Field Sampling . . . . .	3-9
3.4.2 Bottle-Point Isotherm . . . . .	3-9
3.4.3 Bottle-Point Rate Study . . . . .	3-11
3.4.4 Diffusion Column Experiments . . . . .	3-13
3.4.4.1 Description of Apparatus . . . . .	3-13
3.4.4.2 Column Preparation . . . . .	3-15
3.4.4.3 Sampling Procedure . . . . .	3-15
3.4.5 Modeling Methods . . . . .	3-15

	<u>Page</u>
4. Experimental Results . . . . .	4-1
4.1 Field Results . . . . .	4-1
4.2 Sorption Study Results . . . . .	4-5
4.3 Diffusion Column Results . . . . .	4-11
4.4 Modeling Results . . . . .	4-11
5. Discussion . . . . .	5-1
5.1 Diffusivity . . . . .	5-1
5.2 Sorption . . . . .	5-5
5.3 Impact at the Field Scale . . . . .	5-19
6. Conclusions and Recommendations . . . . .	6-1
7. Notation . . . . .	7-1
8. References . . . . .	8-1

## LIST OF FIGURES

	<u>Page</u>
1-1 Groundwater Subsurface Zones . . . . .	1-2
1-2 NAPL in the Vadose Zone . . . . .	1-4
1-3 Partitioning in the Subsurface . . . . .	1-5
3-1 Grain Size Distribution of Pope AFB Soil . . . . .	3-5
3-2 Aqueous Extraction Procedure . . . . .	3-8
3-3 Field Sampling Procedure . . . . .	3-10
3-4 Procedure for Bottle-Point Studies . . . . .	3-12
3-5 Diffusion Apparatus . . . . .	3-14
4-1 Topographic Map of Fire Training Area No. 4. . . . .	4-2
4-2 Groundwater Elevations at Fire Training Area No. 4. . . . .	4-3
4-3 Normalized Concentrations of Hydrocarbons in the Partially-Saturated Zone	4-4
4-4 Results of Bottle-Point Equilibrium Study . . . . .	4-6
4-5 Freundlich and Linear Isotherm Models . . . . .	4-7
4-6 Rate Study Results: Time vs. Concentrations . . . . .	4-9
4-7 Rate Study Results: Time vs. $C/C_0$ . . . . .	4-10
4-8 Results of Column B-1 . . . . .	4-12
4-9 Results of Column C-1 . . . . .	4-13
4-10 Results of Column B-2 . . . . .	4-14
4-11 Results of Column B-3 . . . . .	4-15
4-12 Results of Column C-3 . . . . .	4-16
4-13 Results of Column B-4 . . . . .	4-17
4-14 Comparison of Model: $K_p = 0$ . . . . .	4-20
4-15 Comparison of Model: $K_p = 0.37$ . . . . .	4-21
4-16 Comparison of Model: $K_p = \text{Best Fit}$ . . . . .	4-22
5-1 Comparison of Tortuosities . . . . .	5-4
5-2 Simulation of Column B-1: $K_p = 0$ . . . . .	5-8
5-3 Simulation of Column C-1: $K_p = 0$ . . . . .	5-9

	<u>Page</u>
5-4 Simulation of Column B-2: $K_p = 0$ . . . . .	5-10
5-5 Simulation of Column B-3: $K_p = 0$ . . . . .	5-11
5-6 Simulation of Column C-3: $K_p = 0$ . . . . .	5-12
5-7 Simulation of Column B-4: $K_p = 0$ . . . . .	5-13
5-8 Simulation of Column B-1: Best Fit $K_p$ . . . . .	5-14
5-9 Simulation of Column C-1: Best Fit $K_p$ . . . . .	5-15
5-10 Simulation of Column B-3: Best Fit $K_p$ . . . . .	5-16
5-11 Simulation of Column C-3: Best Fit $K_p$ . . . . .	5-17
5-12 Simulation of Column B-4: Best Fit $K_p$ . . . . .	5-18

## LIST OF TABLES

	<u>Page</u>
3-1 Physical and Chemical Properties of Toluene . . . . .	3-4
4-1 Summary of Experimental Equilibrium Parameters . . . . .	4-8
4-2 Summary of Diffusion Column Data . . . . .	4-18
5-1 Published Tortuosity Factors and Variance with Experimental Data . . . . .	5-3
5-2 Best-Fit Linear Sorption Constants . . . . .	5-7

---

## 1 INTRODUCTION

---

In the United States, groundwater has become one of our most essential and most exploited natural resources. We depend on groundwater for industrial and domestic use for a number of reasons. In some areas, such as the southwest, large influxes of people have raised the demand for water in a region where surface water is not abundant. In other areas of the country groundwater is preferred to surface water because it is a more reliable water source. Annual and seasonal fluctuations are much more pronounced in surface water, and surface water may not be convenient because it occurs at specific points, at springs, lakes or rivers. Dependence on groundwater has also required less long-range planning because there has always been a seemingly endless supply of it; as the population of a region grows we simply install another well. Another advantage of groundwater has been its superior quality; surface water is generally more susceptible to man-made waste, either by run-off or by direct dumping.

Groundwater supplies, however, are neither infinite nor indestructible. Aquifers are fragile, delicately-balanced natural systems which, because of their dynamic nature, are easily contaminated, and difficult to restore. Recharge to an aquifer system occurs mainly through contact with surface water and by infiltration of rain water. This recharge water filters through the subsurface environment, which can be divided into four general regions: the soil zone, where plant life is supported; the vadose, or partially-saturated zone; the saturated zone; and the capillary fringe zone, which is the interface between the saturated and unsaturated zones. Figure 1-1 is a diagram of groundwater subsurface zones.

Groundwater contamination may occur in various ways. Contaminants in surface water or spilled or dumped on the ground surface in a recharge zone may be carried through the soil zone and into the vadose and saturated zones by the natural recharge mechanisms. Another major threat to groundwater supplies comes from underground

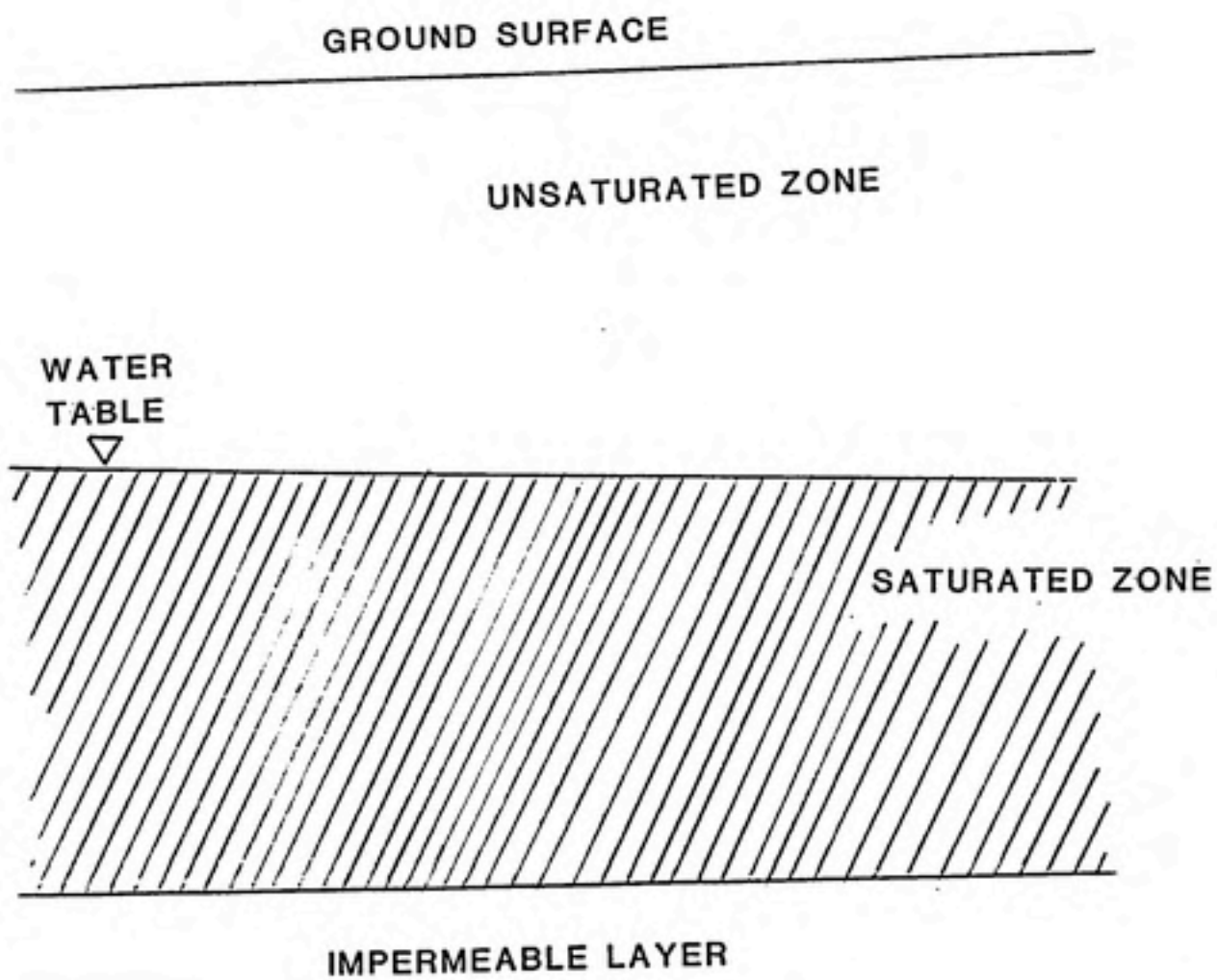


Figure 1-1. Groundwater Subsurface Zones.

storage tanks (USTs), which are used to store gasoline and industrial chemicals. The lifetime of most existing tanks is approximately 18 years, and it was estimated that as many as 100,000 tanks were leaking in the U.S. in 1985 (Mackay et al., 1985).

Contaminants that have a higher density than water that pass through the vadose zone and into the saturated zone may pass through this region and eventually accumulate at the bottom of the aquifer. However, organic compounds that are less dense than water, such as many components of gasoline, will remain at the top of the saturated zone and gradually go into solution in the groundwater. Some contaminants will remain as residuals in the vadose zone as well, as is shown in Figure 1-2. In the saturated zone a contaminant may sorb onto the soil from the liquid phase, and once on the solid it may desorb back into the groundwater. The contaminant may be transported by the bulk movement of the groundwater and it may disperse through the groundwater by molecular movement and mechanical mixing. Many large hydrocarbons will, in time, chemically degrade into smaller chemical species. Biological degradation also accounts for the destruction of many groundwater contaminants.

Contaminants that remain in the partially-saturated zone may partition into the vapor phase as well as sorb onto solids (Figure 1-3). Movement of contaminants in this region can occur by bulk movement of the vapor phase or by vapor-phase diffusion. Both chemical and biological degradation may also occur in this region.

Traditionally, the evaluation of a contamination problem has been based on measurements from the saturated zone. Measurements of the free product, that is the contaminant floating on the groundwater, and of the location of the contaminant plume have been used to determine the extent of a spill and also to identify the source of a contaminant. Relying on measurements from the saturated zone are not always adequate for these evaluations. For the cases where the contamination includes low-density hydrocarbons, a large volume of these compounds may reside in the vadose zone. In this region the movement of the contaminant is not dependent upon the movement of groundwater, but upon the bulk

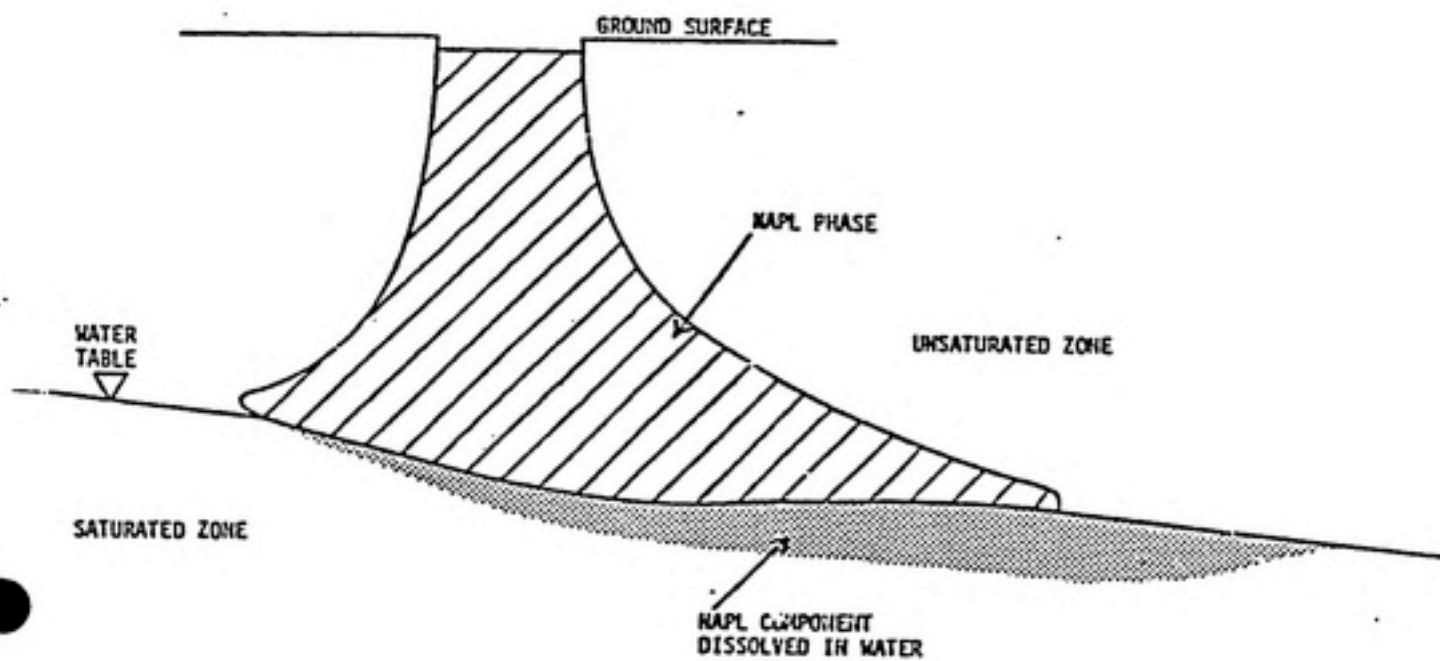


Figure 1-2. Non-Aqueous-Phase Liquid in the Vadose Zone.

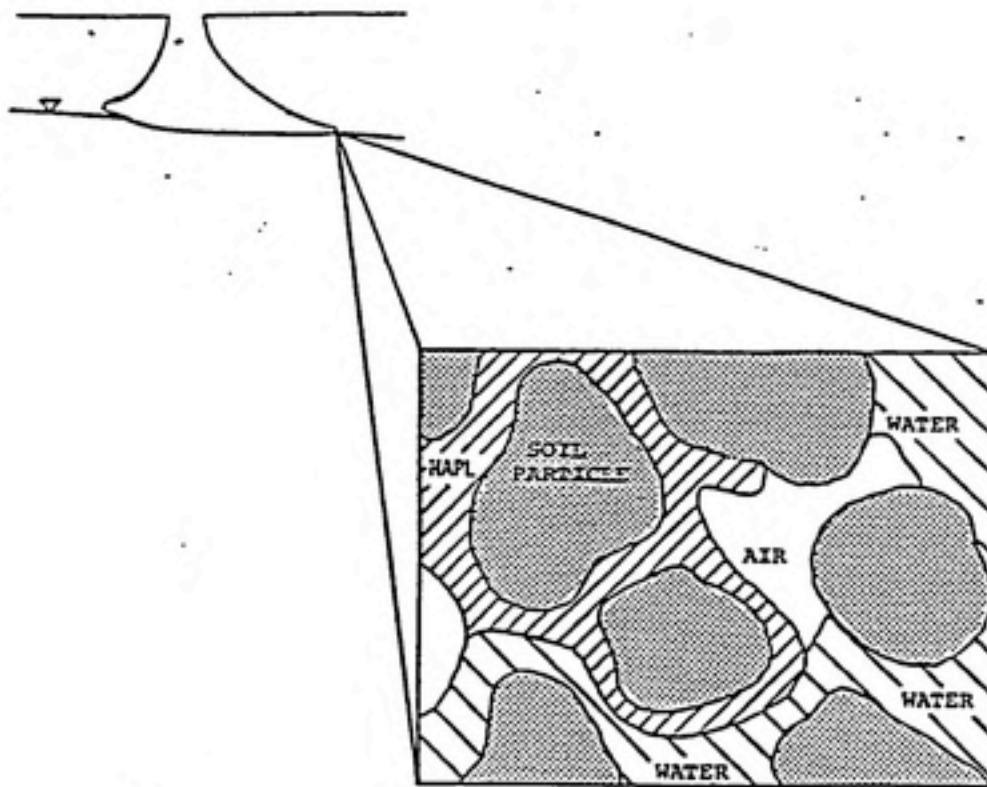


Figure 1-3. Partitioning in the Subsurface.

movement of air, the frequency and amount of recharge, and perhaps most importantly upon the concentration gradient of the contaminant in the vapor phase. Because vapors diffuse from areas of high concentration to areas of low concentration, volatile organic compounds may migrate in any direction away from a source, including up-gradient from that source. Once away from the area of high concentration the volatile organic compounds (VOCs) will establish a new vapor-liquid equilibrium and some will eventually end up in the groundwater even up-gradient from the source.

The partially-saturated zone can hold great volumes of VOC vapor, and migration of these vapors by diffusion, although slow, may occur over large distances. The result is that, over time, the source of a contaminant spreads; what was once a small point source may become a large source area. Diffusion of VOCs not only creates a problem in identifying the source of a contaminant, it also complicates restoration of a contaminated aquifer. The cleanup of contaminants in the subsurface may be a small-scale operation if the remedial action is taken immediately after the release. But the longer the VOCs are left to diffuse through the partially-saturated zone, the larger the source area becomes, and thus, the larger the area requiring remedial action. Restoration of the saturated zone must therefore be coupled with restoration of the vadose zone which, with time, may become a significant source of additional contamination.

Steady-state diffusion through porous media has been studied by some researchers in order to determine the rate of movement of pesticides, herbicides, or nutrients through the soil (van Genuchten et al., 1977; Albertson, 1979). Researchers have also attempted to quantify the rate at which benzene or other industrial waste products vaporize out of landfills (Farmer et al., 1980; Karimi et al., 1987), and others have determined the diffusion parameters at potential hazardous waste disposal sites to determine how effectively the waste will be contained (Weeks, 1982). The characteristics of transient diffusion in porous media have only recently begun to receive attention due to the large number of sites at which VOCs have been released, and due also to the source-spreading problems associated

with these sites, which was discussed earlier. The objective of this work was to quantify the transient nature of vapor-phase diffusion in the partially-saturated zone, while accounting for partitioning into the aqueous and solid phases.

---

## 2 THEORETICAL BACKGROUND

---

### 2.1 Darcy's Law

In the year 1856 a French engineer named Henry Darcy developed an empirical law that governs the flow of water through porous media. Darcy's experimental apparatus consisted of a saturated cylinder of porous media. Water flowed in one end of the cylinder at flow rate  $Q$ , and flowed out the other end at the same flow rate. Each end of the cylinder was connected to a reservoir suspended above it, each at a different height,  $h_1$  and  $h_2$ . The experiments consisted of varying  $h_1$ ,  $h_2$ , and  $\Delta l$ , the length of the column, and measuring the resulting flow rate out of the column. The specific discharge,  $q_x$  is defined as:

$$q_x = \frac{Q}{A} \quad (2-1)$$

where  $A$  is the cross-sectional area of the column and  $q_x$  has units of length per time. Darcy found that the specific discharge is directly proportional to the difference in reservoir elevations,  $h_1 - h_2$ , for constant  $\Delta l$ , and inversely proportional to  $\Delta l$  for constant  $\Delta h$ :

$$q_x = -K \frac{\Delta h}{\Delta l} \quad (2-2)$$

or

$$q_x = -K \frac{dh}{dl} \quad (2-3)$$

$K$  is the constant of proportionality known as the hydraulic conductivity. Hydraulic conductivity is a function of both the media and of the fluid flowing through it.

The hydraulic conductivity was examined more carefully by Hubbert in 1940. Hubbert was looking for a way to separate the effect of the fluid properties from the media properties in the hydraulic conductivity. He defined the hydraulic conductivity as:

$$K = \frac{k\rho g}{\mu} \quad (2-4)$$

where  $\rho$  is the density of the fluid;  $\mu$  is the dynamic viscosity of the fluid;  $g$  is the gravitational constant; and  $k$  is a quantity called the intrinsic permeability of the soil. The intrinsic permeability is a function only of the medium.

## 2.2 Partially-Saturated Flow

The governing equation for the flow of fluid in the partially-saturated zone can be derived using a control-volume approach. A mass balance on a control volume of partially-saturated media may be written:

$$\text{MassAccumulated} = \text{MassIn} - \text{MassOut} \quad (2-5)$$

which can be represented mathematically by:

$$\frac{dM}{dt} = M_{in} - M_{out} \quad (2-6)$$

where  $M$  is the mass of fluid. Describing the mass of fluid passing through the volume in one direction,  $x$ , in terms of the variables of the system, we have:

$$\frac{\partial}{\partial t}(\rho_w V n S) = A \rho_w q_{in} - \left( A \rho_w q_{in} + \frac{\partial}{\partial x} (A \rho_w q_x) \Delta x \right) \quad (2-7)$$

where  $\rho_w$  is the density of water;  $V$  is the volume of the control element;  $n$  is the porosity of the media;  $S$  is the degree of water saturation;  $A$  is the area of the face of the control volume normal to the  $x$  direction; and  $q_x$  is the  $x$  component of the specific discharge vector. This equation simplifies to:

$$\frac{\partial}{\partial t}(\rho_w V n S) = - \frac{\partial}{\partial x} (A \rho_w q_x) \Delta x \quad (2-8)$$

Adding the contributions to the control volume from the  $y$  and  $z$  directions, including the condition that the control volume is constant, and introducing the relationship:

$$S = \frac{\theta_w}{n} \quad (2-9)$$

where  $\theta_w$  is the volumetric fraction of the water phase, we get:

$$\frac{\partial}{\partial x}(\rho_w q_x) + \frac{\partial}{\partial y}(\rho_w q_y) + \frac{\partial}{\partial z}(\rho_w q_z) = -\frac{\partial}{\partial t}(\rho_w \theta_w) \quad (2-10)$$

This equation can also be written:

$$\nabla \cdot (\rho_w \vec{q}) = -\frac{\partial}{\partial t}(\rho_w \theta_w) \quad (2-11)$$

To define the specific discharge vector,  $\vec{q}$ , we start with the general form of Darcy's law:

$$q_x = -K_{xx} \frac{\partial \phi}{\partial x} - K_{xy} \frac{\partial \phi}{\partial y} - K_{xz} \frac{\partial \phi}{\partial z} \quad (2-12)$$

$$q_y = -K_{yx} \frac{\partial \phi}{\partial x} - K_{yy} \frac{\partial \phi}{\partial y} - K_{yz} \frac{\partial \phi}{\partial z} \quad (2-13)$$

$$q_z = -K_{zx} \frac{\partial \phi}{\partial x} - K_{zy} \frac{\partial \phi}{\partial y} - K_{zz} \frac{\partial \phi}{\partial z} \quad (2-14)$$

where  $K_{xx}$ ,  $K_{xy}$ , etc. are elements of the hydraulic conductivity tensor, and  $\phi$  is the hydraulic head defined as:

$$\phi = z + \frac{P}{\rho g} = z + \psi \quad (2-15)$$

If the control volume is aligned with the principal axes we can drop the non-diagonal terms of the hydraulic conductivity tensor. Now, substituting Darcy's law into our working equation gives:

$$\frac{\partial}{\partial x} \left( \rho_w K_x(\psi) \frac{\partial \phi}{\partial x} \right) + \frac{\partial}{\partial y} \left( \rho_w K_y(\psi) \frac{\partial \phi}{\partial y} \right) + \frac{\partial}{\partial z} \left( \rho_w K_z(\psi) \frac{\partial \phi}{\partial z} \right) = \theta_w \frac{\partial \rho_w}{\partial t} + \rho_w \frac{\partial \theta_w}{\partial t} \quad (2-16)$$

If changes in fluid density are assumed to be small compared to changes in moisture content the equation becomes:

$$\frac{\partial}{\partial x} \left( K_x(\psi) \frac{\partial \phi}{\partial x} \right) + \frac{\partial}{\partial y} \left( K_y(\psi) \frac{\partial \phi}{\partial y} \right) + \frac{\partial}{\partial z} \left( K_z(\psi) \frac{\partial \phi}{\partial z} \right) = \frac{\partial \theta_w}{\partial t} \quad (2-17)$$

A more common form of the flow equation for partially saturated media is Richard's equation. In Richard's equation the dependent variable is pressure head,  $\psi$ , rather than having two dependent variables,  $\psi$  and  $\theta_w$ , as in equation 2-17. The use of pressure head as the dependent variable is generally preferred because of the dimensional convenience (Parker et al, 1987). Making this conversion gives:

$$\frac{\partial}{\partial x} \left( K_x(\psi) \frac{\partial(\psi + z)}{\partial x} \right) + \frac{\partial}{\partial y} \left( K_y(\psi) \frac{\partial(\psi + z)}{\partial y} \right) + \frac{\partial}{\partial z} \left( K_z(\psi) \frac{\partial(\psi + z)}{\partial z} \right) = \left( \frac{d\theta_w}{d\psi} \right) \frac{\partial \psi}{\partial t} \quad (2-18)$$

The specific moisture capacity,  $c(\psi)$ , is defined as the slope of the volumetric moisture content as a function of the pressure head:

$$c(\psi) = \frac{d\theta_w}{d\psi} \quad (2-19)$$

Making this final substitution gives Richard's equation:

$$\frac{\partial}{\partial x} \left( K_x(\psi) \frac{\partial \psi}{\partial x} \right) + \frac{\partial}{\partial y} \left( K_y(\psi) \frac{\partial \psi}{\partial y} \right) + \frac{\partial}{\partial z} \left( K_x(\psi) \frac{\partial \psi}{\partial z} + K_z \right) = c(\psi) \frac{\partial \psi}{\partial t} \quad (2-20)$$

The most significant simplifying assumption in Richard's equation is that the pressure in the vapor phase is atmospheric (Faust, 1985).

In this development of Richard's equation both the hydraulic conductivity,  $K$ , and the moisture content,  $c$ , have been described as functions of the pressure head,  $\psi$ . These

functions have been found to be nonlinear and hysteretic in nature (Kool and Parker, 1987; Kool and Parker, 1988). These relationships are important because they determine the relationship between aqueous flow and saturation in the partially-saturated zone. This means that changes in pressure head, hence saturation, has a significant impact on the assumption that the aqueous phase is immobile in this region.

### 2.3 Fluid-Phase Advective-Dispersive-Reactive Equation

The advective-dispersive-reactive (ADR) equation is generally used as the macroscopic equation that governs the fate and transport of groundwater contaminants, though some researchers have proposed other approaches (Gillham et al., 1984; Tompson, 1986). There are several ways to develop the ADR equation, including the use of the control volume approach, as was used in the development of the flow equation. The derivation of the transport equation will not be presented here, however. The general form of the ADR equation is:

$$\frac{\partial C_a}{\partial t} = -\vec{v} \cdot \text{grad } C_a + \text{div} (D_h \text{grad } C_a) + \Gamma(C_a) + \left( \frac{\partial C_a}{\partial t} \right)_{rxn} \quad (2-21)$$

where  $C_a$  is the aqueous concentration of contaminant;  $\vec{v}$  is the vector of average groundwater pore velocity;  $D_h$  is the hydrodynamic dispersion tensor that includes the effects of both mechanical dispersion and molecular diffusion (Bear, 1979); and  $\Gamma(C_a)$  represents either a mass source or sink within the control volume. The reaction term accounts for any mass that is added or removed by reaction. This term includes biological degradation, chemical transformations, sorption onto the solid phase, and desorption from the solid phase.

In the partially-saturated zone contaminant transport may occur in two phases, fluid and vapor, and therefore the ADR equation must be formulated and solved for each phase. For the fluid phase, ignoring any internal sources or sinks, the ADR equation can be written:

$$\frac{\partial C_a}{\partial t} = -\vec{v} \cdot \text{grad } C_a + \text{div} (D_h \text{grad } C_a) + \left( \frac{\partial C_a}{\partial t} \right)_{rxn} \quad (2-22)$$

## Velocity Vector

The pore velocity vector,  $\vec{v}$ , describes the average linear macroscopic velocity of the fluid phase and is obtained by solving Richard's equation for partially-saturated flow. The pore velocity is related to the specific discharge,  $\vec{q}$ , by the relationship:

$$\vec{v} = \frac{\vec{q}}{\theta_w} \quad (2-23)$$

where  $\theta_w$  is the fluid-filled porosity of the media. The specific discharge defines a linear velocity through a control volume of media. The pore velocity refers to the average macroscopic pore velocity of the fluid.

## Hydrodynamic Dispersion

Bear (1979) describes the hydrodynamic dispersion tensor as the sum of a mechanical dispersion term and a molecular diffusion term:

$$D_{ij} = \alpha_T \bar{v} \delta_{ij} + (\alpha_L - \alpha_T) \bar{v}_i \bar{v}_j / \bar{v} + D_m \quad (2-24)$$

where  $D_{ij}$  is the  $i,j$  term of the dispersion tensor;  $\alpha_T$  is the transverse dispersivity;  $\alpha_L$  is the longitudinal dispersivity;  $\bar{v}$  is the average magnitude of the groundwater velocity;  $\delta_{ij}$  is the Kronecker delta function ( $\delta = 1$  for  $i = j$ ;  $\delta = 0$  for  $i \neq j$ ); and  $D_m$  is the effective molecular diffusion coefficient.

Mathematical solutions to the ADR equation have been proposed and have compared well with the results of laboratory experiments. However, discrepancies occur between the results of laboratory experiments and field experiments. Some researchers have concluded that the discrepancies occur because dispersivity is a scale-dependent parameter (Sudicky and Cherry, 1979; Pickens and Grisak, 1981). The dispersivity may be scale-dependent due to heterogeneities in the media (Skibitzke and Robinson, 1963; Bear, 1979).

The product of the flow velocity and the dispersivity is generally known as the mechanical dispersivity. In groundwater systems the molecular diffusion term,  $D_m$ , is often very small relative to the mechanical dispersion, and may be neglected if groundwater velocities are large. One should note that the groundwater velocity is present here in the dispersion term of the ADR equation as well as in the velocity term.

## 2.4 Vapor-Phase Advective-Dispersive-Reactive Equation

In the partially-saturated zone the advective-dispersive-reactive equation can be written to describe contaminant transport in the vapor phase. Assuming that there are no internal sources or sinks the equation is:

$$\frac{\partial C_v}{\partial t} = -\vec{v} \cdot \text{grad } C_v + \text{div} (D_h \text{grad } C_v) + \left( \frac{\partial C_v}{\partial t} \right)_{rxn} \quad (2-25)$$

It is common, though possibly rash, to assume that the pore velocity in the vapor phase is negligible and therefore that the effect of mechanical dispersion is small compared to that of molecular diffusion (van Genuchten and Wieranga, 1976; Weeks et al, 1982; Peterson et al, 1988). If one assumes that the velocity approaches zero the ADR equation reduces to:

$$\frac{\partial C_v}{\partial t} = \text{div} (D_h \text{grad } C_v) + \left( \frac{\partial C_v}{\partial t} \right)_{rxn} \quad (2-26)$$

Also as the velocity approaches zero, the hydrodynamic dispersion tensor can be rewritten. Assuming that the effective diffusivity is the same in all directions, that there are no variations in media properties that could lead to anisotropic diffusion, the governing equation becomes:

$$\frac{\partial C_v}{\partial t} = D_e \nabla^2 C_v + \left( \frac{\partial C_v}{\partial t} \right)_{rxn} \quad (2-27)$$

## 2.5 Diffusion

### Steady-State Diffusion

Steady-state diffusion of a vapor through air was first described by Fick when he drew an analogy between molecular diffusion and heat transfer in solids. Fick recognized that the amount of vapor diffusing along a path length  $x$  is proportional to the concentration gradient across this distance. Just as the conductivity,  $K$ , is the constant of proportionality for heat transfer, Fick defined the diffusivity,  $D^*$ , as the constant of proportionality for diffusion (Bird et al, 1960). Thus Fick's First Law can be written:

$$J = -D^* \frac{dC_v}{dx} \quad (2-28)$$

where,  $J$  is the flux;  $D^*$  is the diffusion coefficient for the diffusion of one pure gas through another; and  $\partial C_v / \partial x$  is the concentration gradient.

In the case where a vapor is diffusing through porous media there are several approaches that may be taken to describe diffusion. One approach is to define an effective diffusivity in which case Fick's first law is written as in equation 2-28. In this case the effective diffusivity is a value that is specific to the media and to the conditions under which the diffusivity was determined. These conditions include temperature, bulk density, water content, and presence of other solutes.

A common way of describing diffusion in porous media is to define a tortuosity factor, which accounts for the geometric effects of the solid media on the apparent diffusion. This tortuosity factor accounts for the increased path length of diffusion and therefore includes effects of water content. The steady-state diffusion equation for porous media can therefore be written:

$$J = -\theta_D \tau D^* \frac{dC_v}{dx} = -\theta_D D_e \frac{dC_v}{dx} \quad (2-29)$$

where  $\theta_D$  is the drained porosity of the soil, or the fraction of the total volume that is occupied by air;  $\tau$  is the tortuosity, and  $D_e$  is an effective diffusivity. Empirical equations for the tortuosity factor have been determined by various researchers (Buckingham, 1904; Millington, 1959; Millington and Quirk, 1961; Albertson, 1979). The most commonly accepted equation has been that proposed by Millington and Quirk (1961). However, even Millington and Quirk's tortuosity has been found to be inaccurate by some recent researchers (Peterson et al., 1988).

#### Transient Diffusion

The ADR equation for vapor-phase contaminant transport, neglecting velocity effects, sorption effects and chemical reactions reduces to:

$$\frac{\partial C_v}{\partial t} = D^* \nabla^2 C_v \quad (2-30)$$

This equation is also known as Fick's second law of diffusion (Bird et al, 1960). Fick's second law is applicable to the movement of one gas through another with no net flow of gas (convection) and under isothermal, constant density conditions. Fick's second law was also originally derived by analogy to heat transfer, and therefore many solutions to the transient diffusion equation under a variety of boundary conditions are available in the literature (Carslaw and Jaeger, 1959; Crank, 1975)

Fick's second law can be adapted to describe diffusion in porous media:

$$\theta_D \frac{\partial C_v}{\partial t} = \theta_D D_e \nabla^2 C_v \quad (2-31)$$

This equation also assumes that molecular diffusion is the only means of vapor transport, neglecting velocity effects and density driven flow.

## 2.6 Reactions

Reactions between volatile organic chemicals (VOCs) and the solid matrix retard the movement of the chemical through that matrix. In the partially-saturated zone, in the absence of advective transport in the vapor phase, vapor-phase diffusion may be the most significant method of transport of VOCs, but there are other physical phenomena that play an important role. By definition the partially-saturated zone retains some residual saturation, which creates a complex and tortuous path through which an organic vapor must move. Throughout this partially-saturated zone the vapor is in contact with water as well as air and partitioning of the organic solute occurs between the aqueous and vapor phases. Because the residual water is in contact with the solid phase, partitioning occurs in turn between the aqueous and solid phases. The result is a dynamic system consisting of three phases.

### Aqueous-Solid Equilibrium

Sorption and desorption refer to the processes of transfer of mass from the fluid phase to the solid phase and from the solid phase to the fluid phase, respectively. The transfer of an organic compound between a fluid and a solid phase is generally believed to be a partitioning phenomena, and this partitioning has been found to be a function of the fraction of organic matter present in the soil (Karickhoff, 1979). When the rate of transfer of mass from the fluid phase to the solid phase is equal to the rate of transfer in the opposite direction, the system is in a state of dynamic equilibrium.

Several models have been used to describe sorption equilibrium. The most common of these is the linear equilibrium model:

$$q_e = K_p C_{ae} \quad (2-32)$$

where  $q_e$  is the equilibrium solid-phase concentration with units of mass of solute per mass

of solid;  $C_{ae}$  is the equilibrium fluid-phase concentration with units of mass per volume; and  $K_p$  is the linear equilibrium partitioning coefficient with units of volume per mass. There are many empirical expressions for the partitioning coefficient. One such expression for the partitioning of organic compounds in sediments has been described as (Karickhoff, 1979):

$$K_p = f_{oc}K_{oc} \quad (2-33)$$

where  $f_{oc}$  is the fraction of organic carbon in the solid; and  $K_{oc}$  is the organic-carbon partition coefficient of the solid. Karickhoff found the organic-carbon partition coefficient to follow the empirical expression:

$$\log K_{oc} = \log K_{ow} - 0.21 \quad (2-34)$$

where  $K_{ow}$  is the octanol-water partition coefficient of the solute. Octanol-water coefficients are compiled in the literature for a variety of compounds (Hansch and Leo, 1979). This relationship was derived for soils of relatively high organic content, and may not yield accurate predictions of  $K_p$  in soils of low organic carbon content (less than 0.1 percent). Also, the expression was derived for use with neutral, non-polar, and hydrophobic compounds and will not give accurate results if used for other types of compounds.

There are also nonlinear equilibrium models. The most common of these is the Freundlich sorption equilibrium model:

$$q_e = K_F C_{ae}^{n_F} \quad (2-35)$$

where  $K_F$  is a sorption capacity constant and  $n_F$  is a sorption intensity constant. Sorption equilibrium curves are often slightly concave in shape and the Freundlich relationship

models this behavior more accurately than a linear model. The great advantage of the linear model, of course, is its simplicity.

### Aqueous-Solid Rate

In a system for which the rates of sorption and desorption have not reached an equilibrium, it is necessary to determine the rate of sorption in order to thoroughly characterize the mass-transfer process. There are several models that are used to describe the rate of sorption of mass from the aqueous phase to the solid phase.

The simplest of these models is the linear local-equilibrium model. Many researchers have used this model, which assumes that local equilibrium is achieved instantaneously (Back and Cherry, 1976; Anderson, 1979; Freeze and Cherry, 1979).

Assuming that the fluid and solid phases are always in equilibrium, the fluid and solid phase concentrations can be related using the chain rule:

$$\frac{\partial q}{\partial t} = \frac{\partial q}{\partial C_a} \frac{\partial C_a}{\partial t} \quad (2-36)$$

The linear local-equilibrium model also assumes that the equilibrium solid-phase concentration is a linear function of the fluid phase concentration:

$$q_e = K_p C_{ae} \quad (2-37)$$

and

$$\frac{\partial q}{\partial C_a} = K_p \quad (2-38)$$

Combining these equations gives an expression for the rate of sorption:

$$\frac{\partial q}{\partial t} = K_p \frac{\partial C_a}{\partial t} \quad (2-39)$$

It has also been suggested by many researchers that sorption rates are not instantaneous and that the rate of sorption is important for certain solute-soil systems (Karickhoff, 1980; Karickhoff, 1984; Miller, 1984; Miller and Weber, 1984; Weber and Miller, 1986).

Another popular sorption model is the two-site model, which assumes that there are two conceptual sorption sites on the solid phase (Cameron and Klute, 1977). The first type of sorption site is one upon which equilibrium between the fluid and solid phases occurs instantaneously, and sorption on the second site follows first-order kinetics. The equilibrium models may be linear:

$$q_{fe} = K_{fp} C_a \quad (2-40)$$

$$q_{se} = K_{sp} C_a \quad (2-41)$$

in which case the rate expressions for these two sorption sites are:

$$\frac{\partial q_f}{\partial t} = K_{fp} \frac{\partial C_a}{\partial t} \quad (2-42)$$

and

$$\frac{\partial q_s}{\partial t} = k(q_{se} - q_s) \quad (2-43)$$

where  $k$  is a mass transfer coefficient,  $q_f$  refers to the solids concentration on the fast sites, and  $q_s$  refers to the solids concentration on the slow sites. Equilibrium may also be described with Freundlich isotherms:

$$q_{fe} = K_{fF} C_a^{n_f} \quad (2-44)$$

$$q_{se} = K_{sF} C_a^{n_s} \quad (2-45)$$

It should be noted that the two-site model with Freundlich equilibria sub-models is a general model, of which the local linear equilibrium model and the local non-linear equilibrium model are special cases.

### Vapor-Liquid Equilibrium

As a volatile organic vapor diffuses through the solid matrix, it will partition into the aqueous phase, which is occupying a portion of the pore space and is surrounding each soil particle. If a soil system is not at equilibrium with respect to the vapor-phase concentration diffusing through the region, then the transfer of material between the aqueous and vapor phases will not be at equilibrium. That is, as the concentration of VOC in the vapor-phase increases, more mass will be transferred into the aqueous-phase and the system will continuously seek a new level of equilibrium. It is common to assume that vapor-liquid equilibrium occurs instantaneously, that at any given instant the concentrations of VOC in the two phases are in equilibrium and can be described by a simple equilibrium model.

A simple way to describe vapor-liquid equilibrium is to assume that there is a linear relationship between the vapor concentration and the aqueous concentration (Smith and Van Ness, 1975). This is Henry's Law and it is written:

$$p_i = H x_i \quad (2-46)$$

where  $p_i$  is the partial pressure of compound  $i$ ;  $H$  is Henry's constant; and  $x_i$  is the mole fraction of compound  $i$  in the aqueous phase. Henry's Law is applicable primarily in cases

when both vapor and liquid concentrations are dilute.

Henry's Law can be restated to describe a linear equilibrium between the vapor and aqueous phases in the partially saturated zone;

$$C_a = K_H C_v \quad (2-47)$$

and

$$\frac{\partial C_a}{\partial t} = K_H \frac{\partial C_v}{\partial t} \quad (2-48)$$

In this case, Henry's constant,  $K_H$ , has units of vapor volume per aqueous volume, but it still defines a linear equilibrium relationship.

## 2.7 Governing Equations

Combining the ADR equation for the vapor-phase with equilibrium and sorption equations, we can arrive at a governing equation for vapor-phase diffusion in the partially-saturated zone. The ADR equation from section 2.4 can be written for porous media:

$$\frac{\partial C_v}{\partial t} = D_e \nabla^2 C_v + \left( \frac{\partial C_v}{\partial t} \right)_{rxn} \quad (2-49)$$

This equation was derived based on the assumption that there is no advection, or net flow of air, in the pore spaces of the vadose zone. This assumption has been made by a number of vapor-phase researchers (Farmer et al, 1980; Karimi et al, 1987; Peterson et al, 1988).

We can now examine the reaction terms of this equation, which must account for any mass that is added or removed from the vapor phase. One of these terms must describe the exchange of mass between the vapor and liquid phases; another must describe the mass which sorbs onto the solid matrix. These two terms can be written with negative signs to denote a loss of mass from the vapor phase:

$$\theta_D \frac{\partial C_v}{\partial t} = \theta_D D_e \nabla^2 C_v - (\theta_T - \theta_D) \frac{\partial C_a}{\partial t} - \rho_s (1 - \theta_T) \frac{\partial q}{\partial t} \quad (2-50)$$

where  $\rho_s$  is the density of the solid;  $\theta_D$  is the drained porosity; and  $\theta_T$  is the total porosity. The porosities are introduced into this equation to account for the actual volumes occupied by the vapor, liquid, and solid phases. The density term is necessary to maintain dimensional consistency.

A linear equilibrium model can be introduced to describe vapor-liquid equilibrium:

$$\frac{\partial C_a}{\partial t} = K_H \frac{\partial C_v}{\partial t} \quad (2-51)$$

and the general two-site sorption model can be used to describe the sorption term:

$$\frac{\partial q}{\partial t} = n_f K_f C_a^{n_f-1} \frac{\partial C_a}{\partial t} + k(K_s C_a^{n_s} - q_s) \quad (2-52)$$

In this case both fast and slow sorption terms have been described with Freundlich isotherm models. Expressing the sorption in terms of the vapor-phase concentration gives:

$$\frac{\partial q}{\partial t} = K_f K_H^{n_f-1} n_f C_v^{n_f-1} \frac{\partial C_v}{\partial t} + k[K_s (K_H C_v)^{n_s} - q_s] \quad (2-53)$$

Substituting the equilibrium expressions into the ADR equation and assuming that the liquid phase completely wets the solid phase, and that gaseous diffusion through the liquid film surrounding the solid particle is instantaneous, the ADR equation can be written:

$$\begin{aligned} \theta_D \frac{\partial C_v}{\partial t} = & \theta_D D_c \nabla^2 C_v - (\theta_T - \theta_D) K_H \frac{\partial C_v}{\partial t} \\ & - \rho_s (1 - \theta_T) K_f K_H^{n_f-1} n_f C_v^{n_f-1} \frac{\partial C_v}{\partial t} - \rho_s (1 - \theta_T) k [K_s (K_H C_v)^{n_s} - q_s] \end{aligned} \quad (2-54)$$

Linear equilibrium models can also be used to describe sorption equilibrium and this greatly simplifies the ADR equation. The linear sorption model can be stated:

$$\frac{\partial q}{\partial t} = K_p \frac{\partial C_a}{\partial t} \quad (2-55)$$

Substituting this expression into the ADR equation gives:

$$\theta_D \frac{\partial C_v}{\partial t} = \theta_D D_c \nabla^2 C_v - [(\theta_T - \theta_D) K_H + \rho_s (1 - \theta_T) K_H K_p] \frac{\partial C_v}{\partial t} \quad (2-56)$$

Combining terms simplifies the equation to:

$$\frac{\partial C_v}{\partial t} = \left[ \frac{\theta_D D_e}{\theta_D + (\theta_T - \theta_D) K_H + (1 - \theta_T) \rho_s K_H K_p} \right] \nabla^2 C_v \quad (2-57)$$

The term in the brackets is a constant with the units of diffusivity,  $L^2/T$ , and can be considered a retarded effective diffusivity through the porous media,  $D_{re}$  (Weeks et al, 1982). Finally, a governing equation for the vapor phase transport of contaminants in the partially-saturated zone, subject to all of the assumptions discussed in this section, may be written:

$$\frac{\partial C_v}{\partial t} = D_{re} \nabla^2 C_v \quad (2-58)$$

---

## 3 EXPERIMENTAL METHODS

---

### 3.1 Introduction

The purpose of this work was to study the diffusion of volatile organic contaminants through partially-saturated porous media. Glass columns packed with both glass beads and soil were used to observe diffusion rates in media of both high and low sorptive capacities. Both glass bead and soil columns were run at various degrees of saturation. Sorption equilibrium and sorption rate studies were also performed in order to separate the sorption effects from the diffusion effects in the experimental columns.

The sorption equilibrium and rate studies both followed the same general procedures. Soil samples were placed in centrifuge vials and then an aqueous solution of toluene was added and the vials sealed. The samples were then shaken vigorously and continuously on an orbit shaker. In the equilibrium studies, the vials were prepared with various initial aqueous concentrations of toluene and all samples were shaken until they approached equilibrium; in the rate studies all the vials were prepared with the same initial concentration of toluene and the samples were analyzed every few hours until equilibrium was achieved. After shaking, the solids were settled by centrifugation and the aqueous toluene concentration was determined by extracting the aqueous phase and analyzing with gas chromatography. The amount of sorbed toluene was calculated by difference based on the final aqueous concentrations of the blanks, which were carried along through the entire procedure.

To prepare the diffusion columns the soil was first saturated in de-ionized water and then slurried into the glass columns which were fitted with frits at one end to contain the soil. Next the soil was drained until some degree of partial saturation was achieved. The columns were then fitted onto the diffusion chamber and sealed with the ball-valve

assembly which allowed for replacement and removal of activated carbon samples at the ends of the columns. The chamber itself was filled with a nitrogen atmosphere that was maintained nearly saturated with toluene and water, which were supplied from constantly stirred reservoirs at the bottom of the chamber.

The activated carbon was left in place at all times to maintain zero concentration at the end of the columns. Samples were taken every 12-24 hours by inserting a fresh plug of carbon into the valve assembly and removing it exactly one hour later. This sample was then extracted and analyzed for the mass of toluene, which could be interpreted as a one-hour integrated flux.

### 3.2 Materials

Toluene was chosen as the contaminant for this study because of its high volatility and its prevalence in gasoline, and therefore in contaminated groundwater systems. The high volatility suggests that toluene should be a major contaminant in the vapor phase of the vadose zone at any gasoline spill site. The physical properties of toluene are listed in Table 3-1.

Toluene that was used in the experiments was reagent grade and was obtained from Fisher Scientific Co., Pittsburgh, PA. All extraction solvents and internal standards (carbon disulfide, ethyl benzene, hexanes and iso-octane) were reagent grade or better and were obtained from Mallencroft, Inc., Paris, Texas.

All soil that was used in diffusion columns, equilibrium studies, and rate studies was obtained from a field site at Pope Air Force Base in Fayetteville, NC. The soil was excavated from three to four feet beneath the surface. Twigs and other large organic material was floated out of the soil using de-ionized water in a five-gallon tank, washing small batches of soil at a time. The fraction of organic carbon ( $f_{oc}$ ) in the soil was 0.004. A grain size analysis of the washed soil is shown in Figure 3-1.

Activated carbon that was used to sample the diffusion columns was ground and sieved to 30-40 mesh. It was subsequently rinsed several times with de-ionized water before use.

All glassware was acid washed in either nitric acid or a mixture of sulfuric acid and chromic acid (*Chromerge*<sup>R</sup>, Fisher Scientific Co.). Glassware was then rinsed several times with de-ionized water and dried at 105°C.

Table 3-1. Physical and Chemical Properties of Toluene

---

Mol. Wt.(g/mol)	92.14
Boiling Pt. (°C)	110.6
Log K <sub>ow</sub> <sup>1</sup>	2.46
Density (g/ml)	0.867
Water Solubility <sup>2</sup> (mg/l)	515
Henry's Constant <sup>2</sup> (atm-m <sup>3</sup> /mol)	6.68 x10 <sup>-3</sup>

---

<sup>1</sup> Hansch and Leo (1979)

<sup>2</sup> Verschuren (1983)

Pope AFB  
Grain Size Analysis

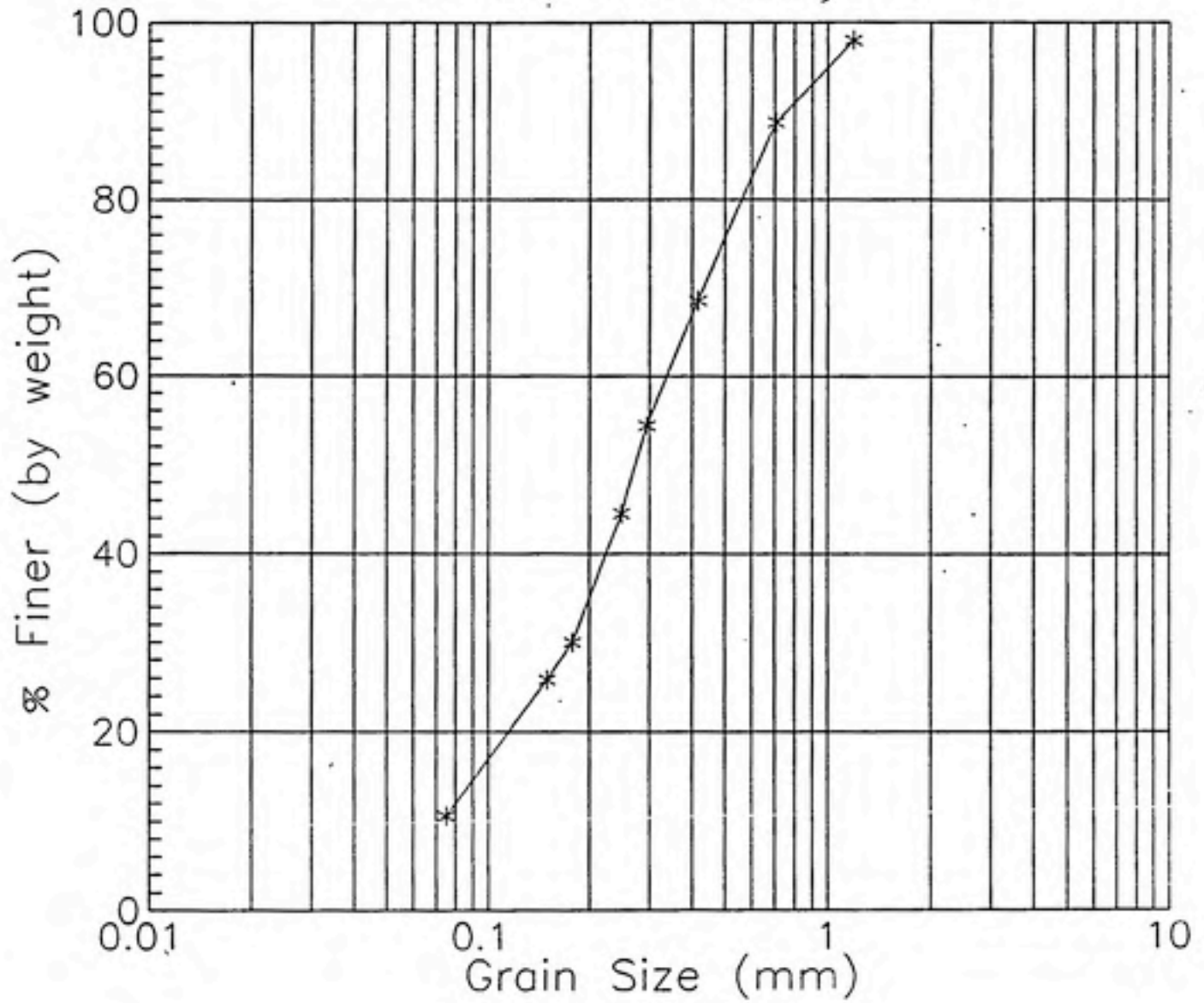


Figure 3-1. Grain Size Distribution of Pope AFB Soil.

### 3.3 Analytical Methods

#### Extractions Methods

In the sorption equilibrium and rate experiments aqueous solutions had to be analyzed for toluene. In each case 10 ml of solution were used for the extraction procedure. The 10 ml of solution were placed in a 20-ml sample vial with 3 ml of hexanes spiked with iso-octane as an internal standard. The concentration of the internal standard was approximately 200  $\mu\text{g/l}$ . The vial was shaken vigorously on an orbit shaker for several minutes. After the two phases were separated, approximately three ml of the organic phase were drawn off using a three ml syringe. The organic phase was then dried in a three-ml sample vial with 0.25 grams of sodium sulfate. The sample was then ready for analysis with a gas chromatogram. The aqueous extraction procedure is illustrated in Figure 3-2.

Activated carbon was used to sample toluene in the diffusion column apparatus. Once an activated carbon sample had been exposed to a column for one hour it was desorbed in three ml of carbon disulfide spiked with ethyl benzene which was used as an internal standard. The concentration of internal standard was approximately 200  $\mu\text{g/l}$ . All samples were shaken continuously for 30 minutes to maximize desorption efficiency. One  $\mu\text{l}$  of the carbon disulfide was then injected into a gas chromatograph for analysis.

A series of experiments were performed to determine the desorption efficiency of the 30-40 mesh granulated activated carbon (GAC) as used to sample the diffusion columns. Several 0.5-gram samples of GAC were placed in small sample vials and then toluene was added with a syringe to each vial. The amount added varied between 25 and 500  $\mu\text{g}$ ; this range was chosen as the range likely to be encountered during the running of the diffusion experiments. After the samples had set for an hour to assure complete sorption, three ml of carbon disulfide spiked with ethylbenzene as an internal standard was added to each. The samples were then shaken for 30 minutes to desorb the toluene from the activated

carbon. After desorption, one  $\mu\text{l}$  injections were analyzed by gas chromatography and the recovery of toluene was calculated to be 92% on the average. These experiments were repeated and recovery was consistently above 90%. Therefore, this became the method of desorption.

#### Measurement Methods

All gas chromatograms were generated by injecting one  $\mu\text{l}$  of sample into a Varian 3700 gas chromatograph equipped with a flame ionization detector (FID), a DB-1 column, and a Hewlett Packard 3390 integrator. The temperature program for the analysis of toluene in hexanes consisted of ramping at four degrees per minute from an initial temperature of  $60^{\circ}\text{C}$  to a final temperature of  $100^{\circ}\text{C}$  and then ramping at ten degrees per minute from  $100^{\circ}\text{C}$  to  $135^{\circ}\text{C}$ . A calibration curve for the gas chromatography was generated by preparing five solutions, each of different concentrations of toluene in hexanes spiked with the internal standard, iso-octane.

The temperature program for analysis of toluene in carbon disulfide consisted of ramping at eight degrees per minute from an initial temperature of  $60^{\circ}\text{C}$  to a final temperature of  $140^{\circ}\text{C}$ . A calibration curve for the gas chromatography was generated by preparing five solutions, each of different concentrations of toluene in carbon disulfide spiked with the internal standard, ethylbenzene.

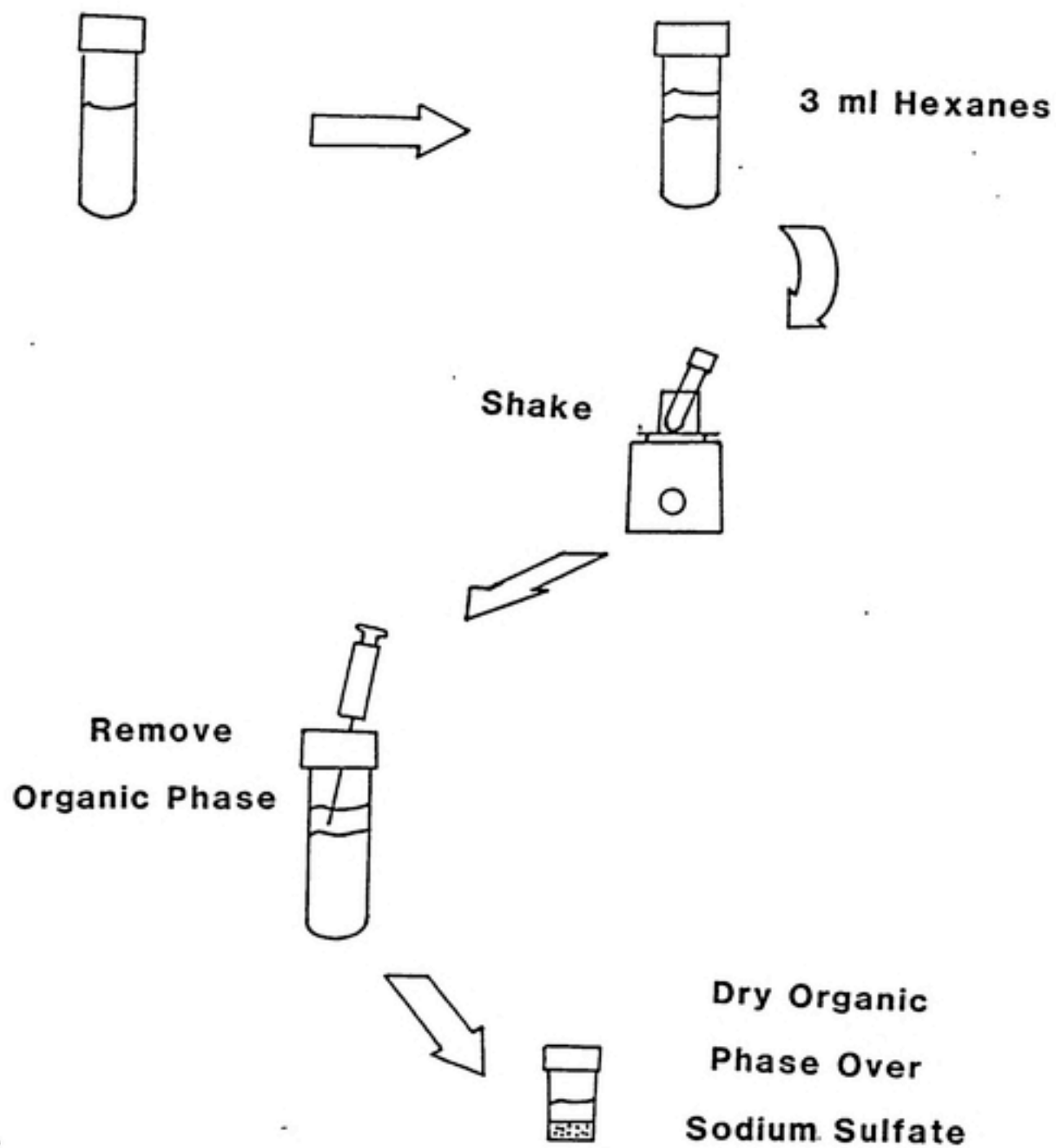


Figure 3-2. Aqueous Extraction Procedure.

### 3.4 Experimental Methods

#### Field Sampling

Vapor-phase sampling at Pope Air Force base was performed with a sampling probe developed by Wallingford et al. (1988). The instrument is shown in Figure 3-3. To take a vapor-phase sample, a 5-cm hole was drilled to a depth of 1.3 m, and then the probe was inserted and pounded another 15 cm into the ground. A diaphragm pump equipped with a Teflon-silica diaphragm was then attached to the top of the probe and soil vapor was pumped at a flow rate of 50 cm<sup>3</sup> per minute for 20 minutes. After passing through the pump, the soil vapor was passed through an activated carbon trap to remove any organic vapors. The carbon trap was then stored on ice until it could be extracted and analyzed back at the laboratory (see sections on extractions and analysis).

#### Bottle-Point Isotherm.

Aqueous-solid isotherms were performed using 24-50 ml centrifuge vials. Samples were run in pairs, and with each pair was a blank that was prepared exactly as the samples but with no soil. Samples consisted of 20 grams of soil and 40 ml of solution. A schematic of the bottle-point sample preparation procedure is shown in Figure 3-4.

Soil was placed in each sample vial and then a solution of calcium chloride and sodium azide was added. This solution was 0.005 molar calcium chloride to help settle the solids during centrifugation, and was 0.045 molar sodium azide to suppress microbiological activity. This solution was added in varying amounts to each sample depending upon the amount of toluene stock solution that would be added to achieve the desired final concentration of toluene.

The stock solution of toluene was prepared in a one-liter bottle. The concentration of this solution was approximately 425 mg/l; the saturation concentration of toluene in water

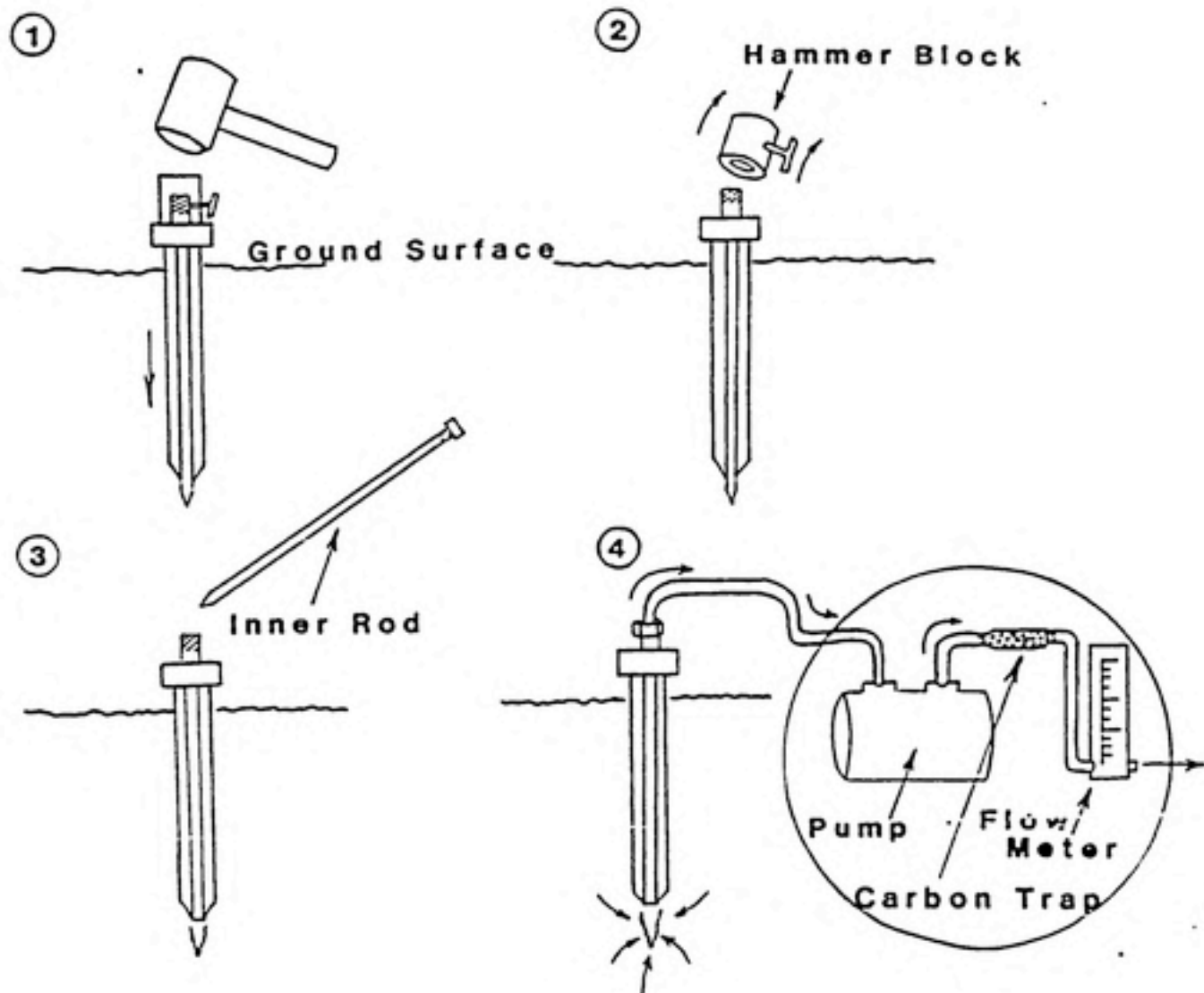


Figure 3-3. Field Sampling Procedure.

water is 515 mg/l. The solution was stirred for 24 hours to allow all the toluene to go into solution before use. Stock solution was withdrawn with a syringe from the septum at the bottom of the bottle and then added to the isotherm vials through the Teflon septa in the vial caps. A second syringe needle was inserted into the vial septa to allow venting of displaced air as the stock was added. This technique is believed to have reduced volatility losses because the solution was never open to the air, but was always contained within either the solution bottle, the syringe, or a sample vial.

During the sample preparation three samples were taken from the stock solution. One sample was taken at the start of the sample preparation; a second was taken after half of the vials were prepared, about 20 minutes later; and the third sample was taken after the last vial was sealed. These three samples were used to detect any change in the concentration of the stock solution during the sample preparation procedure.

At the end of the equilibration period, the samples were placed in a centrifuge for 30 minutes to settle the solids. Ten ml of the supernatant were then removed with a syringe and then extracted with hexanes as described in the extraction section.

#### Bottle-Point Rate Study

The method for bottle point rate studies is very similar to that used in the isotherm experiments. The bottle point samples, however, all start with the same aqueous concentration and each is analyzed at a different time on the rate curve as the system approaches equilibrium.

As with the isotherm experiments, 20 grams of soil sample was weighed into each of 16 50-ml centrifuge vials. Next a solution of toluene in distilled water was added to each of these samples, and also sodium azide to 0.25% and calcium chloride to 0.005 Molar. The initial concentration for each sample was the same: approximately 20 mg/l. Samples were then shaken and one was analyzed every two hours for the first 12 hours and then every 6 hours until the system reached an apparent equilibrium state, which occurred after

is 515 mg/l at 20°C. The solution was stirred for 24 hours to allow all the toluene to go into solution before use. Stock solution was withdrawn with a syringe from the septum at the bottom of the bottle and then added to the isotherm vials through the Teflon septa in the vial caps. A second syringe needle was inserted into the vial septa to allow venting of displaced air as the stock was added. This technique is believed to have reduced volatility losses because the solution was never open to the air, but was always contained within either the solution bottle, the syringe, or a sample vial.

During the sample preparation three samples were taken from the stock solution. One sample was taken at the start of the sample preparation; a second was taken after half of the vials were prepared, about 20 minutes later; and the third sample was taken after the last vial was sealed. These three samples were used to detect any change in the concentration of the stock solution during the sample preparation procedure.

At the end of the equilibration period, the samples were placed in a centrifuge for 30 minutes to settle the solids. Ten ml of the supernatant were then removed with a syringe and then extracted with hexanes as described in the extraction section.

#### Bottle-Point Rate Study

The method for bottle point rate studies is very similar to that used in the isotherm experiments. The bottle-point samples, however, all start with the same aqueous concentration and each is analyzed at a different time on the rate curve as the system approaches equilibrium.

As with the isotherm experiments, 20 grams of soil sample was weighed into each of 16 50-ml centrifuge vials. Next a solution of toluene in distilled water was added to each of these samples, and also sodium azide to 0.045 molar and calcium chloride to 0.005 molar. The initial concentration for each sample was the same: approximately 20 mg/l. Samples were then shaken and one was analyzed every two hours for the first 12 hours and then every 6 hours until the system reached an apparent equilibrium state, which occurred after

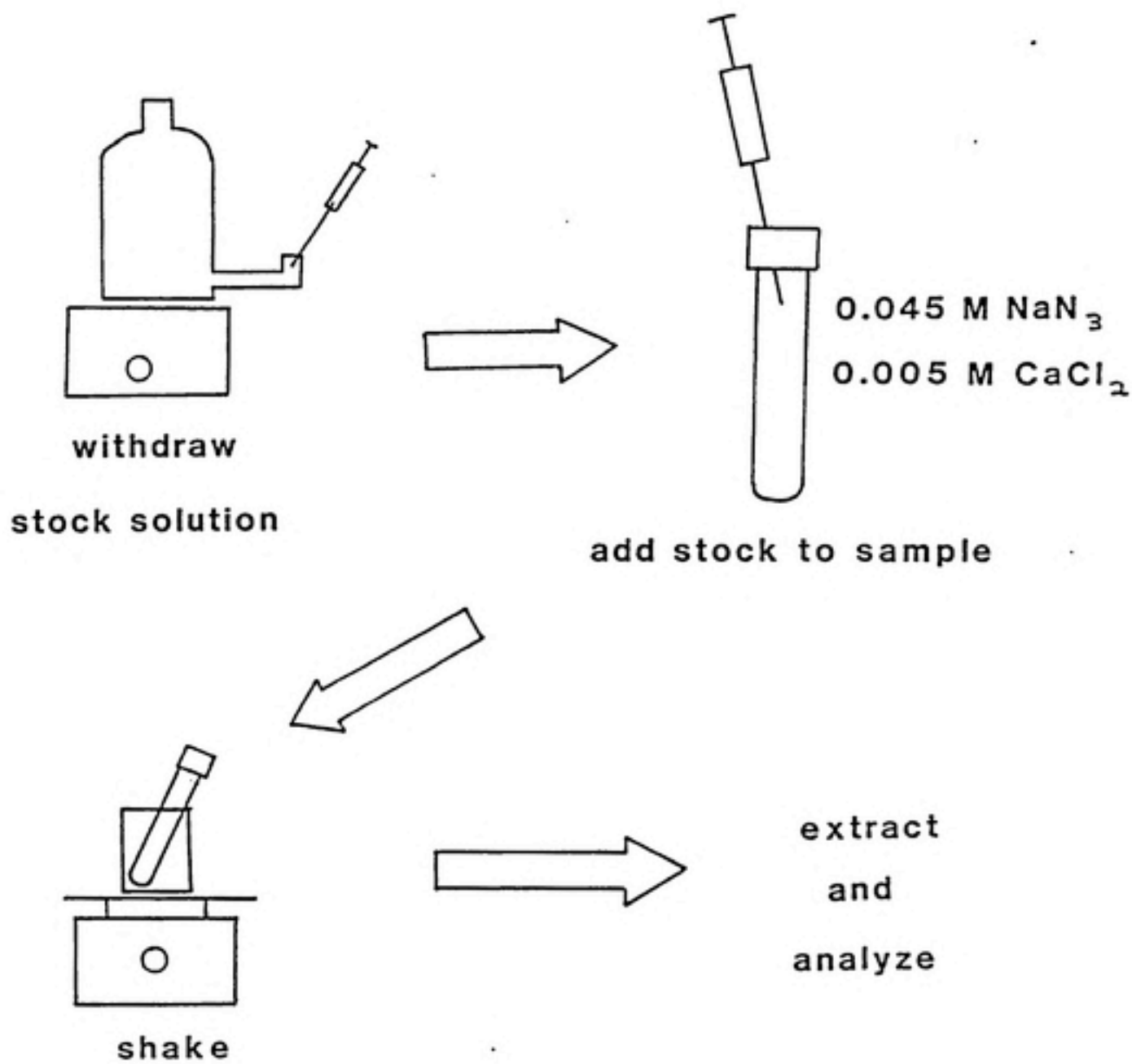


Figure 3-4. Procedure for Bottle-Point Studies.

approximately 24 hours.

Samples were analyzed exactly as they were for the isotherm studies. After centrifugation, 10 ml of supernatant were drawn off with a syringe and then extracted with hexanes.

## Diffusion Column Experiments

### *Description of Apparatus*

The diffusion experimental design is shown in Figure 3-5. The apparatus consists of four glass columns exposed at one end to a chamber which is maintained at a constant concentration of toluene in nitrogen. The other end of the soil columns are exposed to activated carbon to effectively maintain the concentration of toluene at that end of the column at zero.

The chamber is a two-liter glass reaction vessel with four ground-glass ports in a removable lid. The lid is secured to the vessel with clamps that are easily removed, and it is sealed with ground glass. One of the four ports is sealed with a Teflon plug, which has 0.318 cm borosilicate glass tubing inserted and extending well into the chamber. This tubing is for purging the vessel with nitrogen before beginning an experiment. The other three ports are fitted with ground-glass connectors that hold the soil columns. Thus the entire soil column and connector assembly is attached by means of a ground glass fitting.

The glass column is a 0.85-cm diameter glass tube 6 cm in length. The end of the tube which is exposed to the toluene chamber is fitted with a fritted glass plug; the other end is fitted with a ball-valve assembly that is used for inserting and removing activated carbon samples. The carbon is placed in small glass sample vials that are covered with stainless steel screens, which are held in place by Teflon caps. These sample vials are placed into the ball-valve assembly and then rotated into place. In this way the samples may be inserted and removed without ever actually opening the end of the column.

Glass Tubes  
for Purging

Ball-Valve  
Sampling Ports

Soil Column

Toluene

Stir Ring

Magnetic Stirrer

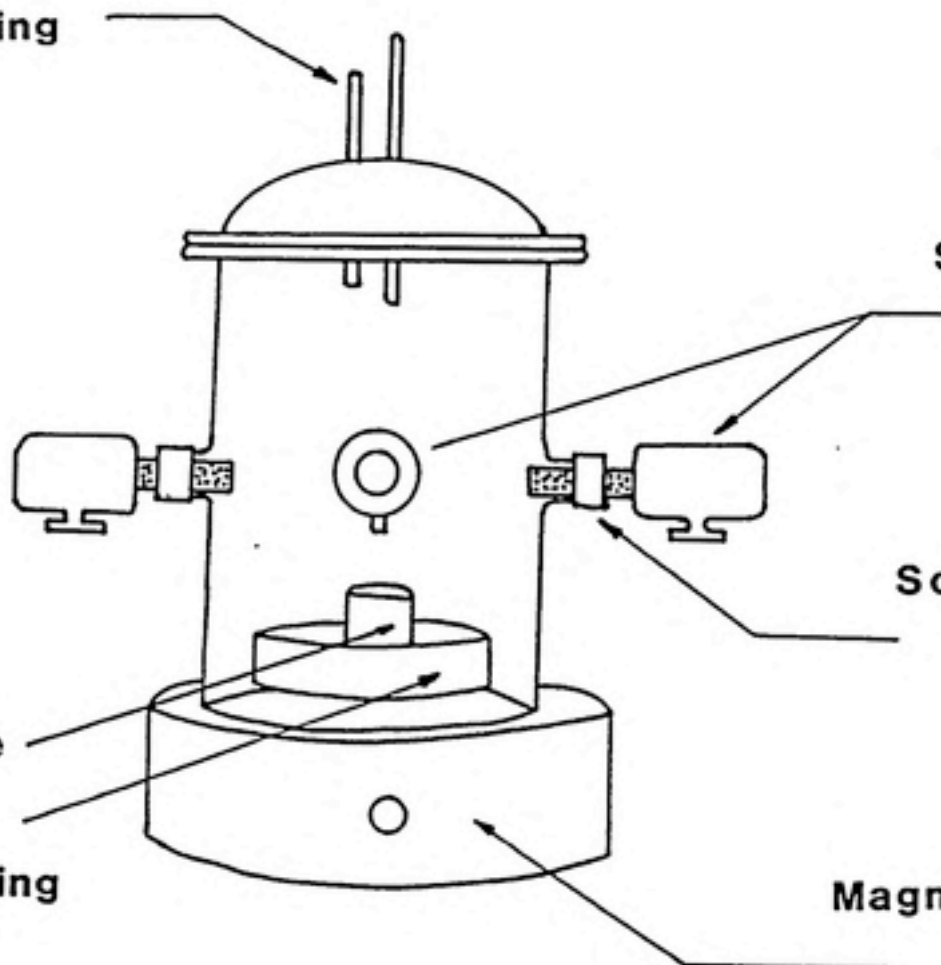


Figure 3-5. Diffusion Apparatus.

### *Column Preparation*

Both soil and glass beads to be used in the columns were first saturated with de-ionized water and then slurried into the glass columns. After weighing, the columns were partially dried by draining and/or blowing nitrogen through them at a very low flow rate and then they were weighed again. After the experiment was finished the columns were dried thoroughly and then weighed again. From the three weights the porosity and the water-filled porosity could be determined.

### *Sampling Procedure*

Samples were taken using 0.5 grams of activated carbon in the sample vial. This vial was inserted into the ball valve assembly, rotated into place and left for one hour. At the end of the hour the ball valve was rotated back, the sample vial removed and a new vial with a fresh sample of carbon was inserted and then rotated into place. Due to the long times required for the columns to reach equilibrium, samples were only taken every 24-36 hours. During the 24-36 hour period between samples 1.5-2 grams of carbon were left inserted in the ball valve to be sure to adsorb all the toluene that diffused through the end of the column during that time. These larger slugs of carbon were first saturated with water before being inserted into the apparatus. This was done to prevent a water vapor gradient occurring across the soil column between a saturated vapor chamber and a dry slug of activated carbon.

Once an activated carbon sample had been exposed to a column for 1 hour it was extracted with carbon disulfide as described in the extraction section.

### *Modeling Methods*

A fully implicit, one dimensional, finite difference model was written to simulate the diffusion in the experimental columns. The model assumes linear local-equilibrium and

utilizes Dirichlet boundary conditions at both ends of the column. The governing equation for the model is:

$$\theta_D \frac{\partial C_v}{\partial t} = \theta_D D_e \frac{\partial C_v}{\partial x} - (\theta_T - \theta_D) K_H \frac{\partial C_v}{\partial t} - \rho_s (1 - \theta_T) K_H K_p \frac{\partial C_v}{\partial t} \quad (3-1)$$

Combining terms gives:

$$\left[ 1 + \frac{(1 - \theta_T) \rho_s K_H K_p}{\theta_D} + \frac{(\theta_T - \theta_D) K_H}{\theta_D} \right] \frac{\partial C_v}{\partial t} = D_e \frac{\partial C_v}{\partial x} \quad (3-2)$$

We can now define a retardation factor,  $R_f$ :

$$R_f = 1 + \frac{(1 - \theta_T) \rho_s K_H K_p}{\theta_D} + \frac{(\theta_T - \theta_D) K_H}{\theta_D} \quad (3-3)$$

and the equation becomes:

$$R_f \frac{\partial C_v}{\partial t} = D_e \frac{\partial C_v}{\partial x} \quad (3-4)$$

Discretizing this equation, and dropping the vapor subscript gives:

$$R_f \frac{C_i^{l+1} - C_i^l}{\Delta t} = D_e \frac{C_{i+1}^{l+1} - 2C_i^{l+1} + C_{i-1}^{l+1}}{\Delta x^2} \quad (3-5)$$

where  $l$  represents the time step, and  $i$  represents the node number. Finally the equation can be rearranged to a form which can be easily programmed in FORTRAN:

$$C_i^{l+1} = \left[ \frac{D_e \Delta t}{\Delta x^2 R_f + 2D_e \Delta t} \right] (C_{i+1}^{l+1} + C_{i-1}^{l+1}) + \left[ \frac{\Delta x^2 R_f}{\Delta x^2 R_f + 2D_e \Delta t} \right] C_i^l \quad (3-6)$$

---

## 4 EXPERIMENTAL RESULTS

---

### 4.1 Field Results

Pope Air Force Base in Fayetteville, North Carolina, was the location chosen for field sampling of organic contaminants in the subsurface. Figure 4-1 is a topographic map of Fire Training Area No. 4, where large amounts of waste jet fuel have been used for decades to fuel training fires. The fires are set within a burn pit, and all fuel that does not burn filters into the soil where it encounters the water table three to six feet below the surface, depending on the location and the season. Figure 4-2 shows the groundwater gradient for the fire training area based on measurements from six groundwater monitoring wells that were installed at the site. From this figure one can see that the groundwater is flowing in a generally westward direction, away from Aldish Road.

Ten soil gas samples were taken at the fire training area to determine the extent of contamination in the partially-saturated zone. The samples contained dozens of compounds found in jet fuel: both light-weight and heavy-weight hydrocarbons. Gas chromatograms of the samples were normalized to the sample with the highest concentration of total organics; this sample was the one taken just down-gradient from and closest to the burn pit. Figure 4-3 is another map of the training area with isopleths of normalized concentrations of hydrocarbons in the partially-saturated zone. Concentrations were normalized to the sample with the highest concentration of total hydrocarbons.

The highest concentrations of hydrocarbons occurred close to and down-gradient from the burn pit, as would be expected. Significant concentrations of contaminants were found up-gradient, however.

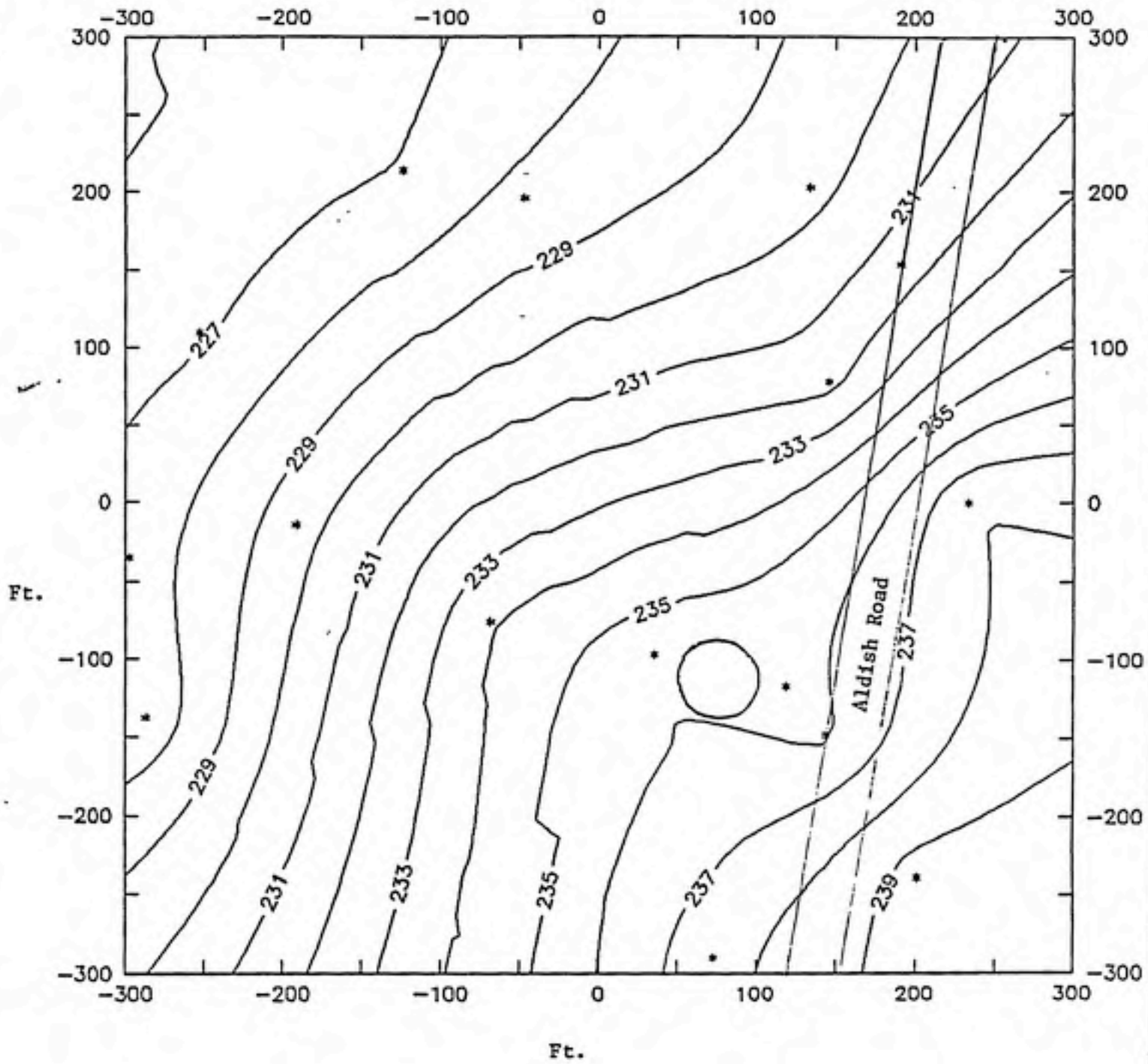


Figure 4-1. Topographic Map of Fire Training Area No. 4.

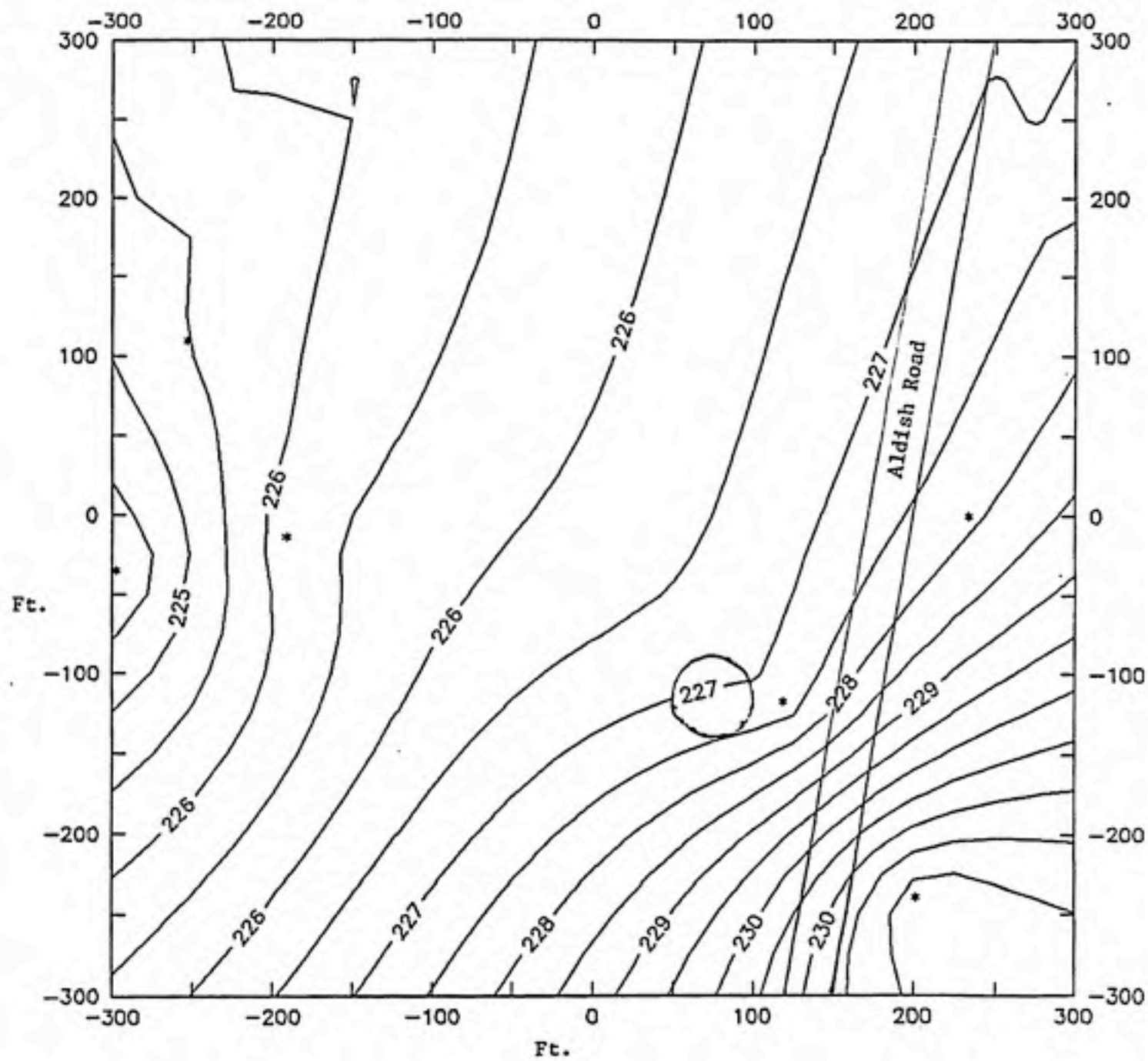


Figure 4-2. Groundwater Elevations at Fire Training Area No. 4.

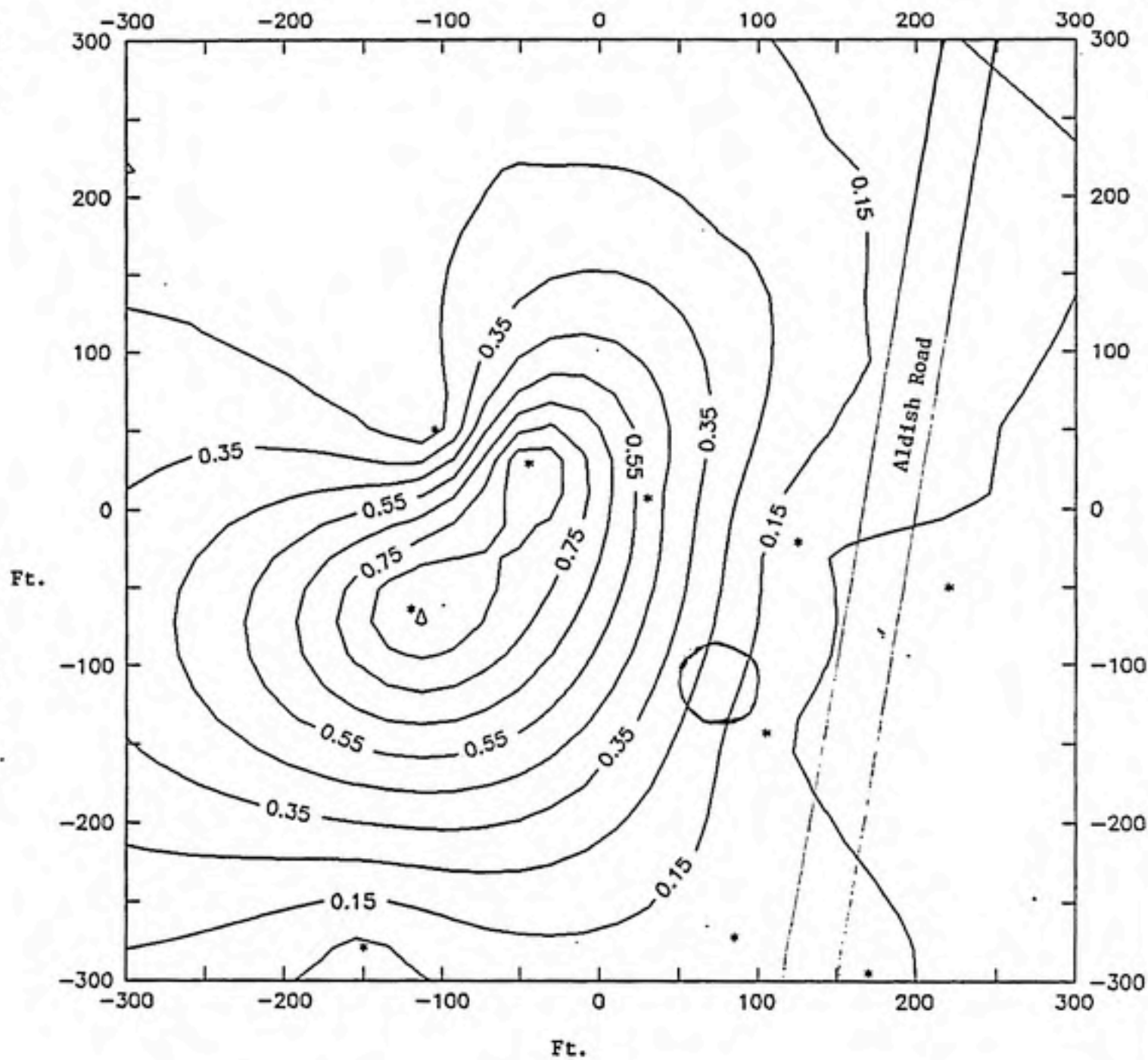


Figure 4-3. Normalized Concentrations of Hydrocarbons in the Partially-Saturated Zone.

## 4.2 Sorption Study Results

### Equilibrium Study

The results from the bottle-point equilibrium study are presented in Figure 4-4. The data was fit to both linear and Freundlich models using a computer program written by Joseph Pedit. The linear and Freundlich models are graphed with the experimental data in Figure 4-5. The linear model gives a partition coefficient,  $K_p$ , of  $0.37 \text{ cm}^3/\text{g}$ . The correlation coefficient,  $R^2$ , for this fit is 0.378. The Freundlich model, however, produces a much closer fit with a correlation coefficient of 0.871. The Freundlich sorption capacity constant,  $K_F$ , is  $0.0077 (\text{cm}^3/\text{g})^n$ , and the sorption intensity constant,  $n_F$ , is 0.685. This data is summarized in Table 4-1.

### Rate Study

The results from the bottle point rate study are presented in Figure 4-6. This graph is a plot of time versus the aqueous concentration of toluene. The samples reached an apparent equilibrium in approximately 24 hours, at a final aqueous concentration of 15 mg/l. The initial aqueous concentration of the samples was 19 mg/l, and Figure 4-7 is a plot of time versus the fraction of initial toluene remaining in the aqueous phase. From this plot one can see that at equilibrium, 20% of the toluene had sorbed onto the solid phase. The equilibrium concentrations in the aqueous and solid phases were used to calculate a linear sorption coefficient,  $K_p$ , equal to  $0.53 \text{ cm}^3/\text{g}$ .

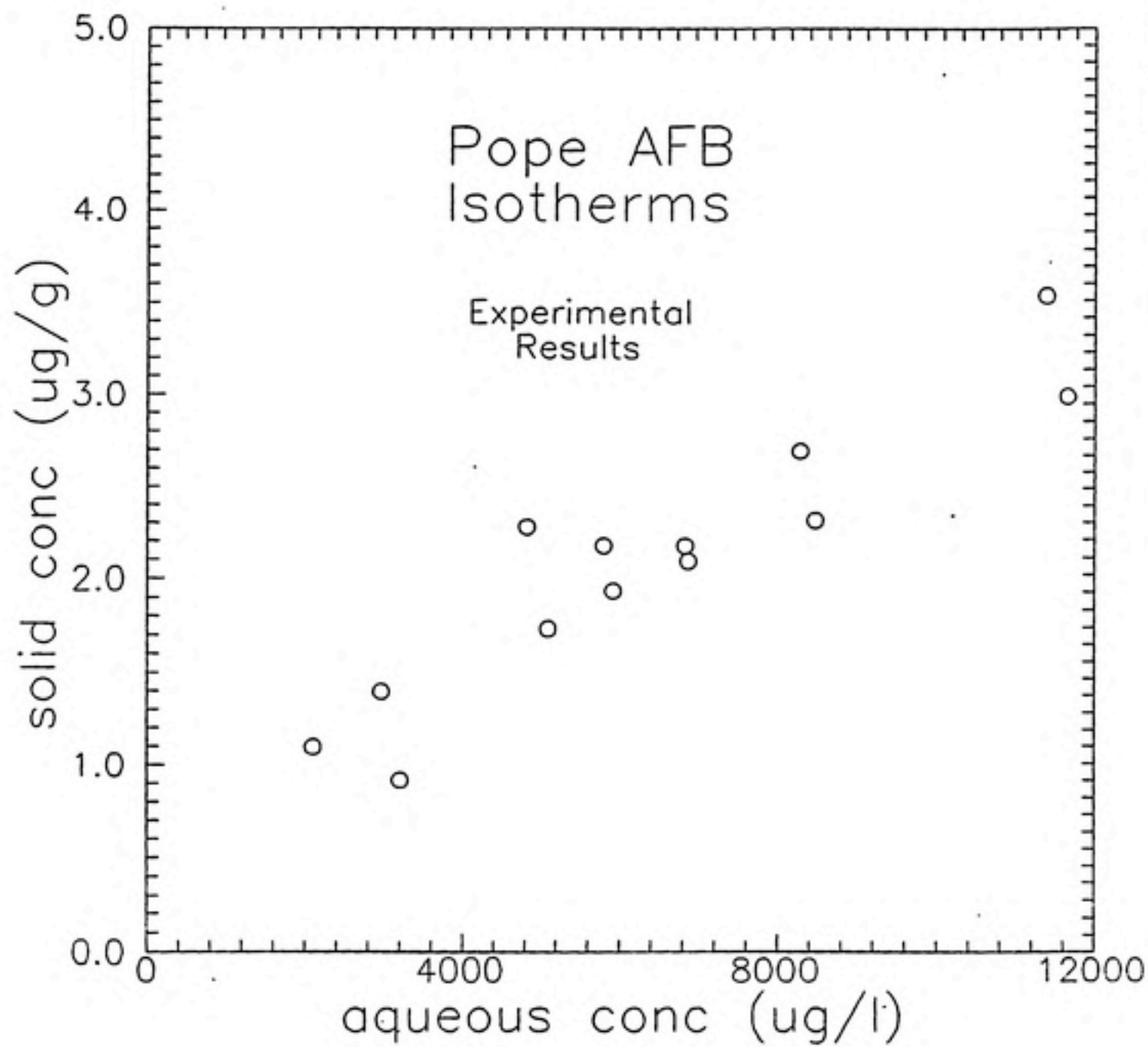


Figure 4-4. Results of Bottle Point Equilibrium Study.

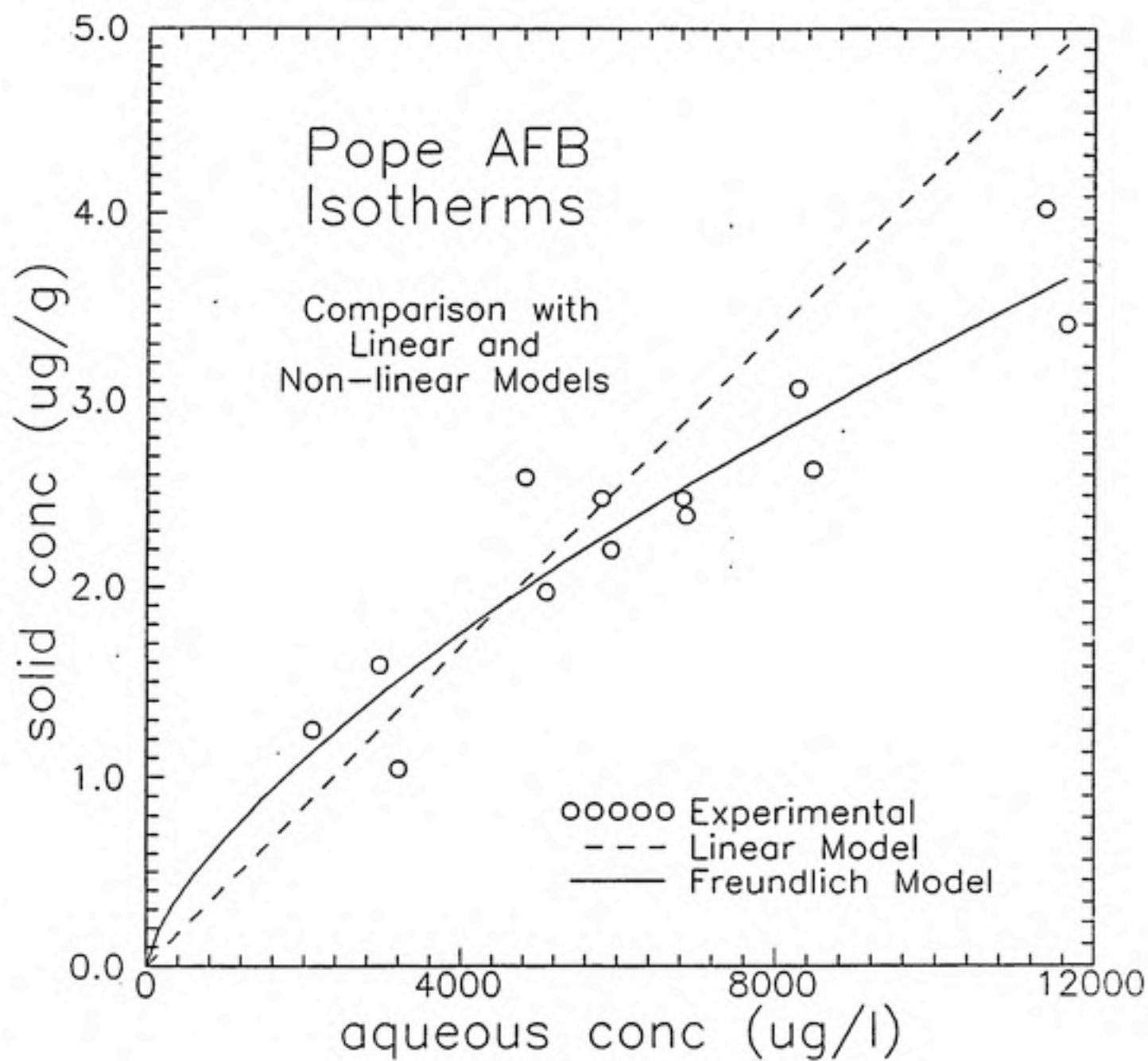


Figure 4-5. Freundlich and Linear Isotherm Models.

Table 4-1 Summary of Experimental  
Equilibrium Parameters.

Isotherm

---

$$K_p = 0.37 \text{ cm}^3/\text{g} \quad (R^2 = 0.378)$$

$$K_F = 0.77 \text{ cm}^3/\text{g} \quad (R^2 = 0.871)$$

$$n = 0.69$$

Rate Study

---

$$K_p = 0.53 \text{ cm}^3/\text{g}$$

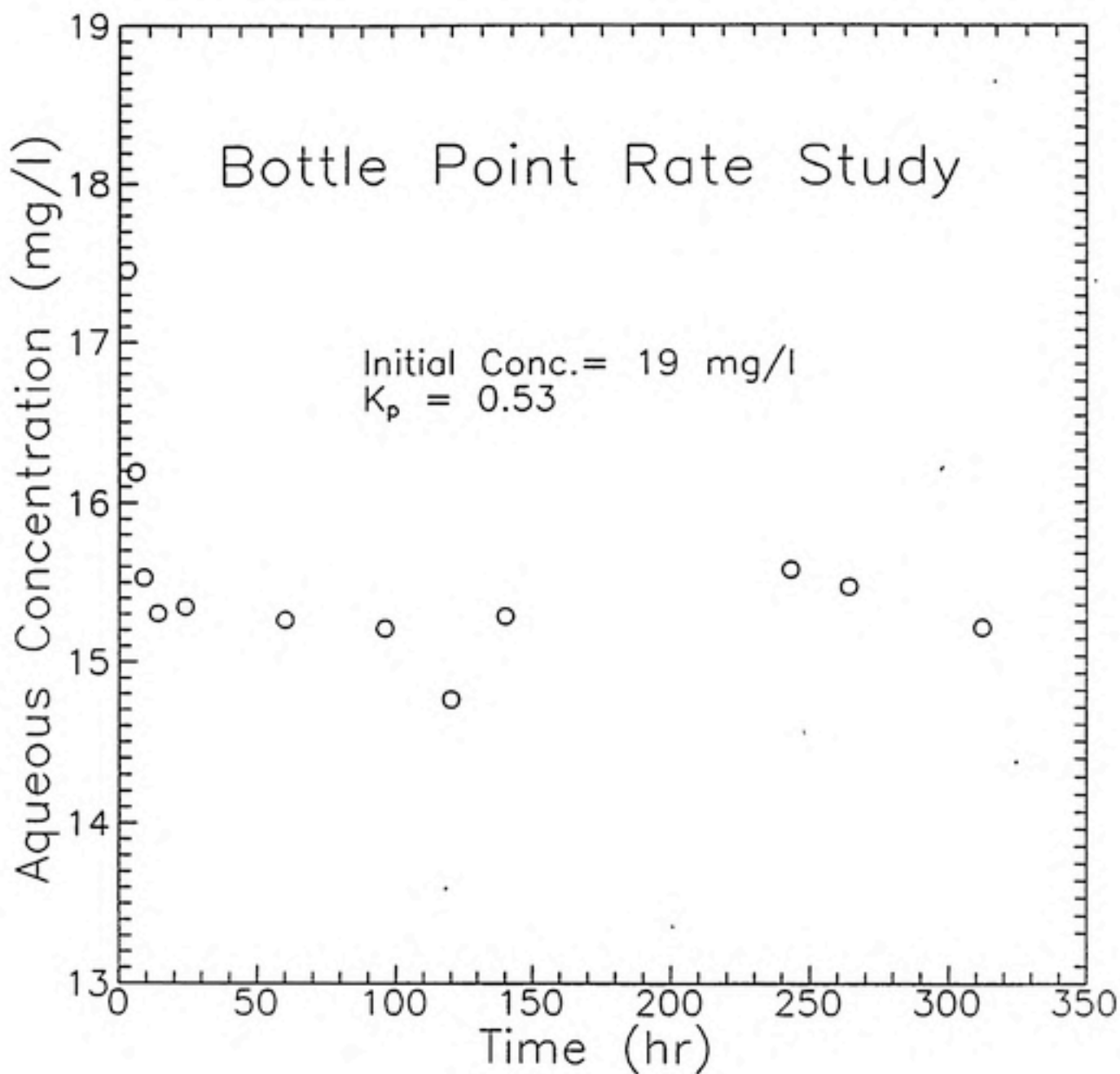


Figure 4-6. Rate Study Results: Time vs. Concentration.

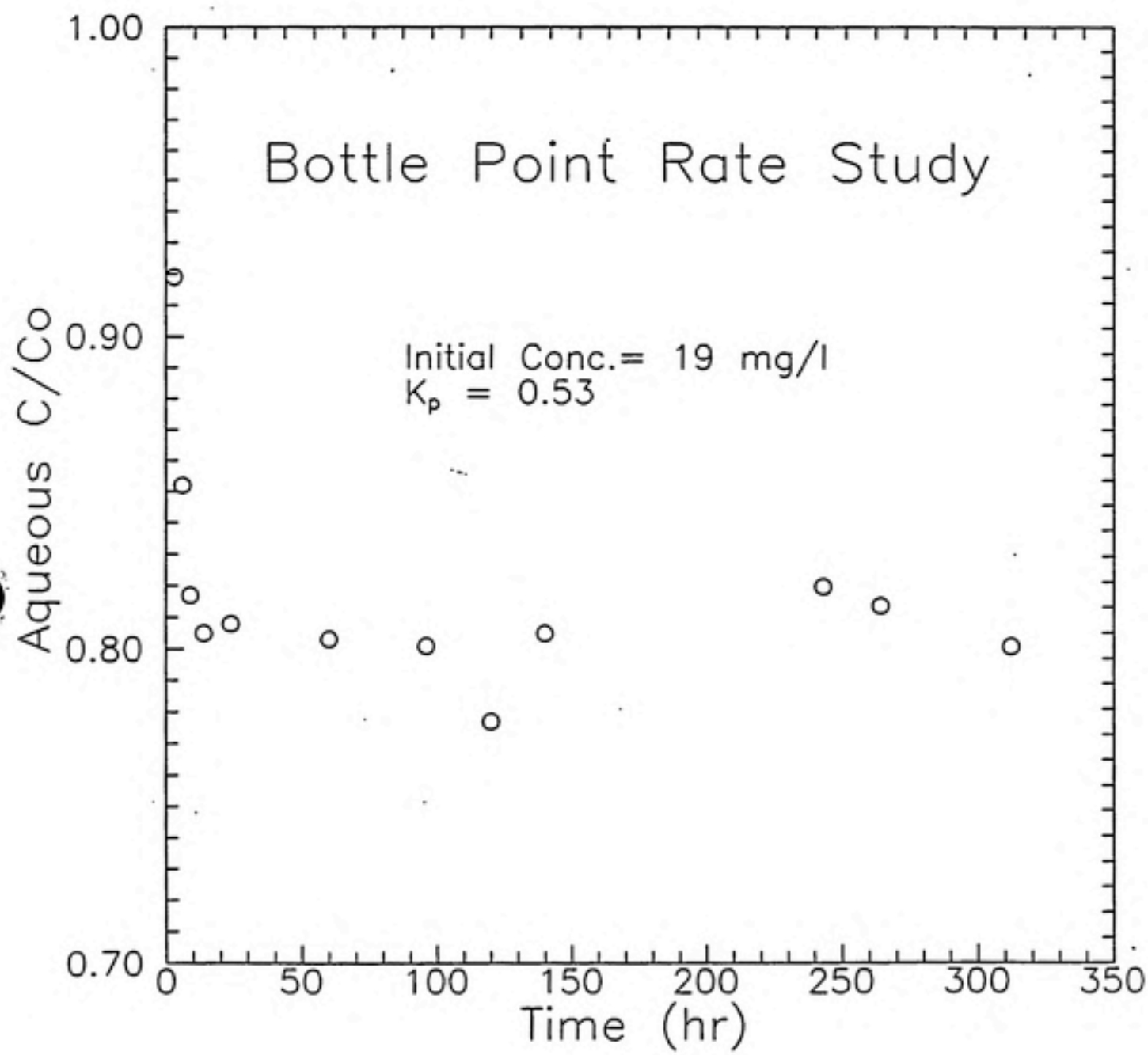


Figure 4-7. Rate Study Results: Time vs.  $C/C_o$ .

### 4.3 Diffusion Column Results

Several runs were made with the diffusion column apparatus. The results of these column experiments are presented in Figures 4-8 through 4-13.

For each column the total porosity,  $\theta_T$ , and the gas-filled, or drained porosity,  $\theta_D$ , were calculated gravimetrically. A summary of these properties are presented in Table 4-2. Also in this table are the effective diffusivities calculated for each column at steady state, and tortuosity factors. Tortuosity factors were calculated from the steady state diffusivity and the diffusivity of toluene in pure nitrogen:

$$D_e = \tau D^* \quad (4-1)$$

All columns were run at constant moisture content except column 1-A. This column gradually dried out completely until  $\theta_D$  equaled  $\theta_T$ . The steady-state data is included in Table 4-2, but a graph of the transient behavior is not presented because the transient diffusion in this column was complicated by the drying process.

### 4.4 Modeling Results

The diffusion columns were modeled using the one-dimensional finite difference model described in the methods section. The porosity, drained porosity and effective diffusivity from each experimental column run were used as parameters for each successive model run. The model is capable of simulating linear partitioning of toluene between the aqueous and vapor phases, and also linear sorption from the aqueous to the solid phase. The model was therefore run with the linear sorption constant,  $K_p$ , that was determined from the bottle-point experiments, but could not be run with the experimental Freundlich parameters,  $K_F$ , and  $n_F$ .

Figure 4-14 is a sample model run plotted with its corresponding experimental column

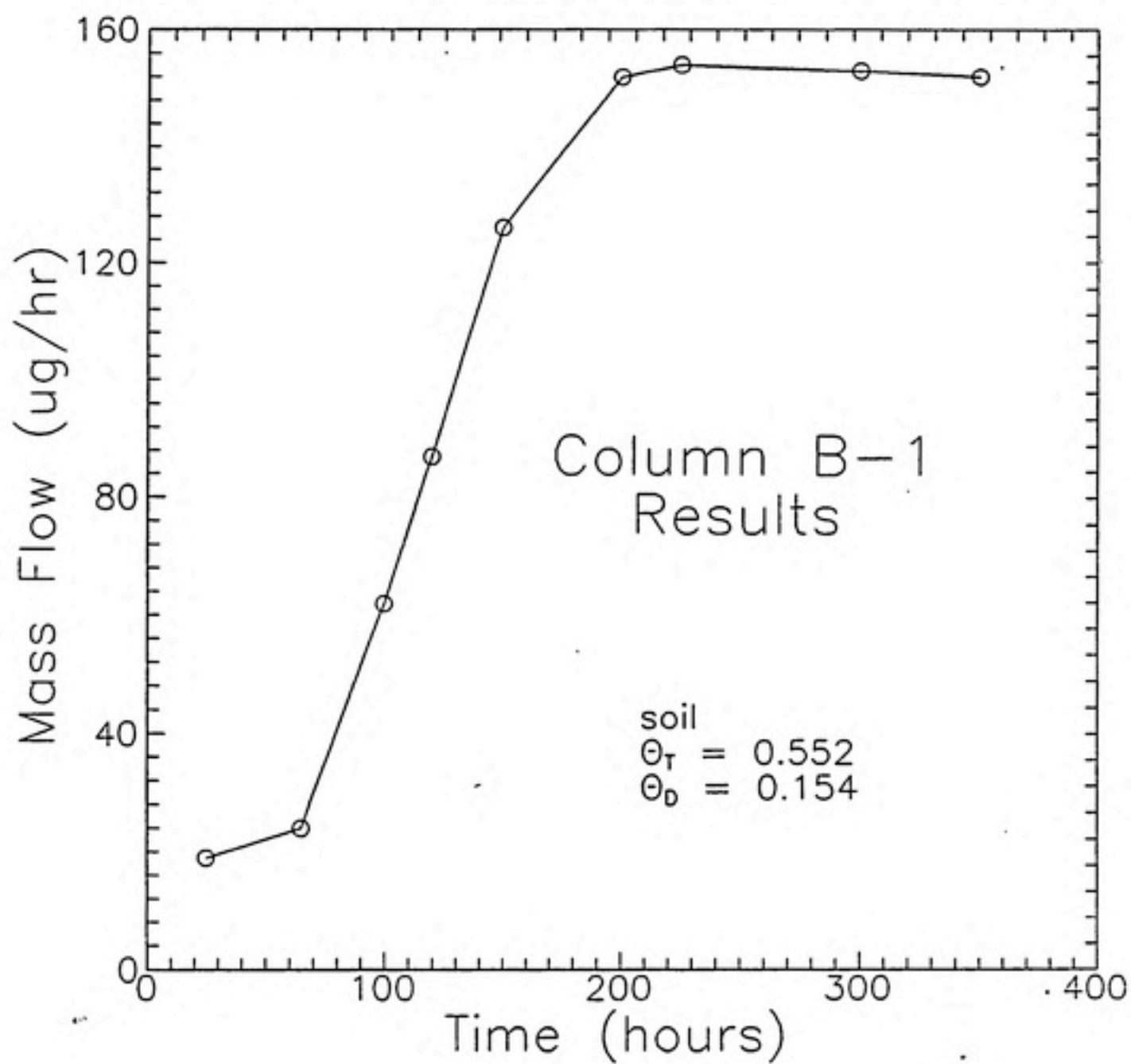


Figure 4-8. Results of Column B-1.

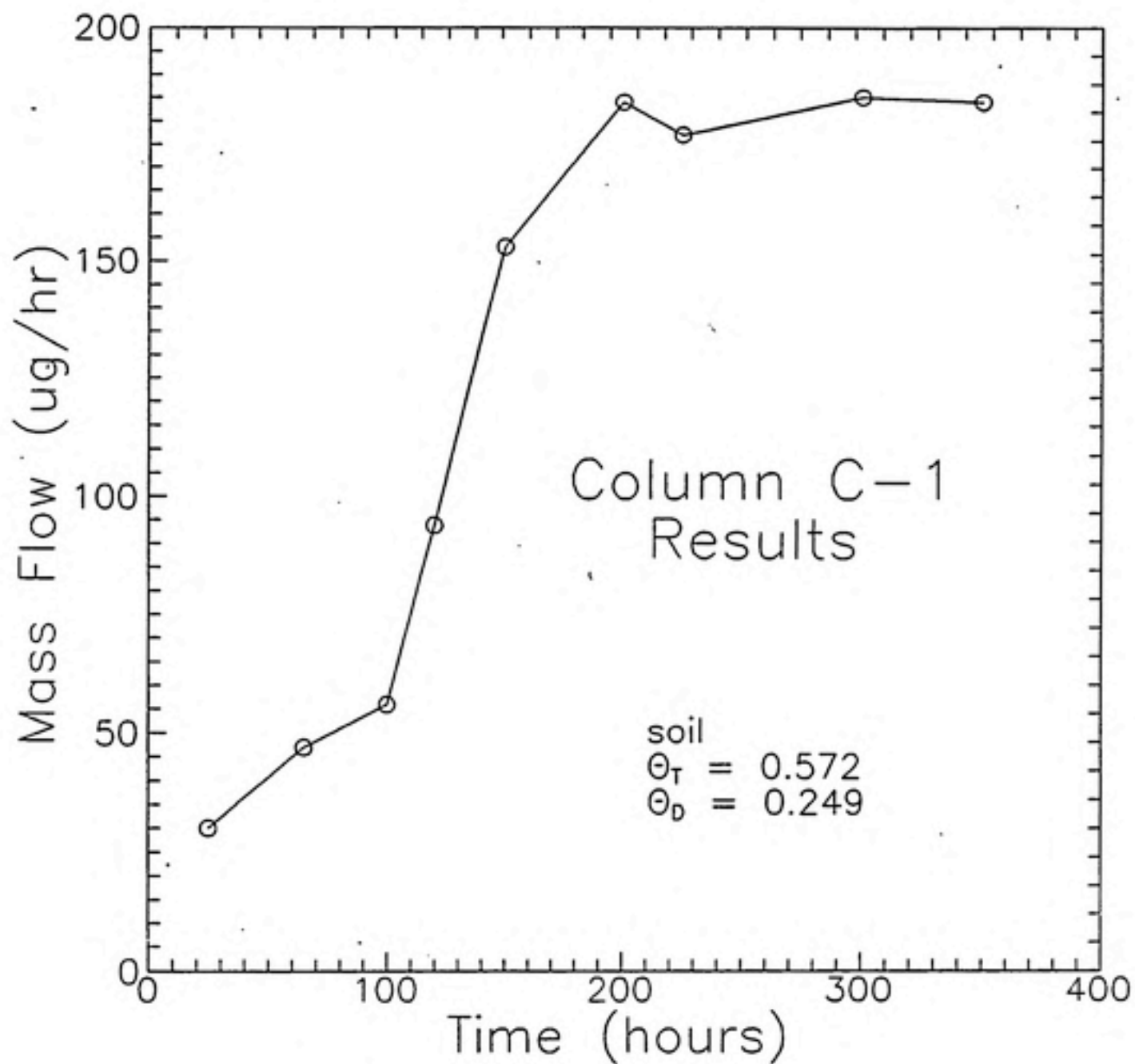


Figure 4-9. Results of Column C-1.

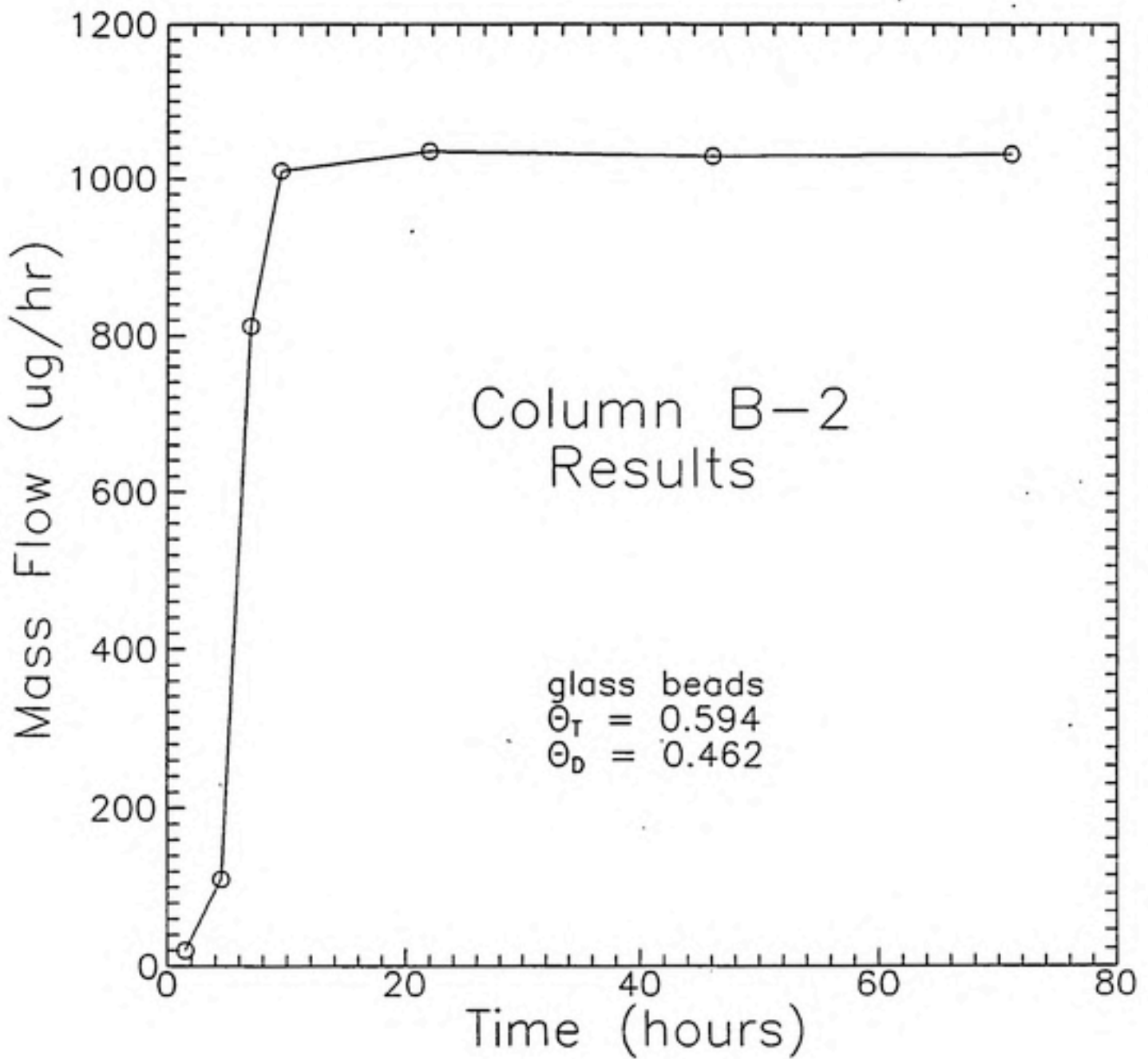


Figure 4-10. Results of Column B-2.

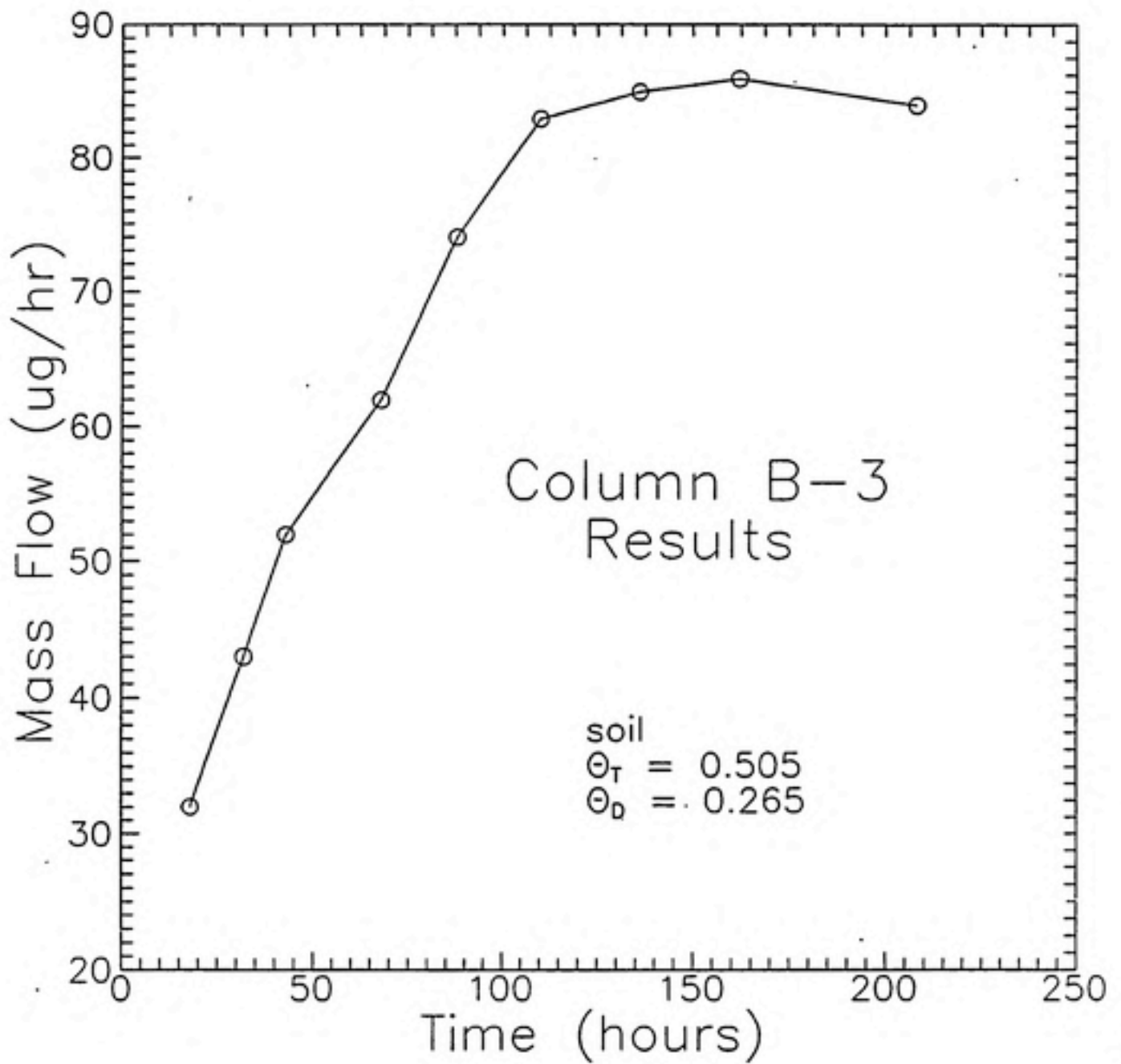


Figure 4-11. Results of Column B-3.

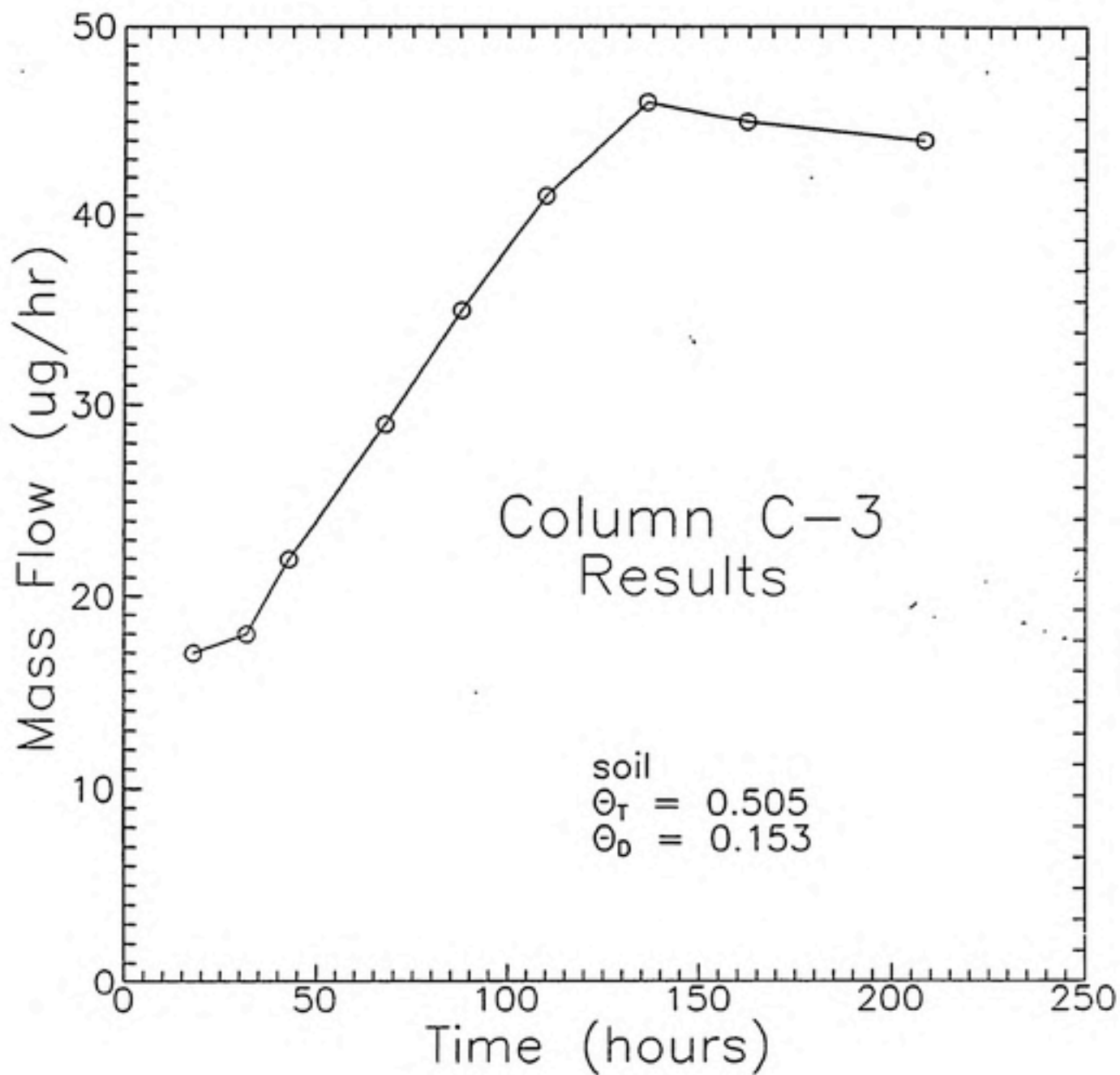


Figure 4-12. Results of Column C-3.

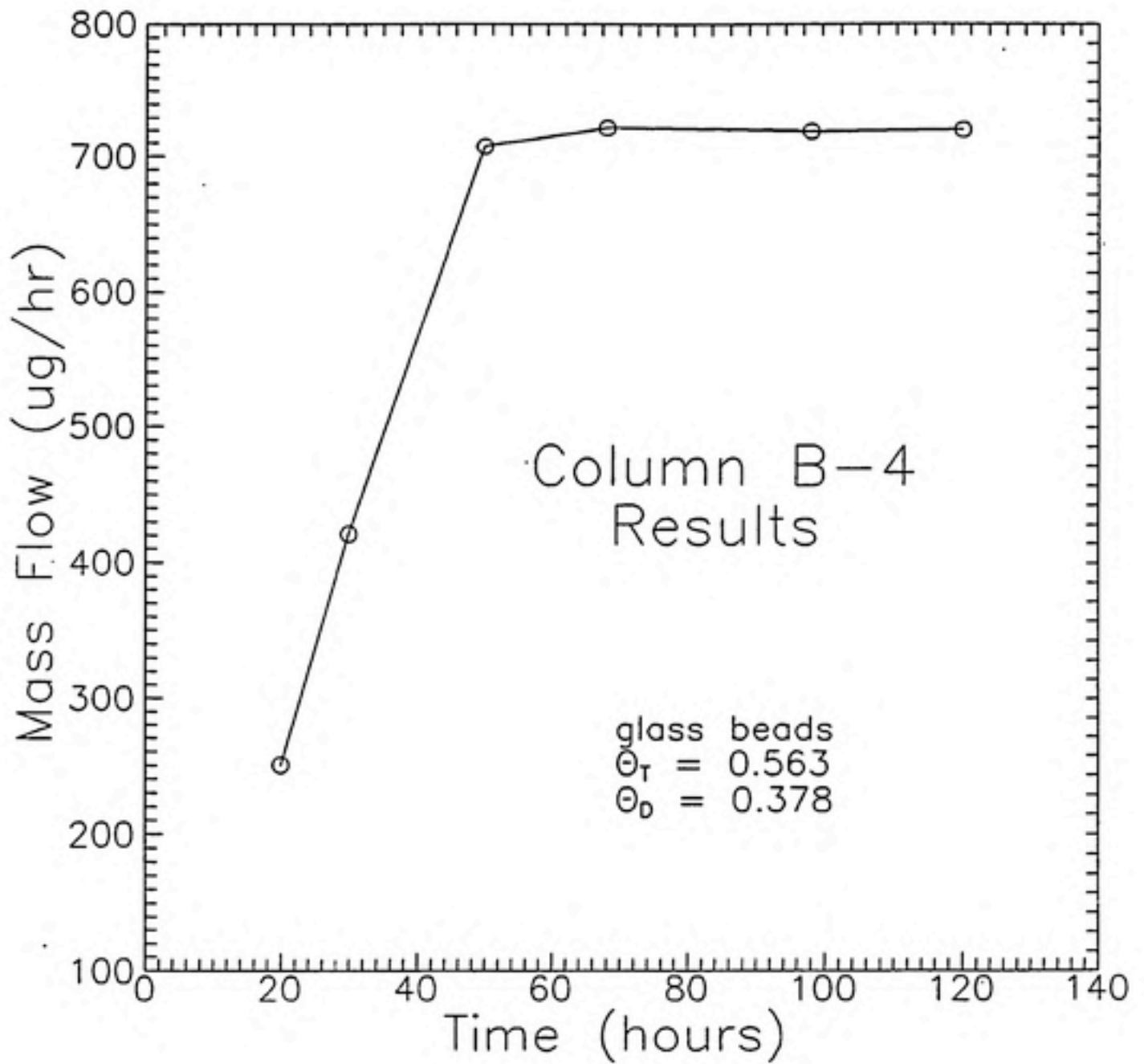


Figure 4-13. Results of Column B-4.

Table 4-2 Summary of Diffusion Column Data.

Column	Media	Column Length (cm)	Steady State Mass Flow ( $\mu\text{g/hr}$ )	$D_e$ ( $\text{cm}^2/\text{hr}$ )	$\Theta_r$	$\Theta_D$	$\tau$
A-1	soil	15	700	233.8	0.550	0.550	0.835
B-1	soil	6	155	74.0	0.552	0.154	0.264
C-1	soil	6	180	53.0	0.572	0.249	0.190
B-3	soil	6	84	23.4	0.505	0.265	0.083
C-3	soil	6	45	21.6	0.505	0.153	0.077
B-2	glass beads	6	1030	163.9	0.594	0.462	0.585
B-4	glass beads	6	721	140.2	0.563	0.378	0.501

$D^* = 280 \text{ cm}^2/\text{hr}$

data. Aqueous- and solid-phase partitioning were not included in this sample run; the results from the model predict the transient diffusion through the soil column assuming that there was no loss of toluene from the vapor phase to either the aqueous or solid phases. The difference in the shape of the two curves, experimental and predicted, suggest that there is some loss of mass from the vapor phase during the transient period.

The experimentally determined linear sorption constant was included in the model and run for each column also. Figure 4-15 is a sample graph of the results of one of these runs. It was found that the model utilizing the experimentally determined linear sorption constant did not describe the transient column behavior well for most of the column runs. A linear sorption constant that best fit the experimental data was determined for each column using the model, and then a simulation was run using that constant. A sample of one of these simulations is presented in Figure 4-16.

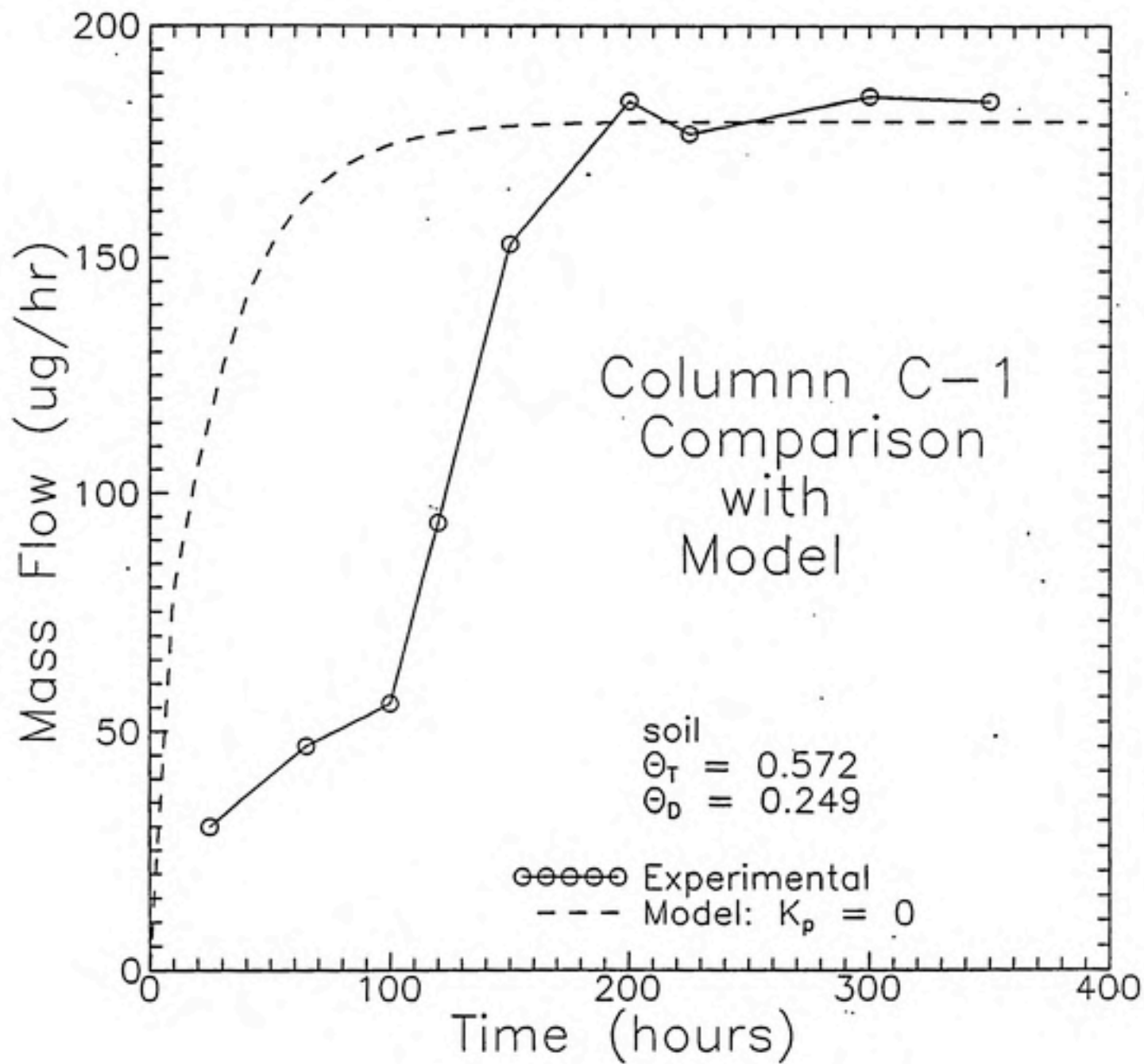


Figure 4-14. Comparison of Model:  $K_p = 0$ .

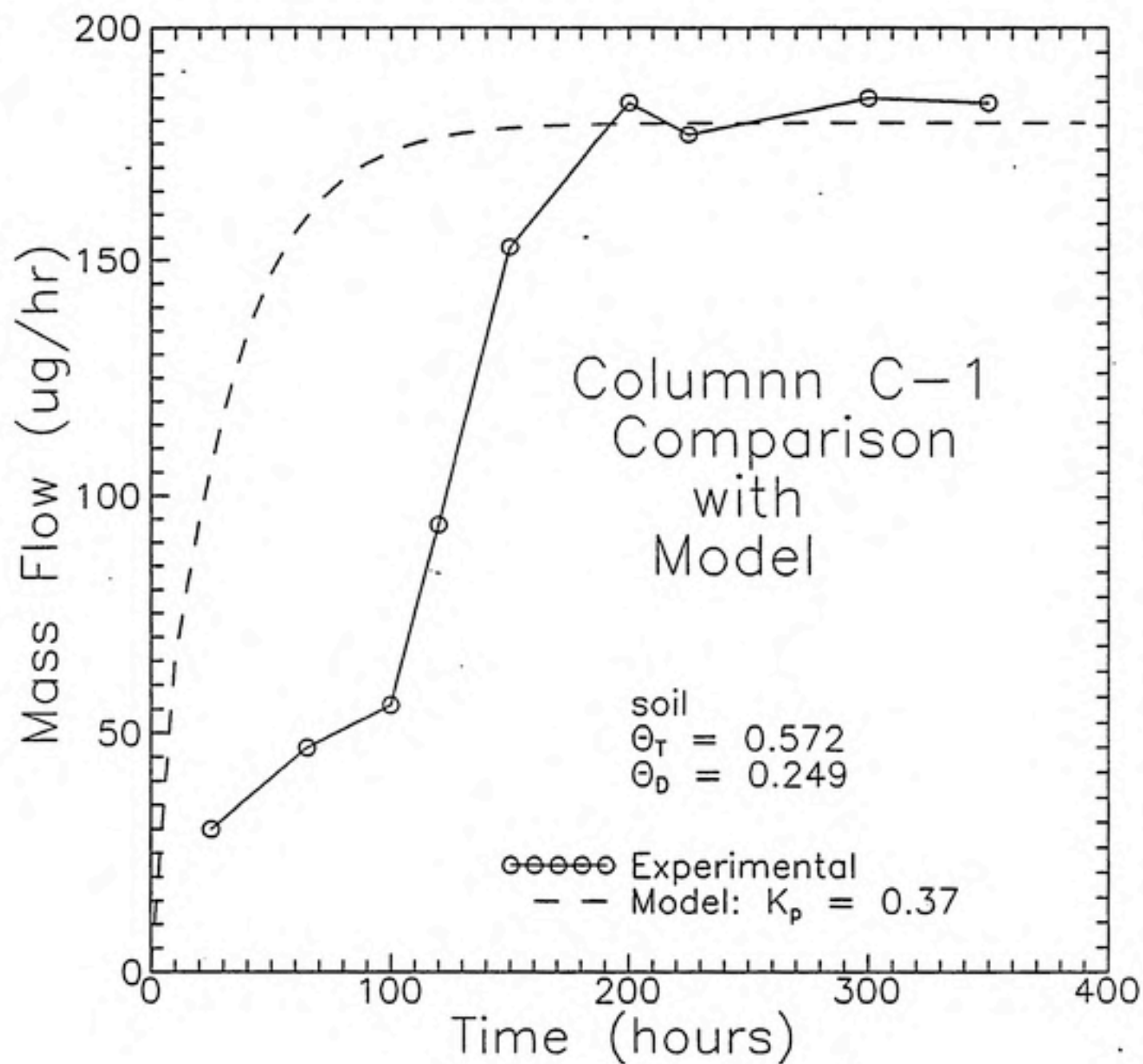


Figure 4-15. Comparison of Model:  $K_p = 0.37$ .

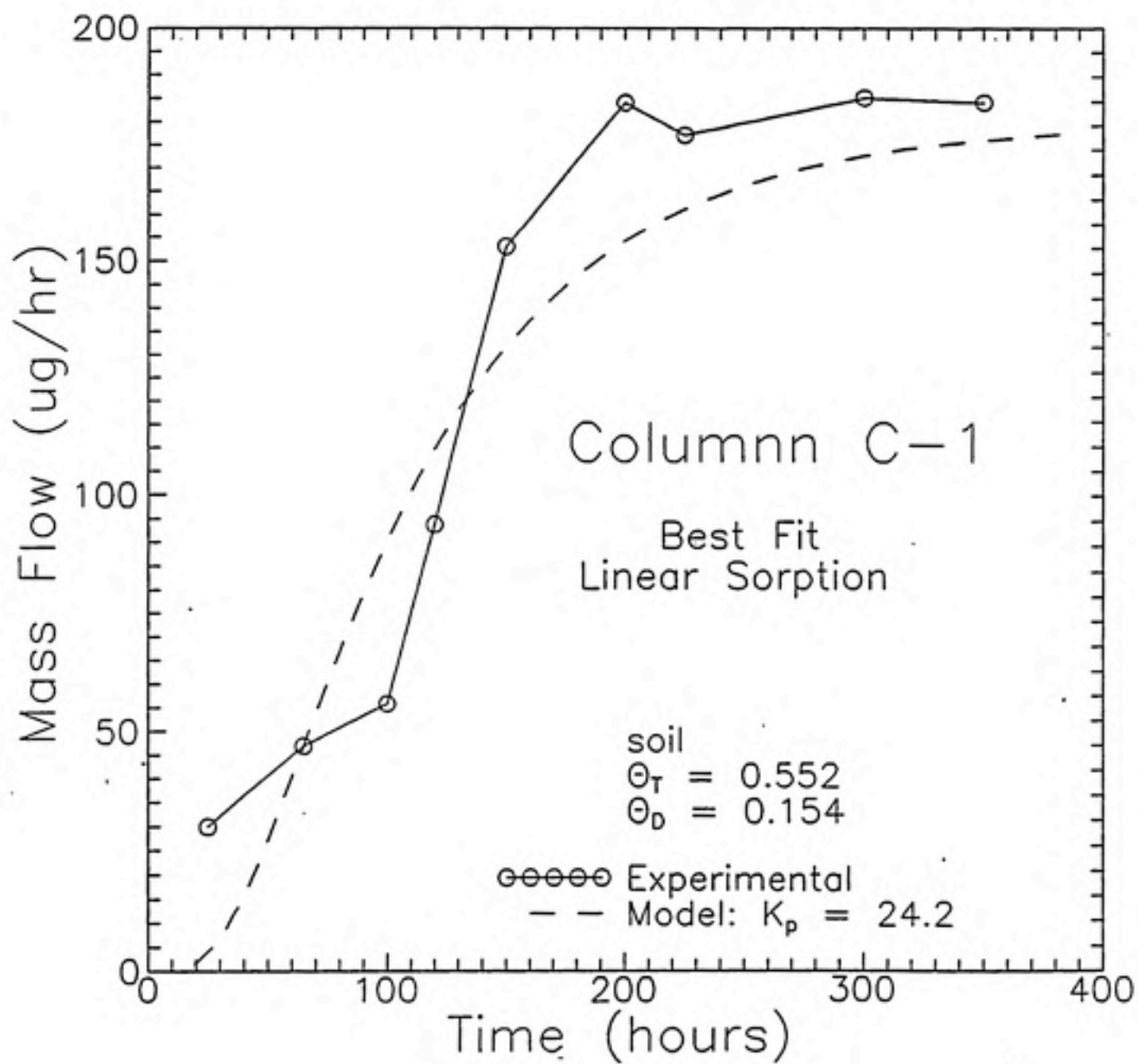


Figure 4-16. Comparison of Model:  $K_p$  = Best Fit.

---

## 5 DISCUSSION

---

### 5.1 Diffusivity

The data for the diffusion column experiments was presented in Table 4-1. The two columns which were run with glass beads resulted in the highest effective diffusion rates at steady state. This is probably due to the low moisture content at which these two columns were run. In fact the drained porosity of these two columns was nearly twice that of the soil columns, which were prepared in the same fashion. After draining the columns, however, the glass beads retained much less water than soil, which resulted in much more air-filled pore space. This in turn resulted in greater movement of toluene vapor through the columns. The increased effective diffusion with decreased moisture content is a well pronounced trend that was expected. The highest diffusion rate for all the columns occurred in column A-1, which was completely dried out at steady state.

This same trend is apparent in the tortuosity constants that were calculated from the effective diffusion coefficients for each column. One would expect the same trend in the tortuosity as in the effective diffusivity because the tortuosity is merely a constant used to describe the diffusion path length. Tortuosity is always less than one and adjusts the diffusivity in pure gas down to account for the tortuous diffusion path through the porous media. As the moisture content decreases, therefore, the tortuosity constant approaches one. Many researchers have described this trend using empirical formulas based upon laboratory experiments. Others have derived formulas based on pore space geometry and porous media packing theories. A short list of these correlations is presented in Table 5-1; the variance between the correlations and the experimental data is also presented in this table. Of the five correlations listed, the data agrees more closely with Millington's predicted values, which are based on a theoretical model. The other four models are based

on experimental data.

It may be noted that as early as 1904 Buckingham was interested in diffusion through porous media, and that new correlations have been proposed as recently as 1979. The most widely accepted tortuosity correlation, however, is the Millington and Quirk formula which was developed in 1961. Figure 5-1 is a graph of three of the correlations from Table 5-1. Values of tortuosity determined from our diffusion columns are plotted on the same graph for comparison. Included on the graph is the tortuosity derived from the dry column run; this is the point with the highest tortuosity constant and a drained porosity equal to its total porosity.

Table 5-1. Published Tortuosity Factors and Variance with Experimental Data.

Investigator	Tortuosity	Variance
+ Buckingham (1904)	$\theta_0$	0.024
* Millington (1959)	$\theta_0^{2.33}/\theta_T^2$	0.015
+ Millington and Quirk (1961)	$\theta_0^{3.33}/\theta_T^2$	0.075
+ Currie (1970)	$\theta_T^{0.5}(\theta_0/\theta_T)^4$	0.038
+ Albertson (1979)	$0.777(\theta_0/\theta_T)-0.274$	0.053

\* Based on theoretical pore size distribution model  
 + Based on laboratory data

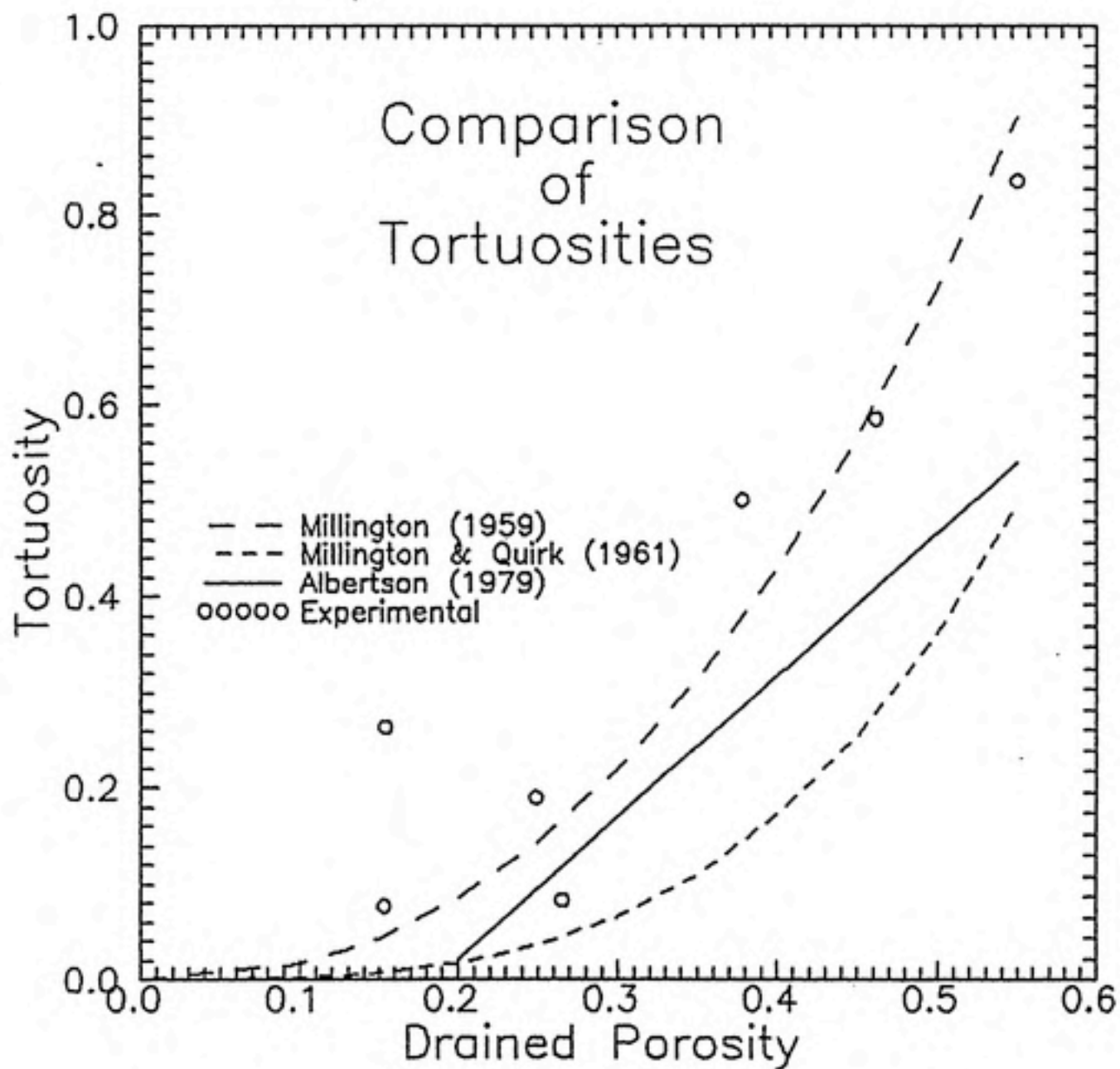


Figure 5-1. Comparison of Tortuosities.

## 5.2 Sorption

Figures 5-2 through 5-7 are graphs comparing the experimental diffusion column data versus the transient diffusion behavior predicted by the model. The model simulations used the effective diffusivities determined at steady state and the sorption constant was set to zero. For each of the soil column runs the difference between the shapes of the two curves is well pronounced. In these cases the model predicts a sharp front, a rapid approach to steady state. The experimental data, on the other hand, suggests a smeared front, a lag time in the approach to steady state. This retardation effect is due to sorption of toluene onto the soil. The data for the two columns that were run with glass beads, columns B-2 and B-4, fall very close to the curves that were predicted for no sorption. This is because the glass beads should sorb very little, if at all. Column B-2 actually displayed a slight 'negative sorption' behavior. This was likely due to preferential flow through the column due to uneven packing or inconsistent draining.

The computer program derived in section 3.4.5 was modified to find the linear sorption coefficient that generated the closest fit to the experimental data for each column run. The best fit was determined by minimizing the sum of the squares of the residuals for each data point. Table 5-2 summarizes the results of these simulations, and Figures 5-8 through 5-12 are plots of the transient diffusion curves that were simulated using the optimized sorption coefficient versus the experimental data. The sorption constant was not optimized for column B-2. The variance for columns B-1, C-1, and B-4 are extremely large and the graphs also reveal a very poor fit with the experimental data. For columns B-3 and C-3, however, the variance was low; the linear sorption model predicted transient behavior that fit the experimental data very closely.

Other researchers have found that in partially-saturated soils sorption increases as the moisture content decreases (Peterson et al., 1988). Examining all of our diffusion column data together does not reveal this same trend. The sorption coefficients range

from 0.4 to 24, but do not follow a trend with moisture content. The results from the third run, columns B-3 and C-3, however, do reveal a trend of higher sorption with decreased moisture content. Working with moisture contents of 8-12 percent, Peterson et al also found that the linear sorption coefficients for these soils was one to four orders of magnitude higher than the linear partition coefficients measured in saturated systems. For columns B-3 and C-3 the sorption constants were 1.0 and 0.4, which are of the same order of magnitude as the sorption constant determined experimentally for the saturated system. The moisture contents of these columns, however, were 52 and 30 percent, respectively. Sorption capacities at such high moisture contents might be expected to approach the sorption capacities of saturated systems.

There was some inconsistency in the data that could be to any of several sources of experimental error. The most serious problem with the diffusion apparatus is the inconsistency of column packing. For the diffusion runs discussed in this report, the length of time in which the soil was hydrated prior to slurring it into the columns was variable. If the soil was not thoroughly hydrated before a run, the sorption capacity would be higher in that column than for a similar column for which the soil was completely wetted. Also, by slurring the soil into the column and then draining it, low moisture contents can not be achieved. Passing nitrogen through the column helped to dry the column, but the pressure may have opened pathways of preferential flow through the soil, or may have dried the column non-uniformly.

Table 5-2. Best Fit Linear Sorption Constants.

Column	$\Theta_0$	$K_p$	SSE	Variance
B-1	0.154	12.5	1581.7	175.7
C-1	0.249	24.2	3956.6	439.6
B-3	0.265	1.0	1129.9	14.4
C-3	0.153	0.4	111.5	12.4
B-4	0.378	5.4	3506.2	584.4

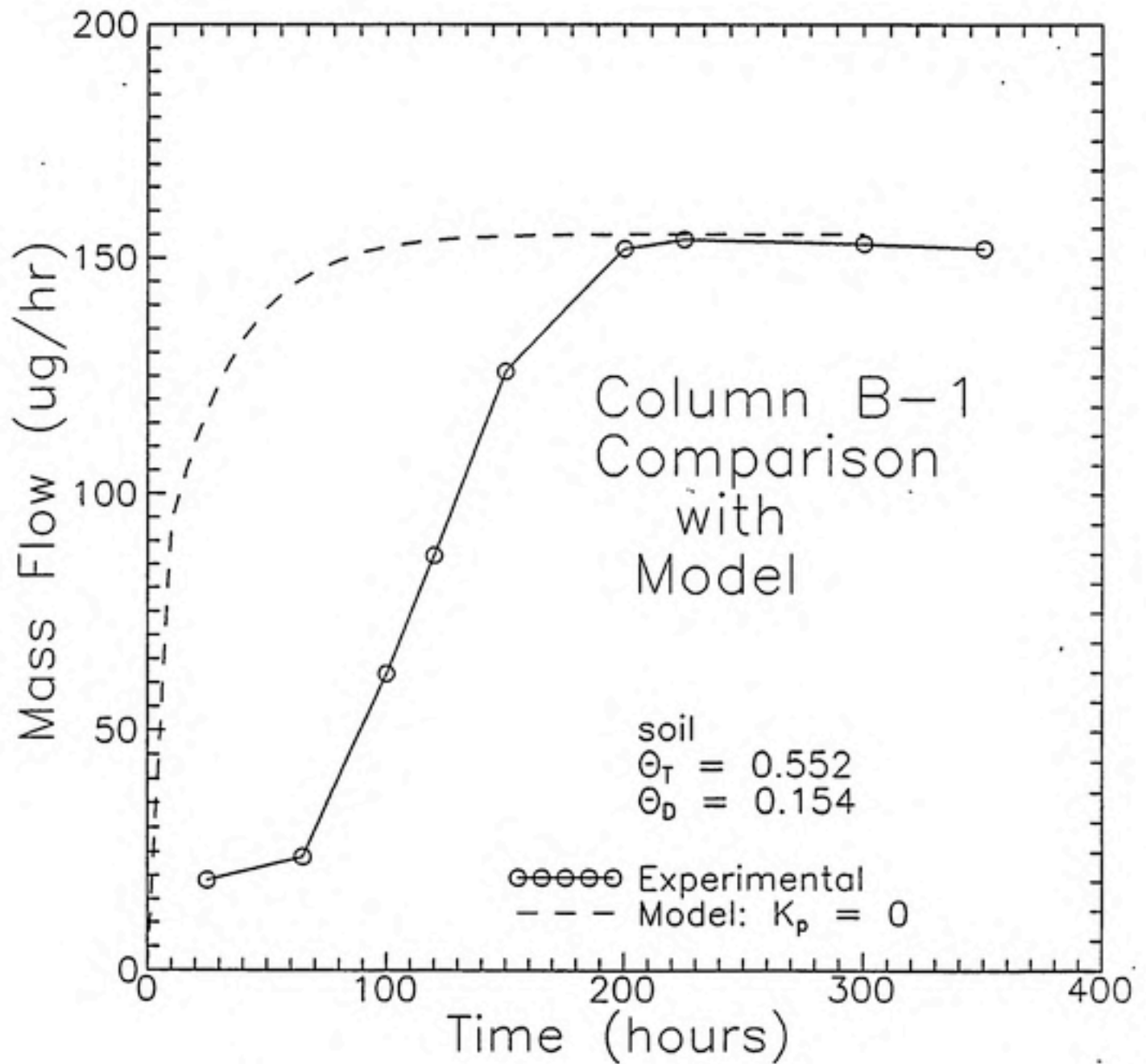


Figure 5-2. Simulation of Column B-1:  $K_p = 0$

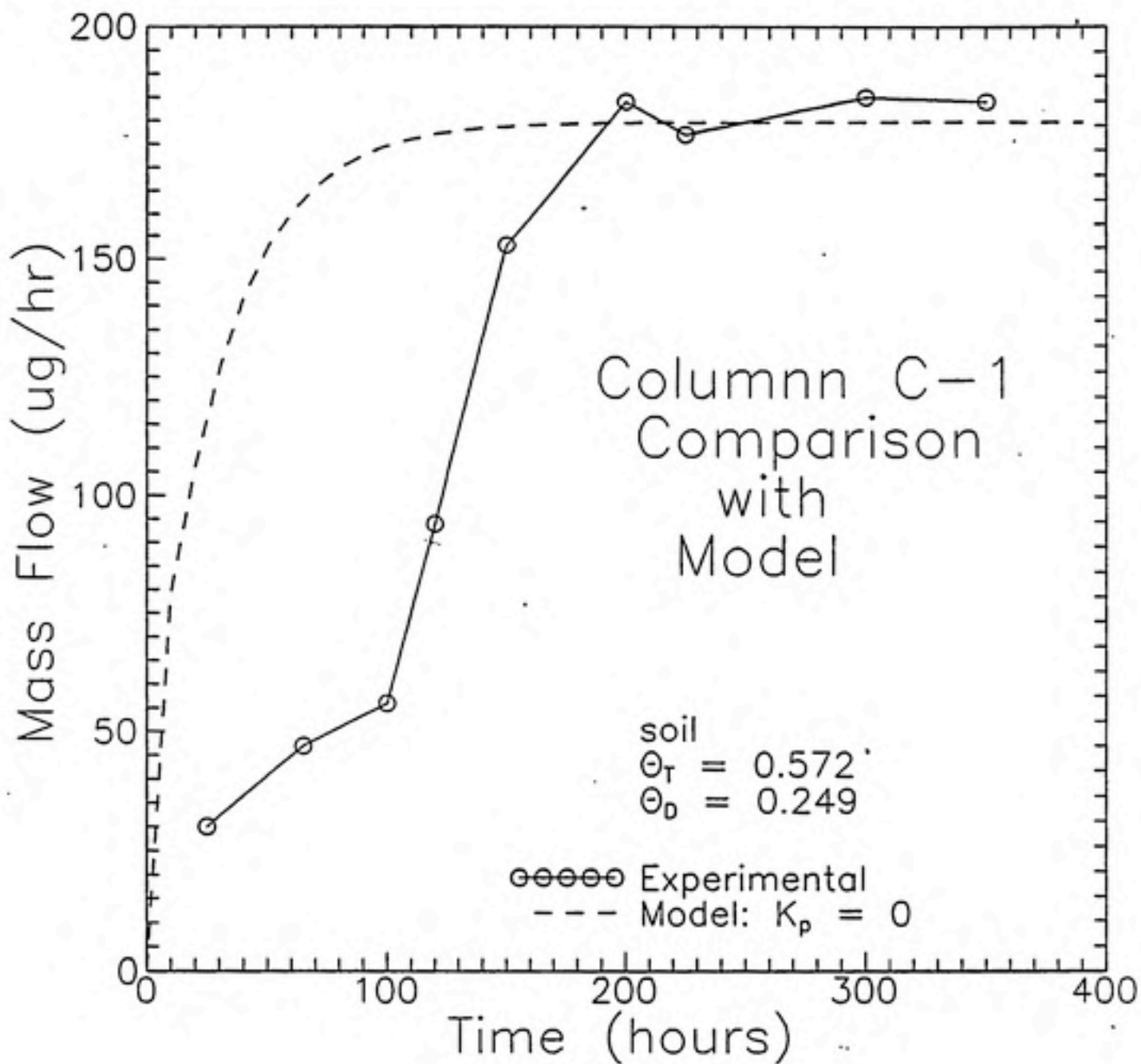


Figure 5-3. Simulation of Column C-1:  $K_p = 0$ .

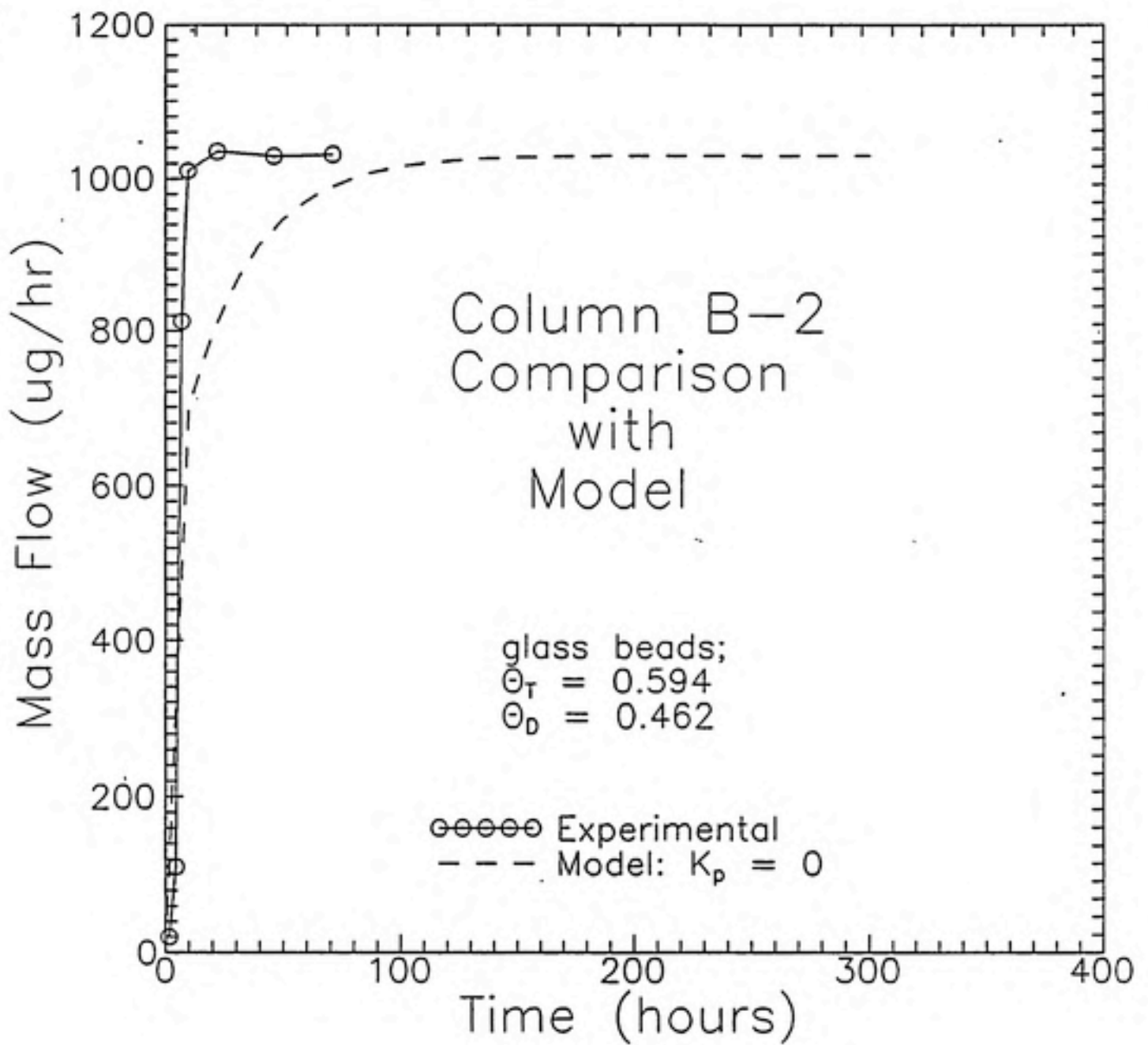


Figure 5-4. Simulation of Column B-2:  $K_p = 0$

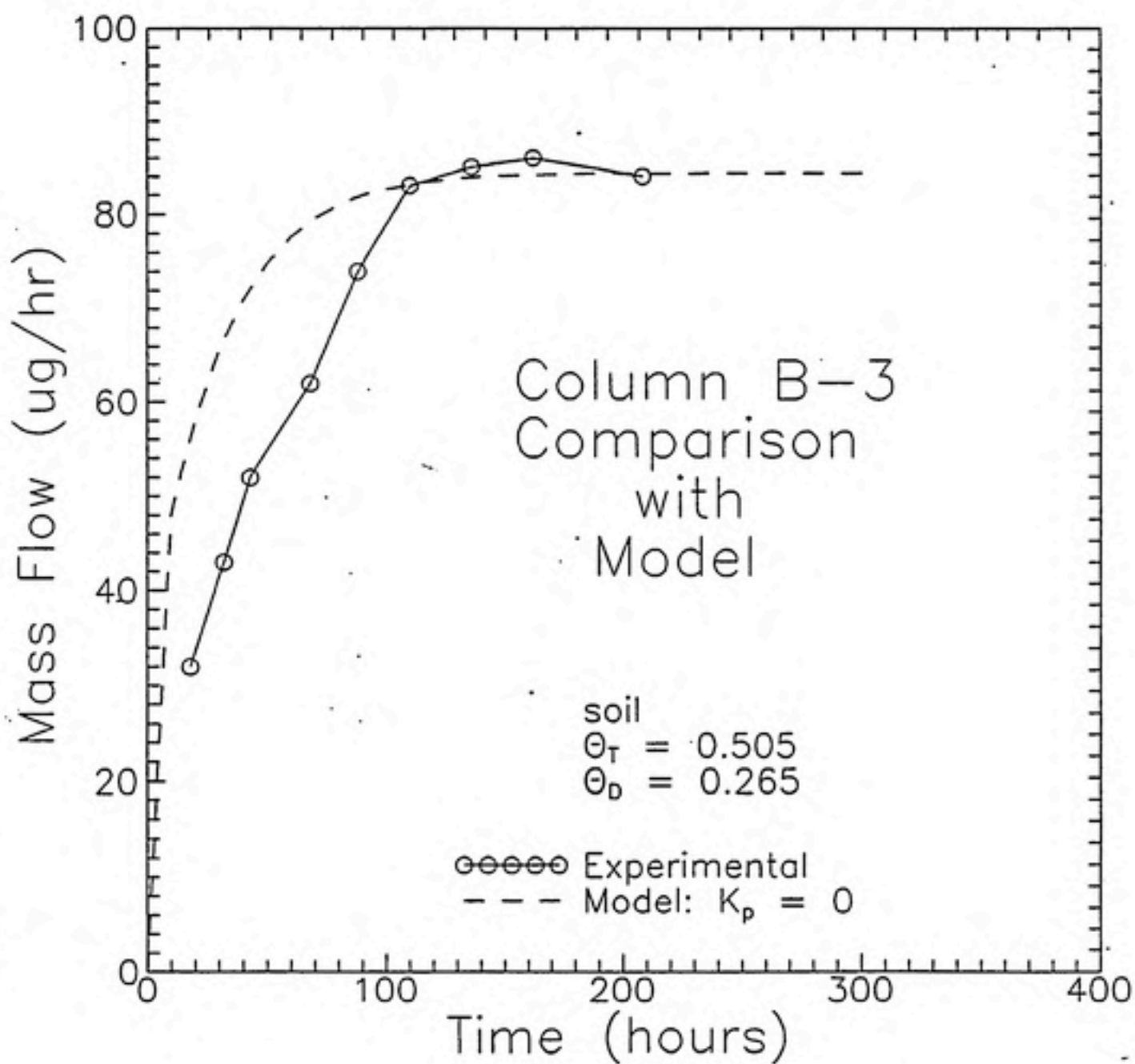


Figure 5-5. Simulation of Column B-3:  $K_p = 0$

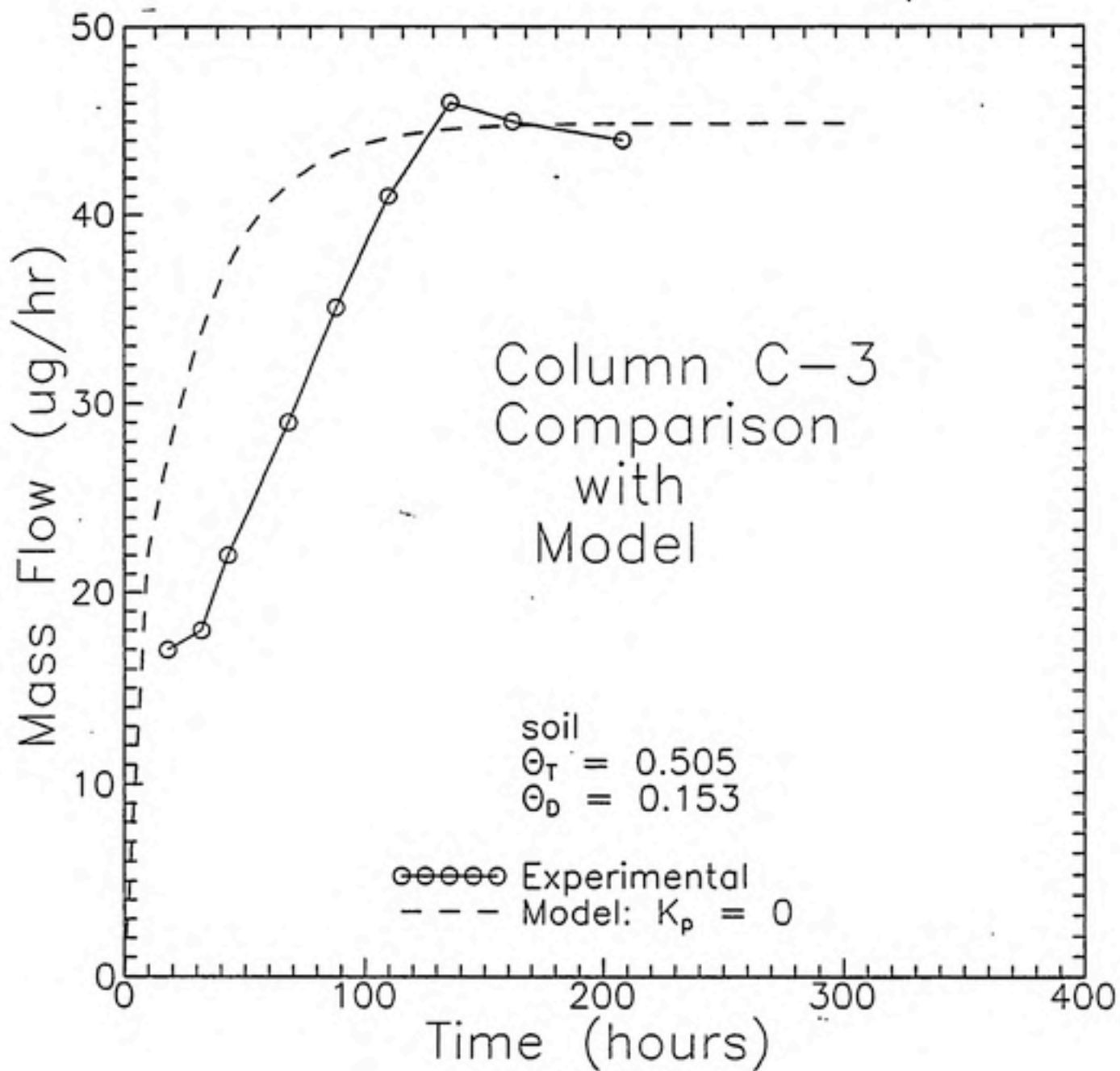


Figure 5-6. Simulation of Column C-3:  $K_p = 0$

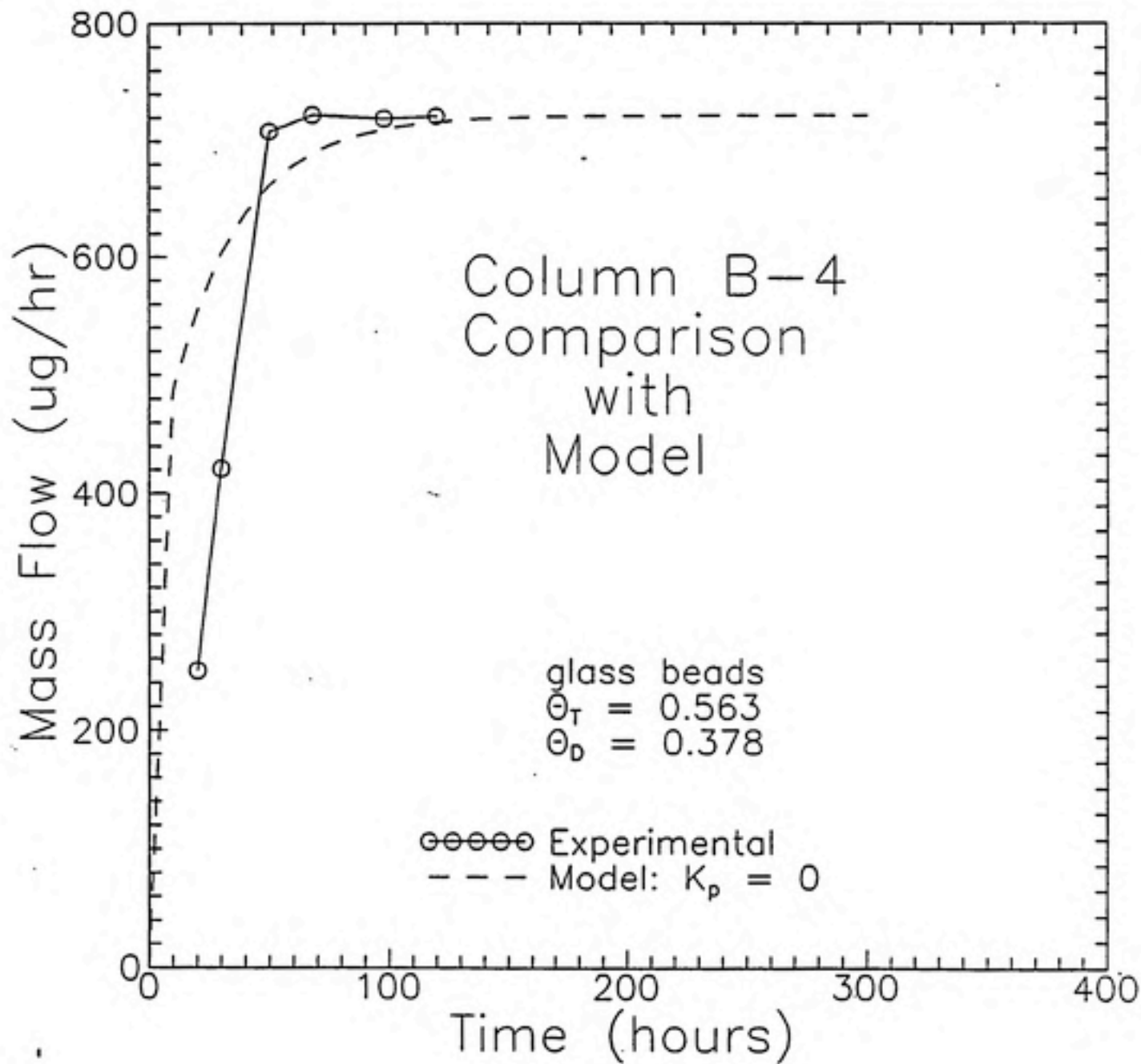


Figure 5-7. Simulation of Column B-4:  $K_p = 0$

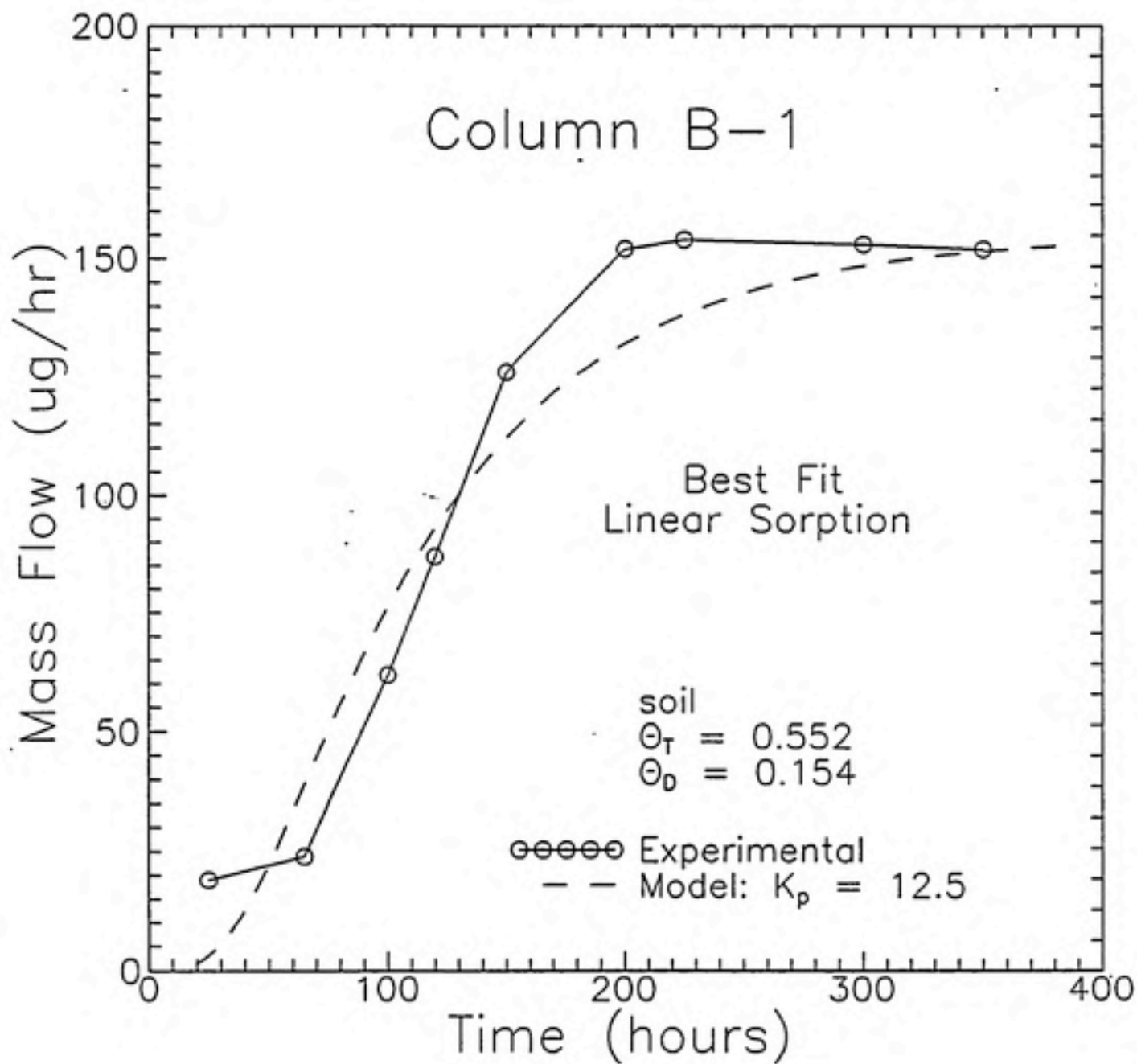


Figure 5-8. Simulation of Column B-1: Best Fit  $K_p$

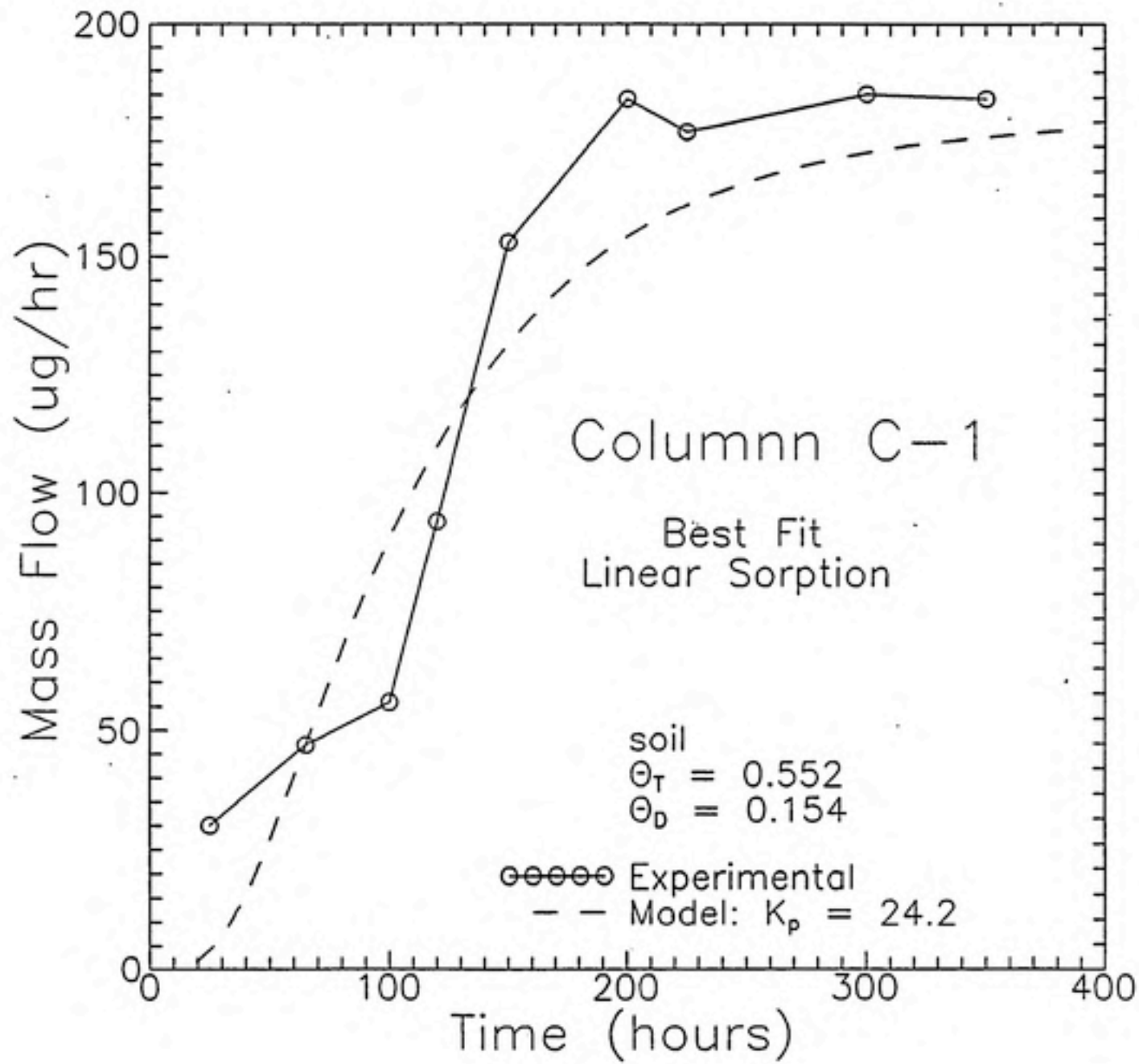


Figure 5-9. Simulation of Column C-1: Best Fit  $K_p$

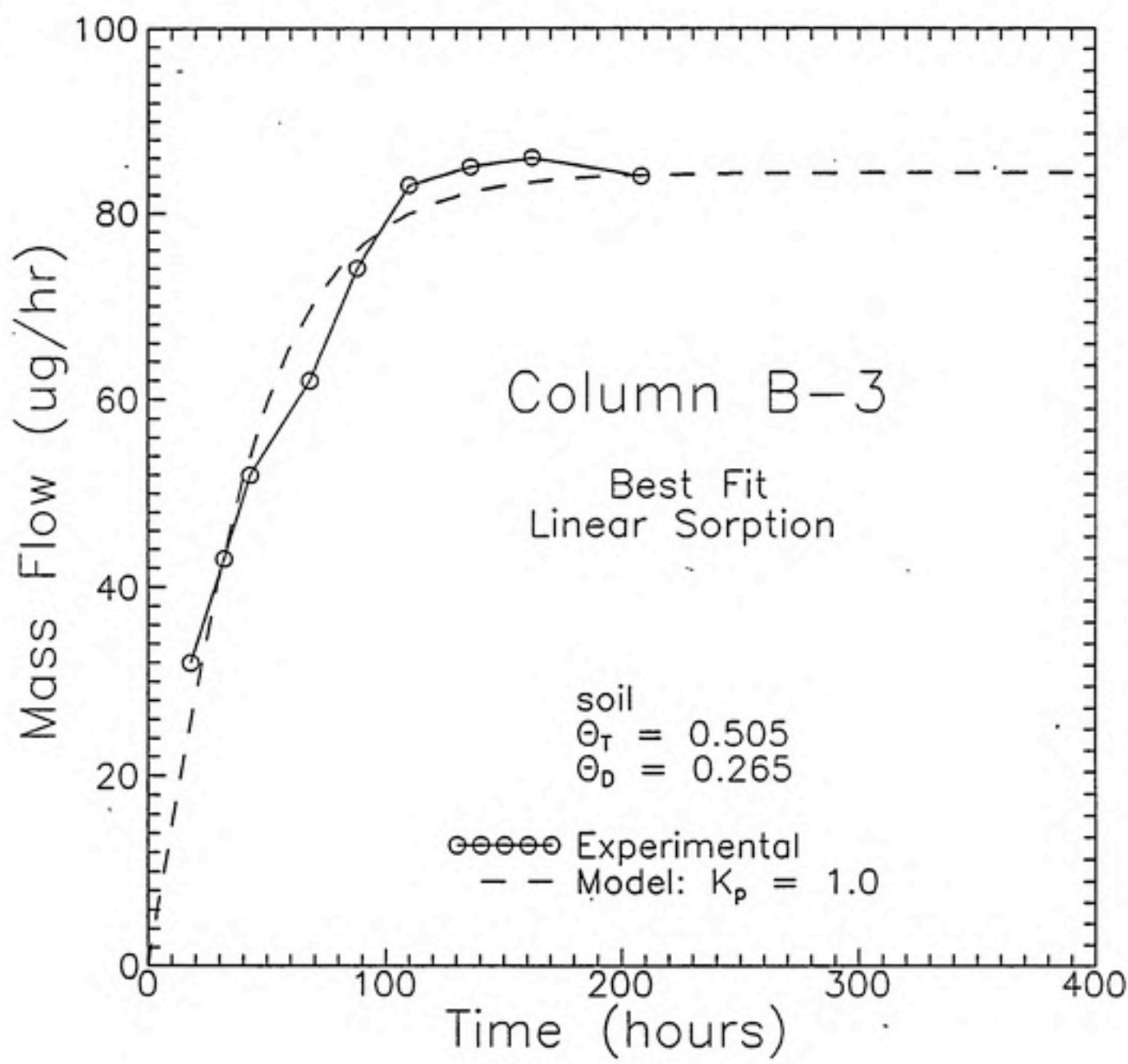


Figure 5-10. Simulation of Column B-3: Best Fit  $K_p$

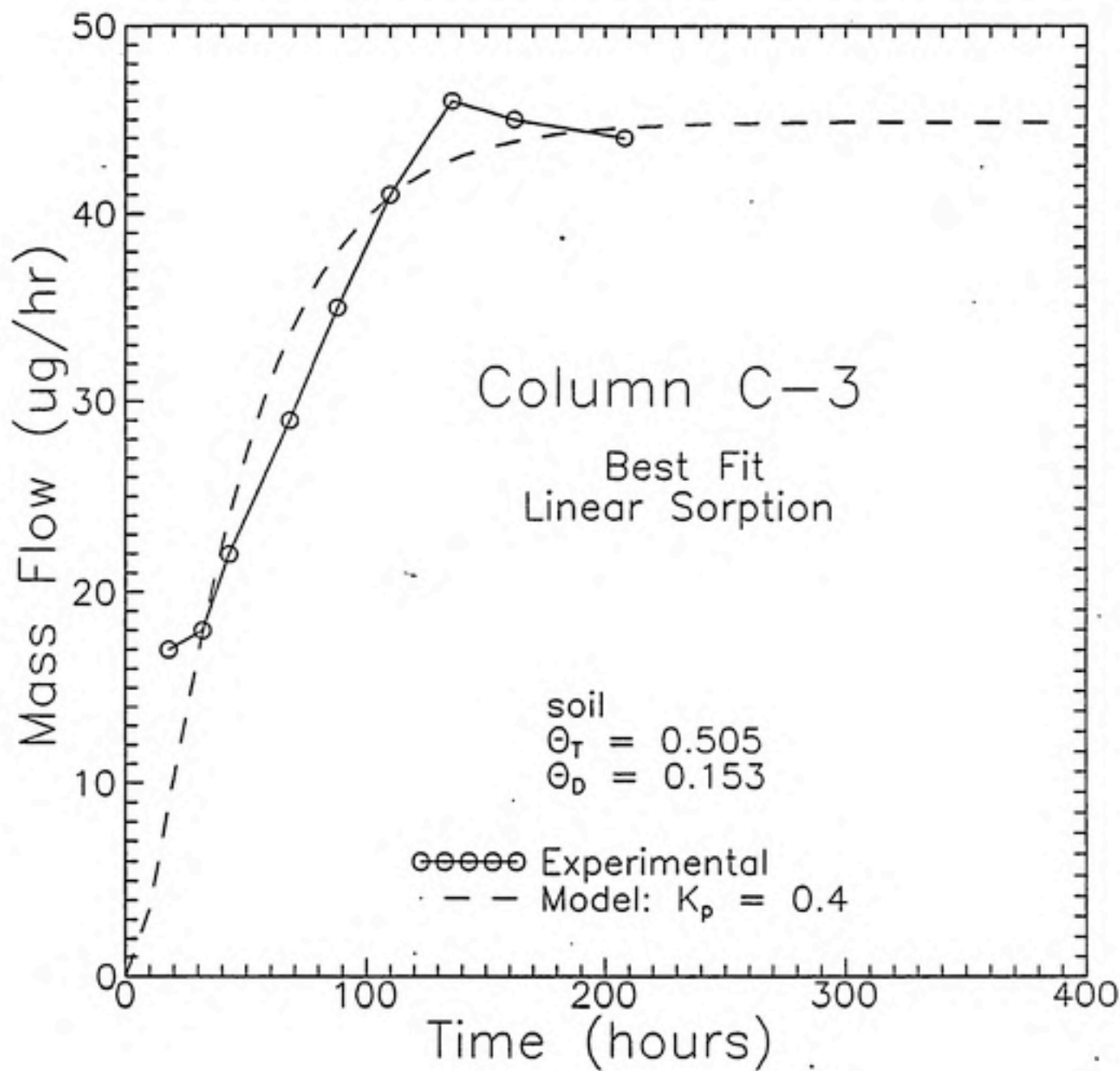


Figure 5-11. Simulation of Column C-3: Best Fit  $K_p$

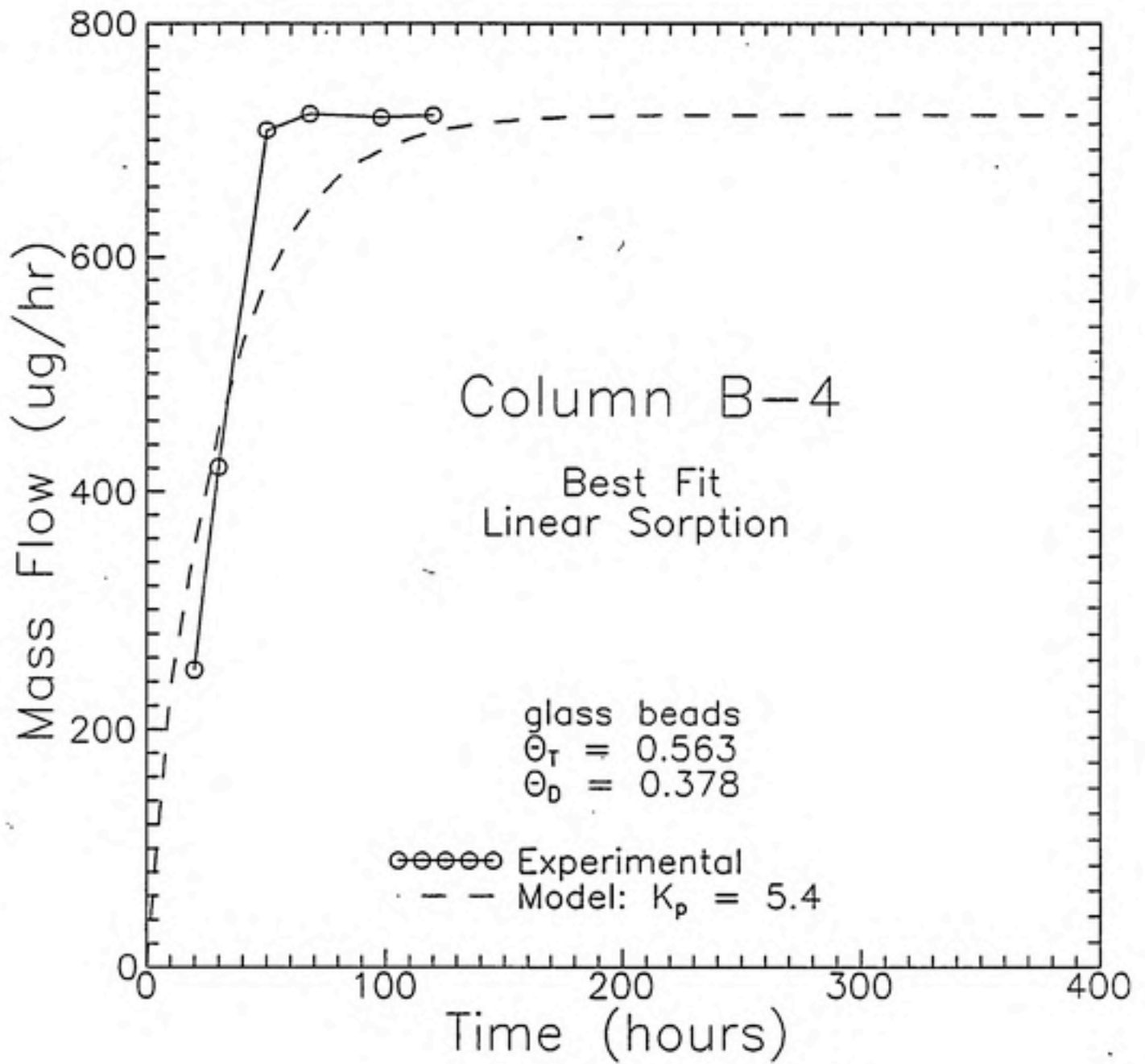


Figure 5-12. Simulation of Column B-4: Best Fit  $K_p$

### 5.3 Impact at the Field Scale

The results of the vapor-phase field sampling clearly shows migration of hydrocarbons up-gradient from the fire training pit. The presence of these vapors up-gradient from the source illustrates the source identification problems created by vapor-phase diffusion in the partially-saturated zone. In this situation the fire training pit was already identified as the source of contamination. But if there were several potential sources in the vicinity of the contaminated region, reliance on groundwater flow data could be misleading.

The fire training area also illustrates the difficulties that vapor migration can pose to remedial action. The area of contamination has spread beyond the immediate area of the site and as it grows it becomes a larger source of contamination that requires a more extensive cleanup.

The results of the laboratory diffusion column experiments suggest that large amounts of volatile compounds can move large distances by diffusion in relatively short times through porous media. At a site like Pope AFB fire training area, in particular, where the soil is exposed to the sun in extreme heat, the moisture level of the soil may be extremely low during many months of the year. These low levels of saturation also increase the amount of sorption from the vapor phase onto the soil. The increased sorption would tend to retard the movement of an organic through the vadose zone, but it would also limit the escape of the contaminant to the atmosphere.

---

## 6 CONCLUSIONS AND RECOMMENDATIONS

---

### Conclusions

1. The glass bead diffusion columns were found to have a much sharper front on the approach to steady-state, while the soil columns exhibited a retardation effect, evidenced by a more smeared front in time.
2. Effective diffusivity increased with decreased moisture content.
3. The tortuosity constant also increased as moisture content decreased.
4. When compared to previously published correlations of tortuosity versus moisture content, the data agreed best with a correlation developed by Millington in 1959, which is based upon theoretical principles and not experimentation.
5. For one set of column runs, run with a high moisture content, the linear sorption coefficient was found to be very close to that found in the bottle-point study. The results of this set of columns suggest that sorption decreases with increased moisture content, and that at high levels of saturation (50-60%), the amount of organic that will sorb to the solid phase approaches that of a saturated system.
6. Sampling soil gas at a fire training area at Pope Air Force Base, North Carolina, revealed contamination at locations that are up-gradient from the actual point of jet-fuel dumping and burning. The transport of volatile organics in a direction opposite to the direction in which free product is moving is concluded to be due to vapor-phase diffusion through the partially-saturated zone.

## Recommendations

1. The diffusion apparatus used in these experiments was found to be a simple and consistent way to measure diffusion through a column of porous media. The only major problem encountered was not in the running of the column, but in the preparation of the column. To obtain better results, a method should be developed that could assure more consistent packing and be able to achieve lower moisture levels.
2. A more sophisticated model that could utilize non-linear equilibrium data would be useful in determining if the linear sorption model is truly adequate. Also, a rate model was never fit to the bottle-point rate study data because the sorption equilibrium model seemed to adequately model the column behavior. The equilibrium assumption should be tested, however, and to do this one must fit the rate data to a rate model, and then incorporate the rate parameters into a diffusion model that does not make the instantaneous equilibrium assumption.

---

## 7 NOTATION

---

- $C_a$  = aqueous concentration ( $M/L^3$ ) .  
 $C_v$  = vapor concentration ( $M/L^3$ ) .  
 $(\frac{\partial C}{\partial t})_{rxn}$  = reactive term ( $M/L^3/T$ ) .  
 $D^*$  = diffusivity in pure vapor ( $L^2/T$ ) .  
 $D_e$  = effective diffusivity ( $L^2/T$ ) .  
 $D_h$  = hydrodynamic dispersion tensor ( $L^2/T$ ) .  
 $D_{ij}$  =  $i, j$  term of dispersion tensor ( $L^2/T$ ) .  
 $D_m$  = effective molecular diffusion coefficient ( $L^2/T$ ) .  
 $D_{re}$  = retarded effective diffusivity ( $L^2/T$ ) .  
 $f_{oc}$  = fraction organic carbon (*dimensionless*) .  
 $g$  = gravitational constant ( $L^2/T$ ) .  
 $h$  = hydraulic head ( $L$ ) .  
 $\frac{\partial h}{\partial x}$  = groundwater gradient (*dimensionless*) .  
 $i, j$  = components of Cartesian coordinate system .  
 $J$  = mass flux ( $M/L^2T$ ) .  
 $k$  = intrinsic permeability ( $L^2$ ) .  
 $K$  = hydraulic conductivity ( $L/T$ ) .  
 $K$  = hydraulic conductivity tensor ( $L/T$ ) .  
 $K_p$  = linear sorption equilibrium constant ( $L^2/M$ ) .  
 $K_F$  = Freundlich sorption capacity constant ( $(L^3/M)^n$ ) .  
 $K_{oc}$  = organic carbon partition coefficient .  
 $K_{ow}$  = octanol water partition coefficient .  
 $K_H$  = Henry's constant ( $L^3/L^3$ ) .  
 $n$  = porosity (*dimensionless*) .  
 $n_F$  = Freundlich sorption intensity constant (*dimensionless*) .  
 $n_f$  = Freundlich fast site sorption intensity constant (*dimensionless*) .  
 $n_s$  = Freundlich slow site sorption intensity constant (*dimensionless*) .  
 $p_i$  = partial pressure of component  $i$  ( $M/L^2$ ) .  
 $q$  = solid phase concentration ( $M/M$ ) .  
 $q_e$  = equilibrium solid phase concentration ( $M/M$ ) .  
 $q_f$  = solid phase concentration of fast sorption sites ( $M/M$ ) .  
 $q_s$  = solid phase concentration of slow sorption sites ( $M/M$ ) .  
 $q_x$  = specific discharge ( $L/T$ ) .  
 $S$  = degree of water saturation (*dimensionless*) .  
 $t$  = time ( $T$ ) .  
 $\bar{v}$  = pore velocity ( $L/T$ ) .  
 $\bar{v}$  = average magnitude of groundwater velocity ( $L/T$ ) .  
 $\Delta x$  = distance between spatial locations in  $x$ -direction ( $L$ ) .  
 $\alpha_T$  = transverse dispersivity ( $L$ ) .

$\alpha_L$  = longitudinal dispersivity ( $L$ ) .

$\nabla$  = gradient operator .

$\Gamma$  = source or sink term ( $M/L^3T$ ) .

$\rho_w$  = density of water ( $M/L^3$ ) .

$\rho_s$  = density of solid phase ( $M/L^3$ ) .

$\phi$  = hydraulic head ( $L$ ) .

$\psi$  = pressure head ( $L$ ) .

$\theta_D$  = drained porosity (*dimensionless*) .

$\theta_T$  = total porosity (*dimensionless*) .

$\theta_w$  = water-filled porosity (*dimensionless*) .

$\tau$  = tortuosity (*dimensionless*) .

---

## 8 REFERENCES

---

- Albertson, M. 1979. Carbon Dioxide Balance in the Gas-Filled Part of the Unsaturated Zone, *Z. Pflanzenernaehr, Bodenkd.*, 142,39-56.
- Baehr, A.L. 1987. Selective Transport of Hydrocarbons in the Unsaturated Zone due to Aqueous and Vapor Phase Partitioning. *Water Resources Research*, 23, p. 1926.
- Bear, J. 1979. *Hydraulics of Groundwater*. McGraw-Hill, Inc., New York.
- Bird, R.B., W.E. Stewart and E.N. Lightfoot. 1960. *Transport Phenomena*, John Wiley, New York.
- Bruell, C.S. and G.E. Hoag. 1986. The Diffusion of Gasoline-Range Hydrocarbon Vapors in Porous Media, Experimental Methodologies. Proceedings of the NWWA/API Conference on Petroleum Hydrocarbons and Organic Chemicals, Nov. 12-14, Houston.
- Buckingham, E. 1904. Contributions to Our Knowledge of the Aeration of Soils. Bull. 25, U.S. Dept. of Agriculture Bur. of Soils, Washington, D.C.
- Cameron, D.R., and A. Klute. 1977. Convective-Dispersive Solute Transport with a Combined Equilibrium and Kinetic Adsorption Model. *Water Resources Research*, 13, pp. 183-188.
- Carslaw, H.S., and J.C. Jaeger. 1959. *Conduction of Heat in Solids*, Oxford University Press, New York.
- Chiou, C.T. and T.D. Shoup. 1985. Soil Sorption of Organic Vapors and Effects of Humidity on Sorptive Mechanism and Capacity. *Envir. Sci. and Technol.*, 19(12), 1196-1200
- Crank, J. 1975. *The Mathematics of Diffusion*. 2<sup>nd</sup> ed. Oxford University Press.
- Farmer, W.J., M.S. Yang, J. Letey and W.F. Spencer. 1980. Hexachlorobenzene: Its Vapor Pressure and Vapor Phase Diffusion in Soil. *Soil Sci. Soc. Am. J.*, 44, pp. 676-680.
- Gierke, J.S. et al. 1985. Modeling the Movement of Volatile Organic Chemicals in the Unsaturated Zone. *Nation Water Well Assoc. Proc.*
- Gillham, R.W., E.A. Sudicky, J.A. Cherry, and E.O. Frind. 1984. An Advection Diffusion Concept for Solute Transport in Heterogeneous Unconsolidated Geological Deposits. *Water Resources Research*, 20(3), pp. 369,378.
- Hansch, C. and A.J. Leo. 1979. *Substituent Constants for Correlation Analysis in Chemistry and Biology*, Wiley, New York.

Jellick, G.J. and R.R. Schnabel. 1985. Field Determination of Gas Diffusion Coefficients in Surface Soils. National Water Well Assoc. Proc.

Karickhoff, S.W., D.S. Brown and T.A. Scott. 1979. Sorption of Hydrophobic Pollutants on Natural Sediments, Water Res. 13, pp. 241-248.

Karimi, A.A, W.J. Farmer and M.M. Cliath. 1987. Vapor-Phase Diffusion of Benzene in Soil. J. Envir. Quality, 16, pp. 38-43.

Kool, J.B. and J.C. Parker. 1987. Development and Evaluation of Closed-Form Expressions for Hysteretic Soil Hydraulic Properties. Water Resources Research, 23(1), pp. 105-114.

Kool, J.B. and J.C. Parker. 1988. Analysis of the Inverse Problem for Transient Unsaturated Flow. Water Resources Research, 24(6), pp.817-830.

Kuhlmeier, P.D. and G.L. Sunderland. 1985. Distribution of Volatile Aromatics in Deep Unsaturated Sediments. National Water Well Assoc. Proc.

Lyman, W.J., W.F. Reehl and D.H. Rosenblatt. 1982. *Handbook of Chemical Property Estimation Methods*. McGraw-Hill.

Mackay, D.M., P.V. Roberts, and J.A. Cherry. 1985 Transportation of Organic Contaminants in Groundwater. Env. Sci. and Technol., 19(5), pp. 384-392.

Marshall, T.J. 1959. The Diffusion of Gases Through Porous Media, J. Soil Science, 10, pp. 79-82.

Miller, C.T. and W.J. Weber Jr. 1986. Sorption of Hydrophobic Organic Pollutants in Saturated Soil Systems, Journal of Contaminant Hydrology, 1, pp. 243-261.

Millington, R.J. 1959. Gas Diffusion in Porous Media, Science, 130, pp.100- 102.

Nielsen, D.R. and J.W. Biggar. 1961. Miscible Displacement in Soils I. Soil Sci. Soc. Am., Proc. 25, pp.1-5.

Nielson, K.K. et al. 1984. Diffusion of Radon Through Soils. Soil Sci. Soc. Am., J. 48, pp. 482-48.

Parker, J.C., R.J. Lenhard and T. Kuppusamy. 1987. Physics of Immiscible Flow in Porous Media. EPA-600/2-87-101.

Peterson, M.S., L.W. Lion and C.A. Shoemaker. 1988. Influence of Vapor-Phase Sorption and Diffusion on the Fate of Trichloroethylene in an Unsaturated Aquifer System. Envir. Sci. and Technol, 22(5), pp.571-578.

Pickens, J.F. and G.F. Grisak. 1981. Modeling of Scale-Dependent Dispersion in Hydrogeologic Systems. Water Resources Research, 17(6), pp. 1701-1711.

Skibitzke, H.E. and G.M. Robinson. 1963. Dispersion in Groundwater Flowing Through Heterogeneous Materials, Geological Survey Professional Paper 386-B, U.S. Government Printing Office, Washington, D.C.

Smith, J.M. and H.C. Van Ness. 1975. Introduction to Chemical Engineering Thermodynamics, McGraw-Hill, New York, 1975.

Sudicky, E.A. and J.A. Cherry. 1979. Field Observations of Tracer Dispersion Under Natural Flow Conditions in an Unconfined Sandy Aquifer. Water Pollution Research in Canada, 14, pp. 1-17.

Thompson, A.F.B., and W.G. Gray. 1986. A Second Order Approach for the Modeling of Dispersive Transport in Porous Media 1: Theoretical Development. Water Resources Research, 22(5), pp. 591-599.

van Genuchten, M.Th. and P.J. Wierenga. 1976. Mass Transfer Studies in Sorbing Porous Media I. Soil Sci. Soc. Am., J., 40, pp. 473-480.

van Genuchten, M.Th. and P.J. Wierenga. 1977. Mass Transfer Studies in Sorbing Porous Media III. Soil Sci. Soc. Am., J., 41, pp. 278-285.

Verschueren, K. 1983. *Handbook of Environmental Data on Organic Chemicals*. Van Nostrand Reinhold Co. New York.

Wallingford, E.D., F.A. DiGiano and C.T. Miller. 1988. Evaluation of a Carbon Adsorption Method for Sampling Gasoline Vapors in the Subsurface. Groundwater Monitoring Review, 8(4), pp. 85-92.

Weeks, E.P. et al. 1982. Use of Atmospheric Fluorocarbons F-11 and F-12 to Determine the Diffusion Parameters of the Unsaturated Zone in the Southern High Plains of Texas. Water Resources Research, 18, pp. 1365-1378.